AFCRL-1071

INFRARED RADIATION OF FLAMES

RICHARD H. TOURIN
HAROLD J. BABROV
GUNTER J. PENZIAS

THE WARNER & SWASEY COMPANY
CONTROL INSTRUMENT DIVISION
32-16 DOWNING STREET
FLUSHING 54, NEW YORK

FINAL REPORT ON CONTRACT AF19(604) - 6106
ARPA ORDER NO. 6-58 TASK 13
PROJECT DEFENDER

OCTOBER 1961

GEOPHYSICS RESEARCH DIRECTORATE
AIR FORCE CAMBRIDGE RESEARCH LABORATORIES
OFFICE OF AEROSPACE RESEARCH
UNITED STATES AIR FORCE
BEDFORD MASSACHUSETTS

Requests for additional copies by Agencies of the Department of Defense, their contractors, and other Government agencies should be directed to the:

ARMED SERVICES TECHNICAL INFORMATION AGENCY
ARLINGTON HALL STATION
ARLINGTON 12, VIRGINIA

Department of Defense contractors must be established for ASTIA services or have their 'need-to-know' certified by the cognizant military agency of their project or contract.

All other persons and organizations should apply to the:

U. S. DEPARTMENT OF COMMERCE
OFFICE OF TECHNICAL SERVICES
WASHINGTON 25, D. C.

ERRATA TO AFCRL-1072, INFRARED RADIATION OF FLAMES.

p. 11 - The second contract report is AFCRL - 848(II).

The third contract report is AFCRL - 1070.

p. 18 - Reference 23 should read AFCRL - 848(II).

p. 19 - Reference 31 should read AFCRL - 1070.

AFCRL-1071

INFRARED RADIATION OF FLAMES

RICHARD H. TOURIN
HAROLD J. BABROV
GUNTER J. PENZIAS

THE WARNER & SWASEY COMPANY
CONTROL INSTRUMENT DIVISION
32-16 DOWNING STREET
FLUSHING 54, NEW YORK

FINAL REPORT ON CONTRACT AF19(604)-6106
ARPA ORDER NO. 6-58 TASK 13
PROJECT DEFENDER

OCTOBER 1961

GEOPHYSICS RESEARCH DIRECTORATE
AIR FORCE CAMBRIDGE RESEARCH LABORATORIES
OFFICE OF AEROSPACE RESEARCH
UNITED STATES AIR FORCE
BEDFORD MASSACHUSETTS

FOREWORD

This work was performed under Contract AF19(604)-6106, ARDC Project No. 4991, with Air Force Cambridge Research Laboratories; Drs. J. N. Howard, J. S. Garing, and R. S. Walker acted as project monitors. The contract was initiated by ARPA Order 6-58, Task 13, under Project Defender, ARPA Code 7200; Dr. Charles W. Cook was project manager for ARPA.

ABSTRACT

Knowledge of the infrared spectral radiance of combustion flames is needed in various military applications of infrared techniques. In an effort to fill this need, infrared spectral emittance and absorptance of flames were studied at various temperatures and for a variety of fuel-oxidizer combinations. Spectral emissivities were measured in the region 1 -- 15-μ, as functions of fuel composition, flame temperature, and mixture ratio. Flame temperatures were determined from the infrared emission and absorption spectra, for various wavelengths.

Methods of extrapolating flame radiance from laboratory to field conditions were investigated. For this purpose, the measurements of infrared flame spectra were correlated with concurrent analyses of molecular population distributions, transition probabilities, and spectral line shape and line width. A sample extrapolation was verified experimentally for a hydrogen-oxygen rocket engine, operating under simulated altitude conditions.

Effects of altitude on the infrared radiation of flames were evaluated, with particular reference to the effects of reduced pressure on spectral line shape, and the applicability of theoretical infrared band models.

CONTENTS

INFRARED RADIATION OF FLAMES

I. INTRODUCTION

Reliable information on the infrared radiation of ballistic missile plumes is needed in the development and design of infrared equipment for detection, identification, and tracking of missiles (1)*. To provide for long range capability in this area, infrared spectral data are required for a variety of fuels, fuel combinations, and combustion conditions which are representative of current and future practice in ballistic missile propulsion (2).

The difficulties and limitations of field measurements of missile plume radiation are well known (1). The opinion has often been expressed that much useful data on missile plume radiation can be obtained, at much less expense than open-air target studies, from laboratory flame and gaseous emission studies (3). Direct observation of missile plume radiation is necessarily restricted to available missiles. Laboratory studies are the only means to obtain data on radiation from flames burning fuels and classes of fuel under development or anticipated for possible future use in ballistic missile propulsion. In addition to the data themselves, laboratory studies provide detailed quantitative analysis of infrared radiation of flames and correlation of the measurements to the basic physics and chemistry of flame radiation. This correlation is an essential step in achieving understanding of radiation processes, which is the basis for long range predictive capability.

The considerations outlined above, combined with the results of previous research on flame radiation (4-21), were the basis for initiating the work described in this report.

The basic data needed to predict missile plume radiation are flame spectral emissivities and flame temperatures, as functions of fuel and combustion conditions. From these basic data, the infrared radiation of a missile plume and its spectral distribution can be determined. Accordingly, the approach followed in this project has been as follows:

1. Measure emissivities and temperatures of flames, using fuels, fuel combinations, and combustion conditions of sufficient variety to be representative of current and future practice in ballistic missile propulsion.

2. Develop suitable extrapolation procedures, to apply the laboratory data to calculation of missile plume emissivities.

---

* Underlined numbers in parentheses refer to references listed in Section X.

3. Verify the extrapolation by field checks made in a controlled environment.

An example of a step-by-step procedure used to predict missile plume emissivities and radiances is described in Section III.

The chief goal of this program is a handbook or "Atlas" of flame emissivities, supplemented by numerical constants and procedures whereby the radiation of missile plumes can be predicted. This Atlas is being issued in parts; the first two parts have been completed under this contract (22,23). Another goal of the program is to achieve basic understanding of flame radiation, and thus help to provide improved predictive capability for the future. This goal has been approached through experimental studies of molecular radiation (24–27) and related physical problems (28–31).

The following are the major accomplishments of the project, as described in detail in the referenced publications and reports. Brief summaries of the principal results are given later in this report.

1. Measurements of hydrocarbon flame emissivities and temperatures have been completed, and an Atlas of these data prepared (22).

2. Measurements of nitrogenous fuel flame emissivities and temperatures have been made (23).

3. The effect of altitude on flame infrared radiation was studied experimentally and evaluated (23,32).

4. A field check was carried out using a hydrogen-oxygen rocket engine under altitude test conditions (32).

5. Progress was made in developing improved extrapolation formulae and procedures (29,31).

6. Methods were worked out for measurement of solid propellant radiation under controlled conditions.

II. MEASUREMENTS OF FLAME SPECTRA

Infrared emission and absorption spectra of flames of various fuels were measured under known, controlled temperature, pressure, and flow conditions. Details of the combustion system, the infrared instrumentation, and the experimental results are given in two technical reports prepared under this contract (22,23).

1. Liquid propellants

Liquid propellant flames were studied in a 3-inch enclosed burner (22). This enabled studies of burning with oxygen and with other oxidizers, such as RFNA, at atmospheric pressure and at reduced pressures. The number of specific examples studied was minimized by concentration on general relationships. The spectra of most hydrocarbon flames are so similar that there is little object to studying a great variety of hydrocarbon fuel mixtures. The combustion products and consequently the gross spectra, are the same for all. The differences are mainly differences due to temperature and pressure, which should be predictable from measurements of a few representative hydrocarbon flames. Methanol-O_2, kerosene-O_2, and hexane-O_2 were studied as representative examples of hydrocarbon combustion. Figure 1 is an example of the type of results obtained.

Nitrogenous fuel systems studied were ammonia-oxygen (23) hydrazine-oxygen (23), and hydrazine-RFNA. Work on nitrogenous fuels is continuing.

2. Gaseous fuels

Gaseous fuels were studied separately from liquid propellants, because the handling problems are different, and gas combustion can be studied with relatively simple burner equipment. Flames of hydrocarbons with oxygen and the hydrogen-oxygen flame were investigated experimentally (23,32).

3. Low pressure flames (high altitude simulation)

Infrared radiation and temperatures of flames were measured as a function of pressure, to aid in evaluating the effect of altitude on flame radiance. Emissivities and equivalent widths of spectral lines were measured in a laboratory burner, and equivalent widths were extrapolated to zero pressure (23). Emissivities of a rocket exhaust plume were measured under controlled conditions simulating altitudes in the range $10^5 - 10^6$ ft. (32). An example of low pressure infrared flame spectra is given in Fig. 2.

4. Solid propellants

Solid propellants require special handling, if the measurements are to be made under controlled, known conditions. Different measurement techniques are required from those used for liquids, because the measurements must be made during the limited time available while the propellant charge is burning. There is nothing in the solid propellant case corresponding to continuous feeding of fuel as in the case of liquid propellants. Preliminary studies were made on an experimental optical bomb and a high speed

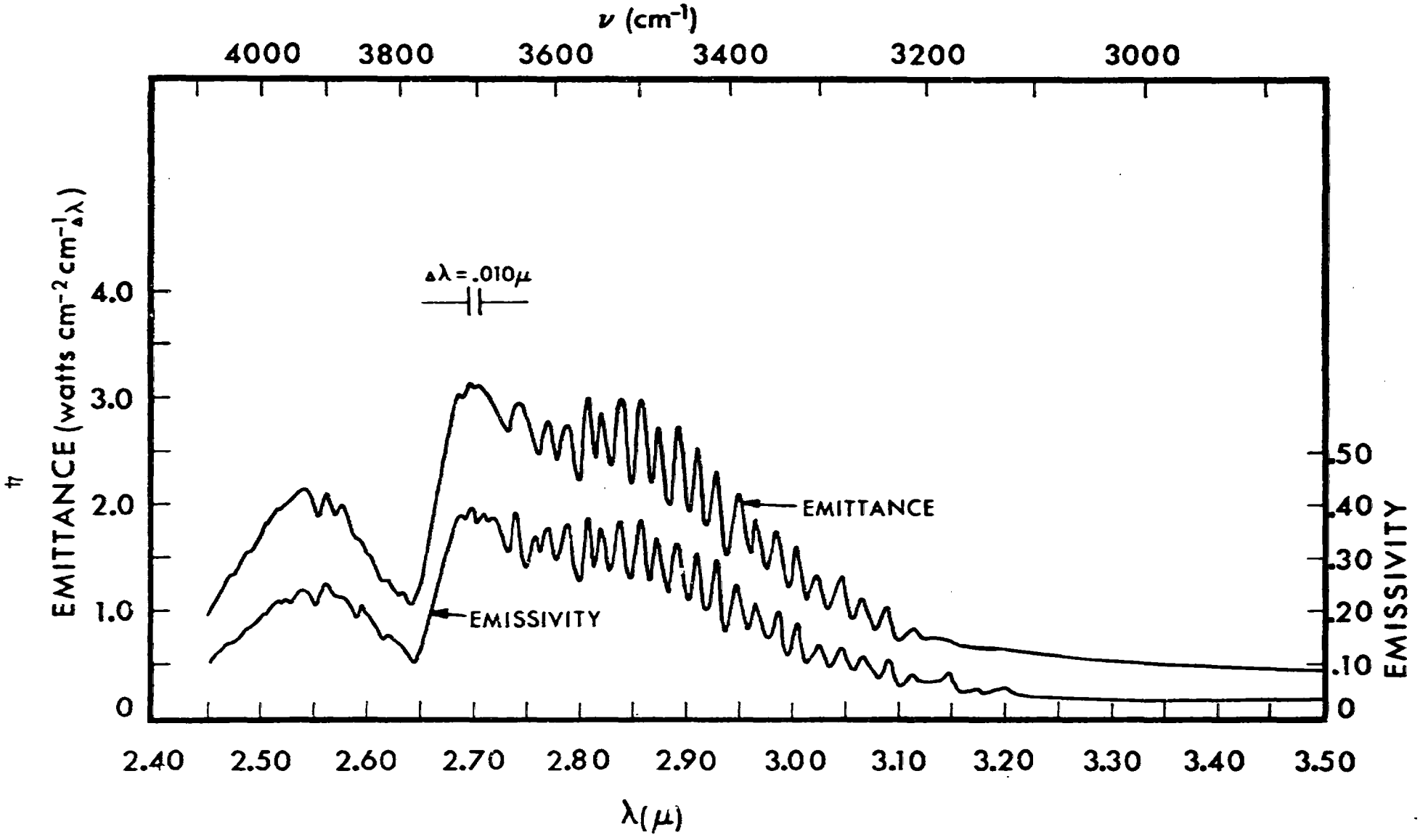

Fig. 1. Typical spectral emittance and spectral emissivity plots for a flame. These curves were obtained from measurements of emission and absorption of a 5-inch diameter methanol-oxygen flame, $5\frac{1}{2}$ inches from the base of the flame.

infrared spectral pyrometer (33), to be used for observing the burning of strands of solid propellants under controlled conditions.

III. PROCEDURE FOR PREDICTING THE RADIANCE OF A MISSILE PLUME

A. General

The radiation measurements outlined in the preceding section are intended for use in predicting missile plume radiation. Methods of prediction were investigated both experimentally and theoretically (31).

The procedure outlined below illustrates how the data obtained from this project may be utilized. The procedure is constantly undergoing improvement as we improve our knowledge of this subject. An experimental example, for a H_2-O_2 rocket at pressures corresponding to altitudes above 10^5 feet, is given in reference 32. For simplicity, only the undisturbed cone of the missile plume was considered in that example; however, this is not an inherent restriction of the general method.

B. Example of Procedure

Consider the case of Fuel X burning in Rocket Y, where Rocket Y may be an operational missile or a hypothetical case.

Step 1. The extrapolation formula appropriate for Fuel X and related conditions is first chosen. The choice of formula is based on previous analyses (31). To simplify this illustration, the Beer-Lambert law will be used*. The choice of formula determines the constants required. In the case of the Beer-Lambert law, only one constant is needed, the absorption coefficient k_λ. The explicit formula is

$$\epsilon_\lambda = 1-e^{-k_\lambda \rho \ell} \quad , \qquad (1)$$

where ϵ_λ is the spectral emissivity at wavelength λ, k_λ is the absorption coefficient, ρ is the density of infrared-active gas and ℓ is the optical path length.

---

* In practice, the Beer-Lambert law is useful mainly as a first approximation.

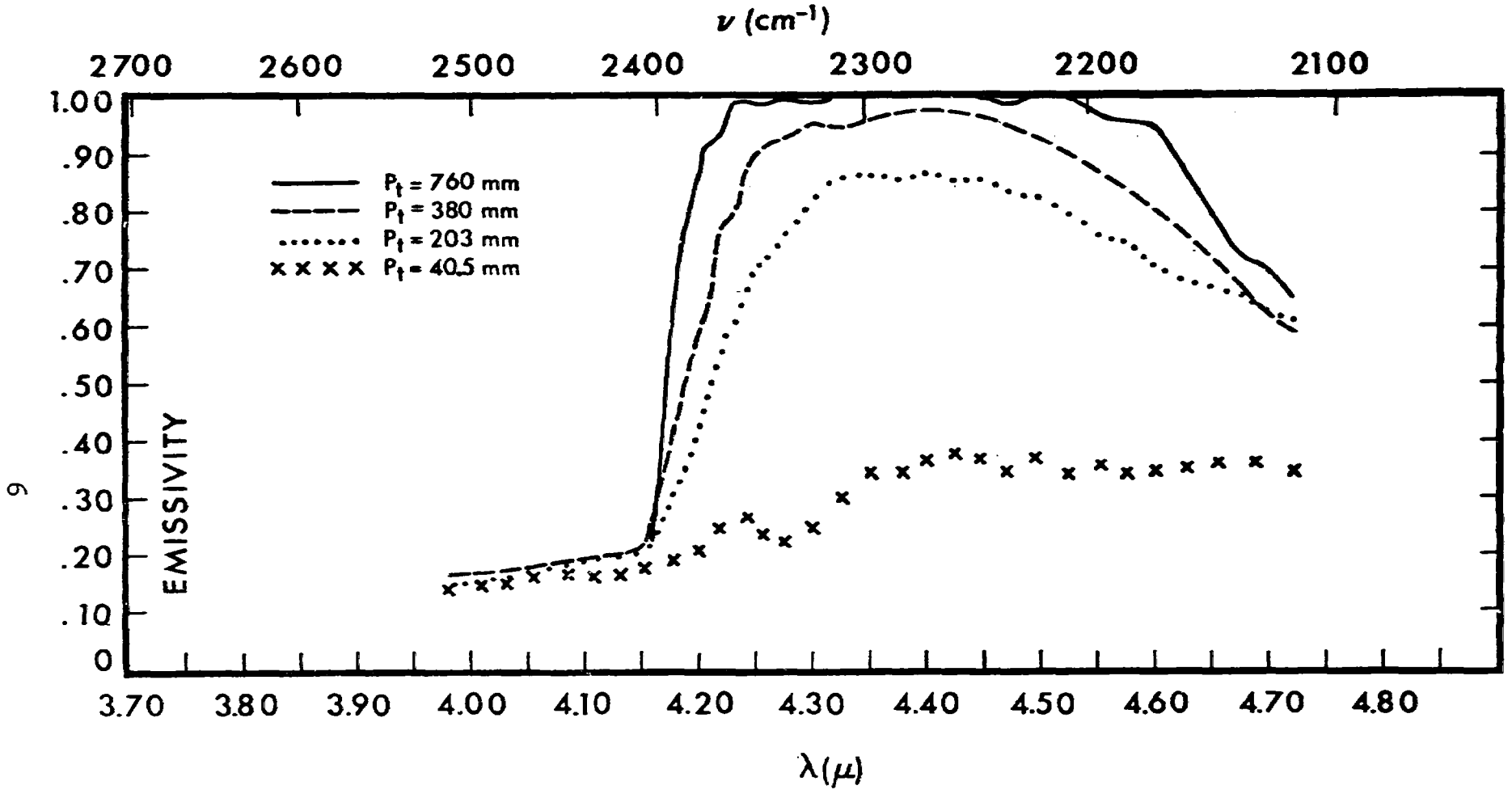

Fig. 2. Emissivity of a kerosene-oxygen flame 11" from nozzle at various pressures. 4.0 – 4.8-μ. O/F = 4.18.

Step 2. The infrared emission and absorption spectra of the flame burning Fuel X are measured in the laboratory. From the spectral data, the emissivity ϵ_λ and flame temperature T are determined and plotted vs λ (22). The absorption coefficient k_λ is then calculated from Eq. (1), for each wavelength of interest.

Step 3. The values of p and ℓ for Rocket Y are now determined by the usual methods (32). In general prediction studies, a series of values of p and ℓ can be used as input data, to obtain curves of plume radiation as a function of missile parameters.

Step 4. Substituting the absorption coefficient k_λ, determined from the laboratory measurements (Step 2) and the values of p and ℓ (Step 3) back into Eq. (1), we compute the plume emissivity ϵ_λ. The calculation is carried out for as many wavelengths as desired.

Step 5. To calculate the spectral radiance of the rocket plume, the calculated emissivity of the plume (Step 4) is combined with the temperature of the flame T, determined from the laboratory measurements (Step 2). The equation used is

$$N_\lambda(T) = \epsilon_\lambda N_\lambda{}^b(T) \quad , \qquad (2)$$

where N_λ is the plume radiance, ϵ_λ is the emissivity, determined from the above procedure, and $N_\lambda{}^b(T)$ is the Planck radiation function at temperature T. Values of the Planck radiation function are readily available from handbooks or radiation slide rules.

C. Improved Extrapolation Procedures

The Beer-Lambert law, used in the above example, is admittedly inadequate as a general extrapolation formula. In order to improve this situation, the following basic studies were carried out. This work is described in reference 31.

1. Line width studies

Spectra of pure gas samples were measured at room temperature and at temperatures up to 1300°K in an electric furnace. The first purpose of this work was to determine width of spectral lines in the infrared spectra of flame combustion products, and to aid in evaluation of various models of infrared bands for practical application.

2. Molecular population distributions and transition probabilities

Population factors were calculated and tabulated in order to provide a basis for calculating infrared emission of flames from fundamental constants, and also as an aid in extrapolating from laboratory measurements to field conditions.

3. Absorption laws

Various absorption laws and extrapolation formulae were studied both theoretically and in relation to the measurements mentioned above, in order to provide data and techniques for extrapolating from laboratory data to systems of different chemical and physical properties from those studied in the laboratory.

4. Thermochemical relations

Equilibrium compositions of flames were calculated from thermochemical data, based on temperatures determined from the infrared spectral measurements. These measurements are applicable to calculation of the energy distributions in the gas and the concentration of each radiating species present.

5. Instrumental distortion

The effect of spectral resolving power on the infrared measurements was studied both experimentally (31) and analytically (28). It was found that correction for this effect can be made in many cases even if the transmission function of the infrared instrument is unknown.

IV. FIELD CHECK OF EXTRAPOLATION OF INFRARED EMISSIVITIES

Rocket exhaust temperatures and emissivities were measured under simulated altitude conditions (32). The test program was conducted at the Rocket Test Facility, Arnold Center, Tennessee, with the cooperation of ARO, Inc., operator of the Arnold Center. The tests were conducted on May 9 and 10, 1961.

Infrared spectral emission and absorption of the exhaust plume of a hydrogen-oxygen rocket engine were measured, as a check on extrapolations from laboratory flame measurements. Firings were made in an altitude test chamber under conditions simulating altitudes from 96,000 to 145,000 feet. Exhaust gas temperatures and emissivities were determined from the infrared spectral measurements. Laboratory measurements of hydrogen-oxygen flame emissivities

were extrapolated to the conditions of the rocket engine tests. The measured results verified the extrapolation within the range of error determined by experiment and by limitations of the extrapolation procedure.

It was concluded that the results support the extrapolation from laboratory flame measurements, and that refinement of both theory and experiment are required to improve accuracy. The tests also demonstrated the utility of the infrared technique and instrumentation for measuring gas temperatures in rocket engines.

V. CONCLUSION

A three-part program has been carried out to provide basic data for prediction of missile plume radiation. The three parts of the program were (1) measurement of laboratory flame radiation, (2) extrapolation from laboratory flames to rocket exhaust plumes, (3) a controlled field test of the extrapolation. The results obtained have confirmed the utility of this approach, and indicated where refinement is needed.

Additional work is planned, to obtain data on a greater variety of fuel-oxidizer combinations, and to improve the extrapolation procedures. During the next phase of work, emphasis will shift from liquid to solid propellant radiation.

The gross characteristics of missile plume radiation are similar to those of radiation from other flame sources. Accordingly, it appears desirable to focus attention on those detailed characteristics, such as spectral energy distribution and flame temperature profile, which are likely to be most helpful in providing unique characterization of a rocket exhaust as against other similar radiation sources. This is a basic practical reason for trying to achieve complete, quantitative understanding of the processes of flame radiation. The achievement of this aim is the long range goal of the present work.

VI. ACKNOWLEDGEMENTS

E. T. Liang was mainly responsible for construction and operation of the experimental burners used in this work. The infrared instrumentation was designed and set up by S. A. Dolin. L. R. Ryan and S. Gillman performed the laborious tasks of spectrum recording and data reduction,

and P. M. Henry assisted in spectroscopic analysis.

The authors are also indebted to Dr. A. G. Gaydon, Dr. W. S. Benedict, and Mr. G. A. Hornbeck, for invaluable discussions and criticisms.

VII. PUBLICATIONS AND REPORTS PREPARED UNDER CONTRACT AF19(604)-6106

The following reports and publications were prepared wholly or in part with the support of this contract:

A. Papers Published (reprints attached)

R. H. Tourin, J. Opt. Soc. Am. 51, 175 (1961). Measurements of Infrared Spectral Emissivities of Hot Carbon Dioxide in the 4.3-μ Region.

H. J. Babrov, J. Opt. Soc. 51, 171 (1961). Instrumental Effects in Infrared Gas Spectra and Spectroscopic Temperature Measurements.

R. H. Tourin, Temperature, Its Measurement and Control in Science and Industry, Vol. III, C. M. Herzfeld, ed. (Reinhold, New York, 1962), Part 2, Ch. 46. Monochromatic Radiation Pyrometry of Hot Gases, Plasmas, and Detonations.

R. H. Tourin, J. Opt. Soc. Am. 51, 799 (1961). Spectral Emissivities of Hot CO_2-H_2O Mixtures.

R. H. Tourin, Infrared Physics 1, 105 (1961). Infrared Spectral Emissivities of CO_2 in the 2.7-μ Region.

R. H. Tourin, J. Opt. Soc. Am. 51, 1225 (1961). Some Spectral Emissivities of Water Vapor in the 2.7-μ Region.

B. Papers Read at Meetings

R. H. Tourin, Fourth Symposium on Temperature (Columbus, Ohio, March 1961), Paper No. B11.3. Monochromatic Radiation Pyrometry of Hot Gases, Plasmas, and Detonations.

H. J. Babrov and P. M. Henry, Symposium on Molecular Structure and Spectra (Columbus, Ohio, June 1961). Paper #M3. Experiments on the Applicability of the Beer-Lambert Absorption Law to the Spectra of Hot CO_2 and H_2O.

H. J. Babrov, G. Ameer, and W. Benesch, Symposium on Molecular Structure and Spectra (Columbus, Ohio, June 1960). Paper #F7. Collision Cross Sections from Measurements of the Infrared Absorption of Molecular Lines.

C. Contract Scientific and Technical Reports

L. R. Ryan, G. J. Penzias, and R. H. Tourin, AFCRL-848, Geophysics Research Directorate, Hanscom Field, Bedford, Mass. (1961). An Atlas of Infrared Spectra of Flames. Part One. Infrared Spectra of Hydrocarbon Flames in the 1 – 5-μ Region.

G. J. Penzias, S. Gillman, E. T. Liang, and R. H. Tourin, AFCRL- , Geophysics Research Directorate, Hanscom Field, Bedford, Mass. (1961). An Atlas of Infrared Spectra of Flames. Part Two. Hydrocarbon-Oxygen Flames 4 – 15-μ, Ammonia-Oxygen 1 – 15-μ, Hydrazine-Oxygen 1 – 5-μ, and Flames Burning at Reduced Pressures.

H. J. Babrov, P. M. Henry, and R. H. Tourin, AFCRL- , Geophysics Research Directorate, Hanscom Field, Bedford, Mass. (1961). Methods for Predicting Infrared Radiance of Flames by Extrapolation from Laboratory Measurements.

S. A. Dolin, G. J. Penzias, and R. H. Tourin, AFCRL-881, Geophysics Research Directorate, Laurence G. Hanscom Field, Bedford, Mass. (1961). Determination of Rocket Exhaust Gas Temperatures and Emissivities by Infrared Spectral Methods.

APPENDIX I.

NOTE ON APPLICATION OF INFRARED FLAME RADIANCE DATA

The measurements described in this report were made to provide basic information on flame processes as they relate to infrared radiance. The information obtained is to be applied to development of system parameters and limitations of infrared early warning systems. Although these developments are not part of the present project, it may be helpful to point out some possibilities for the use of absolute spectral intensity and spectral energy distributions as system parameters.

In principle, the techniques for identifying a hot gas target from its spectrum are known, and are used in analytical infrared absorption spectroscopy. However, the standard techniques are insufficient in the present application, because the characteristics usually used to identify chemical compounds (e.g. group frequencies) are rather sparse in flame spectra, and are similar for a wide variety of different cases. For example, all hydrocarbon combustion gases show the characteristic CO_2 and H_2O bands. Accordingly, more subtle distinctions between spectra must be sought. For example, "hot" bands occur in the spectra of flames, and the relative spectral intensities observed depend upon temperature and upon characteristics of the fuel and oxidizer used; also shapes and widths of spectral lines vary with temperature and pressure.

Figure 3 illustrates some possibilities for utilizing spectral data in infrared early warning systems. The output of a wavelength scanning device is fed into a Wiener filter network. The feedback loop adjusts the wavelength response of the Wiener filter, proportional to

$$S(\lambda)/\ (S(\lambda)+N(\lambda))\qquad ,$$

where $S(\lambda)$ is the signal and $N(\lambda)$ the background radiation; thus optimizing the signal response. This "suppresses" the random noise and non-periodic signals, and the output is in the form of a series of varying amplitude pulses at prescribed wavelength values. This principle permits low intensity detail to be picked up out of the noise.

The output of the Wiener filter is fed into a synchronous multiplier, which is part of a cross-correlation network. The purpose of this network is to minimize electronic noise and further suppress non-periodic signals, without altering the signal wave shape. The principles of cross-correlation are well known; in practice it provides

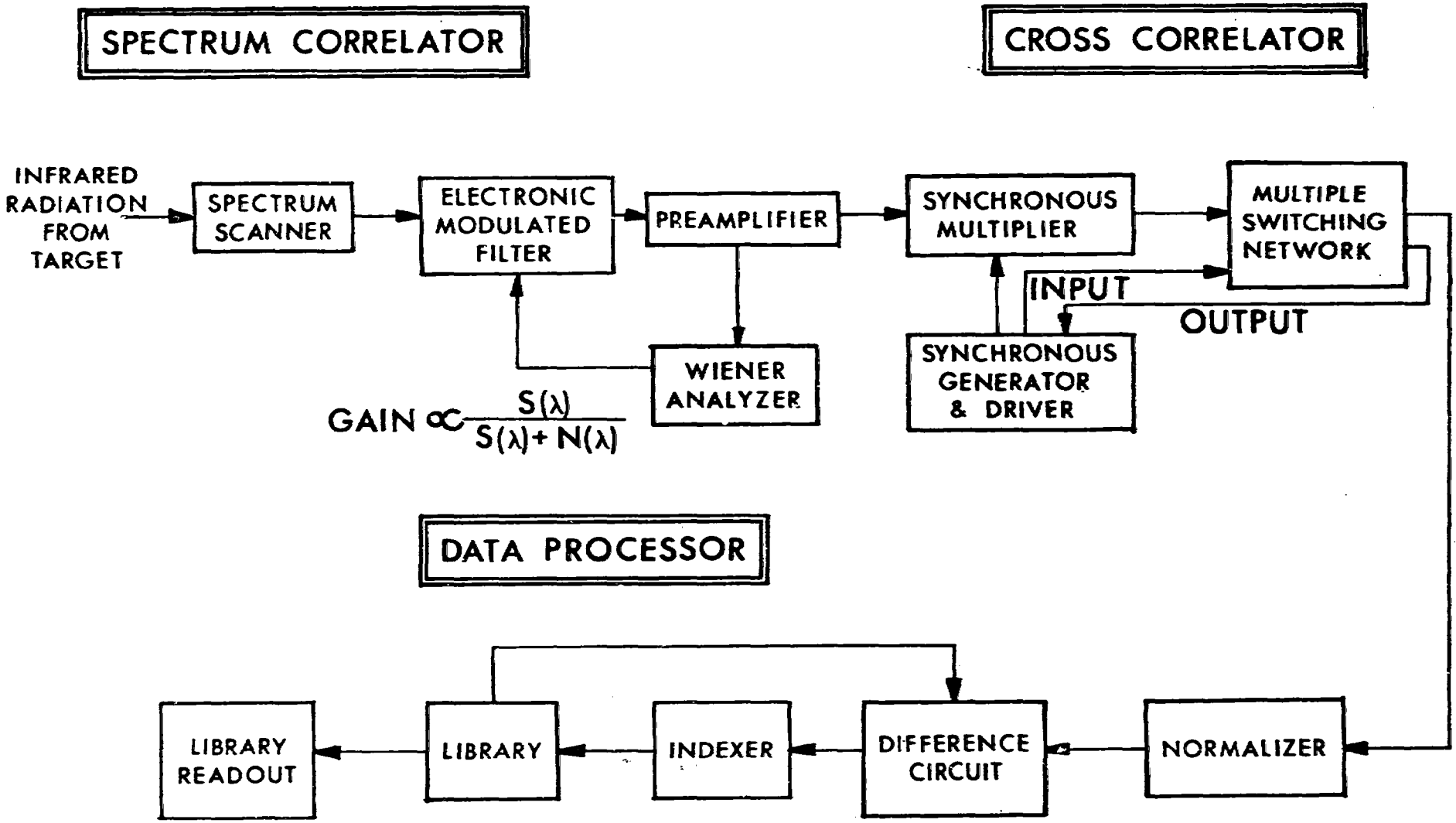

Fig. 3. Schematic diagram of infrared spectral correlation and identification system.

for integration, thus reinforcing only periodic signals.

The resultant pulses from the cross-correlation network are fed into a normalizer that adjusts the peak amplitude to a predetermined height, so that it can be compared to a library of spectral data. The library data are obtained from laboratory flame measurements. The comparison continues between the unknown and the library until a match is obtained. The identification is then complete and may be indicated in terms of a recorder trace or coded output.

APPENDIX II.

NOTE ON POSSIBLE EFFECTS OF FUEL ADDITIVES ON INFRARED RADIATION OF FLAMES

The addition of foreign substances to the fuel to suppress the infrared radiation from flames, or to change the character of the infrared spectrum, is suggested by the well known results of such additions upon spectra in the visible and ultraviolet. Small amounts of metallic salts, for example, can cause very large and striking changes in the appearance of the visible radiation of a flame.

No adequate experimental or theoretical evidence is available to indicate that the molecular infrared radiation of flames can be suppressed to a significant degree by small amounts of fuel additives. The available experimental data bearing on this point were obtained primarily from rocket motor observations. The lack of known, controlled conditions and the large experimental uncertainties inherent in these measurements, as well as inadequate theoretical background, make the results inconclusive. Carefully controlled laboratory experiments on the effects of additives on infrared spectra of flames, coupled with a quantitative study of radiation mechanisms, would be of value.

In considering possibilities for suppression of infrared radiation from flames, it is essential to distinguish between the continuous infrared spectrum and the discontinuous molecular band spectrum. The latter is an intrinsic property of hot polyatomic and heteronuclear diatomic gases. The continuous spectrum in liquid propellant combustion is largely due to inefficient combustion and we may expect it to be reduced substantially on the basis of future improvements. In the case of solid rockets, it is reasonable to assume that the continuous spectrum will always play an important role, because the materials added to the solid fuel matrix to increase thrust are such as to necessarily increase the infrared radiation also.

The large variation in transition probabilities for different types of radiation is likely to be a key factor in the question of suppressing radiant emission of hot sources. Atomic resonance lines in the visible and ultraviolet spectrum, such as those of the alkali metals, have very high transition probabilities, of the order of $10^{8} sec^{-1}$. As a result, a relatively small number of atoms can emit or absorb a large amount of radiation. Molecular transition probabilities for infrared radiation, on the other hand, are much smaller, by a factor of perhaps 10^{-5}. Since the strength of radiation effects (emission or absorption) is roughly proportional to the product: transition probability X particle population, the bulk of material required to

produce in the infrared an effect equivalent to that produced in the visible spectrum by a given quantity of, say, sodium is 10^5 times the corresponding quantity of sodium.

There is certainly no direct way to reduce the infrared radiation from hot polyatomic and heteronuclear diatomic gases, except by cooling. Due to the intrinsic thermal nature of infrared radiation from a hot gas, any appreciable change in the radiant power emitted corresponds to a change in temperature and consequently in heat transfer. In a rocket engine, changes in heat transfer conditions may entail significant changes in rocket performance.

It is possible to shift the spectral distribution of flame radiation, without necessarily an overall reduction in radiant power, by changing the fuel composition. However, a very large change in exhaust gas composition is required to change infrared spectral distribution appreciably, because of the small effect per particle (low transition probability). A change in temperature distribution in a flame will also change the spectral energy distribution, but this cannot be accomplished merely by adding materials to the fuel, since the temperature distribution is a function of the rocket nozzle configuration.

Another possibility is the use of catalysts, to hasten the reaction of radiating species in the exhaust. This does not apply to most infrared radiation, since nearly all this radiation comes from unreactive end products of combustion. It might be applied to the more chemically active radiators, such as HCl and HF, which would result in production of more radiation from some other molecule, e.g., H_2O.

Other methods than fuel additives to reduce the radiation of rocket exhausts may be imagined. Some monopropellants theoretically yield only homonuclear diatomic gases as combustion products, and these have no infrared spectra. One can also imagine various schemes for shielding the infrared radiation of a rocket plume. For example, the exhaust might be surrounded by shields of very low emissivity material, or the heat of combustion could be liberated in a heat exchanger, which would then eject a stream of homonuclear diatomic exhaust gas, without an infrared spectrum.

In sum, the infrared spectrum of a ballistic missile exhaust plume is, and may be expected to remain, an intrinsic characteristic of the missile system. Controlled experiments and detailed theoretical analysis would doubtless be helpful in clarifying this subject.

REFERENCES

1. Private communications from S. S. Ballard, J. N. Howard, E. Welmers, G. J. Zissis, and others. Also various articles in Proceedings of IRIS, 1957-61.

2. Statement of Work, Contract AF19(604)-6106.

3. J. A. Sanderson (in AF memorandum by J. N. Howard, April 1957); R. H. Tourin, Warner & Swasey Proposal No. Q401.1, April 1958; S. S. Penner, Symposium on Quantitative Spectroscopy, Pasadena, California, March 1960.

4. S. Silverman, G. A. Hornbeck, and R. C. Herman, J. Chem. Phys. 16, 155 (1947). The Infrared Emission and Absorption of the Carbon Monoxide-Oxygen Flame.

5. E. K. Plyler, J. Research Natl. Bur. Stds. 40, 113 (1948). Infrared Radiation from a Bunsen Flame.

6. E. K. Plyler and C. J. Humphreys, J. Research Natl. Bur. Stds. 40, 449 (1948). Infrared Emission Spectra of Flames.

7. E. K. Plyler and C. J. Humphreys, J. Research Natl. Bur. Stds. 42, 567 (1949). Flame Spectrum of Acetylene from 1 to 5-μ.

8. S. Silverman, J. Opt. Soc. Am. 39, 275 (1949). The Determination of Flame Temperatures by Infrared Radiation.

9. S. Silverman and R. C. Herman, J. Opt. Soc. Am. 39, 216 (1949). The Infrared Emission Spectra of the Oxy-Hydrogen and Oxy-Deuterium Flames.

10. E. K. Plyler and J. J. Ball, J. Chem. Phys. 20, 1178 (1952). Infrared Emission Spectra of OH, CO, and CO_2 from 3 to 5.5-μ.

11. J. H. Taylor, W. S. Benedict, and J. Strong, J. Chem. Phys. 20, 1884 (1952). Infrared Spectra of H_2O and CO_2 at 500°C.

12. R. H. Tourin, J. Chem. Phys. 20, 1651 (1952). Infrared Spectra of Thermally Excited Gases.

13. R. H. Tourin, Natl. Bur. Standards Circ. No. 523, p. 87 (1954). Infrared Spectra of Thermally Excited Gases.

14. A. G. Gaydon, The Spectroscopy of Flames (John Wiley, New York, 1957).

15. G. A. Hornbeck and L. O. Olsen, WADC Tech. Rept. 57-516 (1957). Emission and Absorption Studies of Jet Engine Hydrocarbon Combustion Products.

16. R. H. Tourin, Combustion and Flame 2, 353 (1958). Spectroscopic Studies on Temperature Gradients in Flames.

17. R. H. Tourin and P. M. Henry, AFCRC-TN-59-262, Geophysics Research Directorate, Hanscom Field, Bedford, Mass., 1958. Infrared Spectral Emissivities and Internal Energy Distribution of Carbon Dioxide at High Temperatures. Part I. Internal Energy Calculations.

18. R. H. Tourin and P. M. Henry, AFCRC-TR-60-203, Geophysics Research Directorate, Hanscom Field, Bedford, Mass., 1959. Infrared Spectral Emissivities and Internal Energy Distributions of Carbon Dioxide and Water Vapor at High Temperatures.

19. H. W. Neill, J. Opt. Soc. Am. 49, 505A (1959). Measurements of the Self Absorption of Carbon Dioxide in the 4.3-μ Band.

20. R. H. Tourin and P. M. Henry, J. Opt. Soc. Am. 49, 512 (A) (1959). Infrared Spectral Emissivities and Vibrational Energy Distribution of Water Vapor at High Temperatures.

21. E. E. Bell, P. B. Burnside, and F. P. Dickey, J. Opt. Soc. Am. 50, 1286 (1960). Spectral Radiance of Some Flames and Their Temperature Determination.

22. L. R. Ryan, G. J. Penzias, and R. H. Tourin, AFCRL-TR-848, Geophysics Research Directorate, Hanscom Field, Bedford, Mass., 1961. An Atlas of Infrared Spectra of Hydrocarbon Flames. Part One.

23. G. J. Penzias, S. Gillman, E. T. Liang, and R. H. Tourin, AFCRL-[illegible](I)Geophysics Research Directorate, Hanscom Field, Bedford, Mass. (1961). An Atlas of Infrared Spectra of Flames. Part Two.

24. R. H. Tourin, J. Opt. Soc. Am. 51, 175 (1961). Measurements of Infrared Spectral Emissivities of Hot Carbon Dioxide in the 4.3-μ Region.

25. R. H. Tourin, Infrared Physics 1, 105 (1961). Infrared Spectral Emissivities of CO_2 in the 2.7-μ Region.

26. R. H. Tourin, J. Opt. Soc. Am. 51, 799 (1961). Spectral Emissivities of Hot CO_2-H_2O Mixtures in the 2.7-μ Region.

27. R. H. Tourin, J. Opt. Soc. Am. 51, 1225 (1961). Some Spectral Emissivities of Water Vapor in the 2.7-μ Region.

28. H. J. Babrov, J. Opt. Soc. Am. 51, 171 (1961). Instrumental Effects in Infrared Gas Spectra and Spectroscopic Temperature Measurements.

29. H. J. Babrov and P. M. Henry, Symposium on Molecular Structure and Spectroscopy (Columbus, Ohio, 1961). Experiments on the Applicability of the Beer-Lambert Absorption Law to the Spectra of Hot CO_2 and H_2O.

30. R. H. Tourin, Temperature, Its Measurement and Control in Science and Industry, Vol. III, C. M. Herzfeld, ed., Part II, Ch. 46 (Reinhold, New York, 1962). Monochromatic Radiation Pyrometry of Hot Gases, Plasmas, and Detonations.

31. H. J. Babrov, P. M. Henry, and R. H. Tourin, AFCRL- , Geophysics Research Directorate, Hanscom Field, Bedford, Mass. (1961). Methods for Predicting Infrared Radiance of Flames by Extrapolation from Laboratory Measurements.

32. S. A. Dolin, G. J. Penzias, and R. H. Tourin, AFCRL-881, Geophysics Research Directorate, Laurence G. Hanscom Field, Bedford, Mass. (1961). Determination of Rocket Exhaust Gas Temperatures and Emissivities by Infrared Spectral Methods.

33. R. H. Tourin, M. L. Hecht, and S. A. Dolin, J. Opt. Soc. Am. 50, 1129 (A) (1960). High Speed Monochromatic Radiation Pyrometer for Measurement of Detonation Gas Temperatures.

34. W. S. Benedict and E. K. Plyler, Natl. Bur. Stds. Circular #523, 64 (1954). High-Resolution Spectra of Hydrocarbon Flames in the Infrared.

Monochromatic Radiation Pyrometry of Hot Gases, Plasmas, and Detonations

Richard H. Tourin

The Warner & Swasey Company, Control Instrument Division
32-16 Downing Street, Flushing 54, New York

(Reinhold Publishing Corp., New York, 1962)

Presented at the Fourth Symposium on Temperature
Its Measurement and Control in Science and Industry,
Columbus, Ohio, March 29, 1961

Sponsored by the American Institute of Physics,
National Bureau of Standards,
and
Instrument Society of America

CONTENTS

MONOCHROMATIC RADIATION PYROMETRY OF HOT GASES, PLASMAS, AND DETONATIONS*

Richard H. Tourin

ABSTRACT

Techniques of infrared monochromatic radiation (IMRA) pyrometry have been developed to measure the high temperatures encountered in hot gases, such as flames and plasmas. Hot gases generally radiate heat only at certain characteristic infrared wavelengths which are determined by the structure of the gas molecules. As a result, the familiar T^4 radiation law of Stefan-Boltzman — based on the assumption of a continuous blackbody or graybody spectrum — is inapplicable to gases, and a different principle is required. The IMRA method, like optical pyrometry, is based on the radiation laws of Planck and Kirchhoff, which relate it to the International Temperature Scale. But it differs from optical pyrometry in at least three respects: (1) the wavelength used for measurement must be selected from among the characteristic infrared wavelengths of the gas; (2) it is not necessary, and usually not possible, to match the spectral brightness of a standard to the spectral brightness of the hot gas; (3) the assumption of constant emissivity is untenable for gases, and the infrared spectral emissivities of the gas must be determined explicitly from its infrared absorption spectrum. The IMRA method is adaptable to direct recording of gas temperatures. No spectroscopic analysis is involved, although spectroscopic instrument techniques are used. Moderate spectral resolution is adequate; spectral resolution does not affect the measurements significantly.

The IMRA method has been applied to measurement of gas temperatures in flames, combustion exhaust gases, plasmas, and transient combustion waves. Steady-state temperatures have been measured, as well as temperature transients having duration of the order of a millisecond. Representative instrumentation and results are described. The IMRA-measured temperatures, when plotted against wavelength, reflect the temperature gradient across a flame. Good agreement was obtained between measurements made in the 2.7-μ bands of H_2O and the 4.3-μ band of CO_2. An experimental comparison was made between IMRA and thermocouple temperature measurements. This showed that accuracy of $\pm 1\%$ in temperature is achievable.

---

* Supported in part by Advanced Research Projects Agency and U. S. Air Force, through Geophysics Research Directorate, Bedford, Massachusetts, and Aeronautical Research Laboratories, Wright Field, Ohio.

I. INTRODUCTION

High gas temperatures are difficult to measure with thermocouples and other immersion-type temperature sensors. At the higher temperatures of combustion flames and plasmas, the use of temperature probes to sense the gas temperature becomes impracticable. Determination of gas temperatures from the heat radiation they emit is a natural alternative to immersion devices. A radiation pyrometer measures temperature without being in contact with the hot body, and its temperature measuring range has no upper limit. Since the measurement is based upon use of the natural infrared radiation emitted by the hot gas, it is unnecessary to add anything to the gas for measurement purposes, and it is immaterial whether the gas is luminous or not. Since no probe is used, the measurement is uninfluenced by gas velocity, and one measures the static temperature.

Gas radiation pyrometry is quite different from radiation pyrometry of solids and melts, because the radiation emitted by hot gases is of a different spectral character from the emission of a hot solid or melt. The solid or melt emission is typically a continuous spectrum, similar to the spectrum of a blackbody radiator[1,2]. The emission spectrum of a hot gas, on the other hand, is discontinuous, consisting of narrow emission bands at a few infrared wavelengths, with no emission at other wavelengths[3,4,5,6]. As a result, conventional radiation pyrometry, based on the familiar T^4 law of Stefan-Boltzmann[1], is not applicable to gases, and a different principle of temperature measurement must be used.

The infrared monochromatic radiation (IMRA) method of gas pyrometry was first suggested by Schmidt[7] in 1909. After forty years of relative obscurity, the method was revived in modified form, with the aid of modern infrared techniques[8,9,10,11,12]. The IMRA method is similar in principle to conventional optical pyrometry[13], but is considerably different in detail. The principles of monochromatic radiation pyrometry, and some results achieved by its use for gas temperature measurement are discussed in this paper. The methods described are intended for practical pyrometry, where direct indication of gas temperature is desired. Spectroscopic methods of gas temperature measurement, which are based on detailed analysis and theoretical interpretation of the emission spectra of hot gases, have been described elsewhere[14,15,16,17].

II. PRINCIPLES OF MEASUREMENT

A. Characteristics of Hot Gas Radiation

Before discussing temperature measurement by radiation, let us first consider the nature of radiation emitted by hot gases. Figure 1 shows schematically an emission spectrum of an

ideal blackbody radiator and the emission spectra of some typical molecules found in hot combustion gases and flames. As shown by Fig. 1, gas radiation, as well as most blackbody radiation, is emitted at wavelengths in the infrared region of the electromagnetic spectrum. The significant feature of radiation from solids is the fact that the emission spectrum of a solid is continuous; that is, heat energy is emitted from the hot object at all wavelengths throughout the spectrum. The emission of solids (and liquids) is continuous because the strong coupling of the particles (atoms, ions, or molecules) causes the individual particle vibration frequencies to be "smeared out"[18]. In this respect solid radiation is similar to blackbody radiation. The emission of a gas, on the other hand, consists of a few narrow bands scattered over the infrared spectrum; i.e. the emission spectrum of a gas is essentially discontinuous. The wavelengths at which gas radiation occurs correspond to the characteristic internal vibration frequencies of the gas molecules.

At temperatures up to about 3000°K, polyatomic molecules are plentiful in combustion gases, and are the chief contributors to gas radiation. CO_2 and H_2O predominate in hydrocarbon flames and combustion gases[3,4]. At temperatures above 3000°K, polyatomic molecules become scarce, due to dissociation, but diatomic molecules are common. For example, ordinary air, when heated to temperatures between 3000°K and 10,000°K, radiates in the infrared due to formation of molecules of NO[19,20]. At still higher temperatures, found in arc-heated plasmas, there is infrared radiation from atoms and possible from "abnormal" molecules like Ar_2.

Flames and combustion gases always emit their characteristic discontinuous infrared radiation. In some cases, flames exhibit a continuous radiation spectrum in addition. The continuous spectrum of a sooty hydrocarbon flame, for example, is the graybody emission of suspended carbon particles. As a rule, the continuous spectrum cannot be depended upon to occur, and is therefore of limited value for gas temperature measurement. In this paper, we consider only the always-present infrared band spectrum of the gas itself. Continuous spectra in plasmas have a different origin; these continua do not generally follow the Planck curve[21]. Plasma continua will not be discussed in this paper.

Fully combusted exhaust gases are essentially nonluminous, i.e. they show no emission in the visible part of the spectrum. In the reaction zone of a flame, and in plasmas, visible and ultraviolet radiation are observed in addition to infrared radiation. Even in such cases, it is usually desirable to use the infrared radiation of the gas for temperature measurement purposes, to be sure of obtaining a true equilibrium temperature. This point is elaborated upon later.

B. The Infrared Monochromatic Radiation Method

The intensity of radiation emitted by a hot gas depends upon the gas temperature and upon the number of gas molecules or atoms contributing to the radiation. In addition to measuring the radiant emission of the gas, we must account for the effect of the quantity of gas radiating, in order to determine gas temperature. This can be done by the well-known technique of infrared absorption spectroscopy[22], in which an infrared radiation beam of known intensity is sent through the gas, and its loss of intensity measured. The fraction of beam energy lost in the gas at a particular wavelength depends upon the number of gas particles which emit and absorb energy at that wavelength. This fraction is the spectral absorptivity of the gas, which is equal to its spectral emissivity[1]. Knowing the gas spectral emissivity, as well as the gas spectral emission, at a particular infrared wavelength, we can readily determine the gas temperature. It is apparent that the spectral emissivity of a gas is a function of the gas density and of the length of optical path over which the measurement is made. Unlike the case of solids and melts, gas emissivity is not a surface phenomenon. Accordingly, gas spectral emissivity must be measured explicitly each time we desire to measure temperature; gas spectral emissivities are not unique for a given gas molecule and hence cannot be tabulated for use in temperature measurement*.

Figure 2 illustrates the principle of monochromatic radiation pyrometry for gas temperature measurement. The source of infrared radiation to the left of the flame emits a primary radiation beam of constant, but arbitrary, intensity $I_o(\lambda)$ at wavelength λ. This primary radiation, represented by the barred arrow to the left of the flame, is sent through the flame towards the radiation detection system. The convergence of the Source beam through the flame in Fig. 2 represents the attenuation of the beam by absorption in the flame. The transmitted beam is represented by the upper portion of the double arrow to the right of the flame. Added to this transmitted radiation is the radiation $I_g(\lambda)$ from the flame itself, represented by the lower portion of the double arrow. Both of these radiation beams are sent through an infrared monochromator, symbolized by the prism, which is set to transmit only radiation in a narrow band at wavelength λ. The wavelength λ is selected from the spectrum of emission bands which were discussed previously. The radiation transmitted by the monochromator at a narrow wavelength band,

---

* The spectral absorption coefficient, related to the spectral emissivity through the Beer-Lambert law, is a unique constant for a given molecule. However, spectral absorption coefficients are of little value for gas temperature measurement, because the Beer-Lambert law is usually invalid for gases[6,23,24].

consisting of contribution $I(\lambda)$ from the reference source, attenuated by the gas, and contribution $I_g(\lambda)$ from the gas, is sensed by the infrared detector. This detector may be a photocell, bolometer, or other detector, depending upon the wavelength range being used. The output of the radiation detector is stepped up by an amplifier and sent to the computer. The computer computes the ratio of the spectral emission of the gas to the spectral emissivity of the gas, corresponding to the two radiation signals. This ratio is equal to the Planck radiation function, which gives the temperature of the gas on the International Temperature Scale[2]. The instrument is calibrated by reference to the blackbody standard at one convenient temperature.

The necessary mathematical relationships are simple, and are easily derived. The transmitted source intensity $I(\lambda)$ at wavelength λ is equal to the primary intensity $I_o(\lambda)$ times the fraction of $I_o(\lambda)$ remaining after absorption in the gas, or

$$I(\lambda) = I_o(\lambda)(1-a_g(\lambda)) \quad , \qquad (1)$$

where $a_g(\lambda)$ is the spectral absorptivity of the gas, i.e., the fraction of incident radiation which the gas absorbs at wavelength λ. Since the spectral absorptivity $a_g(\lambda)$ at a given wavelength equals the spectral emissivity $e_g(\lambda)$ at the same wavelength[1], we can write

$$I(\lambda) = I_o(\lambda)(1-e_g(\lambda)) \quad , \qquad (2)$$

from which $e_g(\lambda)$ can be readily found, once $I(\lambda)$ and $I_o(\lambda)$ have been measured.

According to Kirchhoff's radiation law[1], the ratio of the gas spectral emission $I_g(\lambda)$, at a particular wavelength, to the gas spectral emissivity $e_g(\lambda)$, at the same wavelength, is equal to the spectral emission of a blackbody at the same temperature, i.e.

$$I_b(\lambda) = I_g(\lambda)/e_g(\lambda) \quad . \qquad (3)$$

The emission of a blackbody is given by the Planck radiation law,

$$I_b = c_1\lambda^{-5}(e^{c_2/\lambda T}-1)^{-1} \quad , \qquad (4)$$

which is the basis for the accepted definition of the temperature scale for temperatures above the gold point (1063°C), as adopted in the International Temperature Scale[25]. Because of this fact, the gas temperatures obtained by IMRA pyrometry are absolute temperatures, and do not require empirical calibration. Planck law curves, of the type shown in Fig. 3, are the calibration curves for IMRA pyrometry. A specific instrument is calibrated by checking against a blackbody radiator at a single convenient temperature, such as the gold point.

It is important to keep in mind that Kirchhoff's law, equation (3), holds for a gas only in a narrow spectral band. The emission and absorption of a gas vary strongly with wavelength, as shown in Fig. 1, and therefore a gas is not only not a blackbody, but is not a gray body either. This is one of the basic reasons for using a monochromatic method. In practice, one measures a narrow band of radiation extending over a wavelength interval $\Delta\lambda$, centered at λ. The results of the measurement are independent of the value of $\Delta\lambda$, within rather broad limits[9,10,24,26].

C. Theoretical Basis of the IMRA Method

The elementary derivation of the IMRA method given above is incomplete from the theoretical standpoint, for a number of reasons, which do not, however, affect the validity and utility of the method. A detailed analysis is beyond the scope of this paper, but a few of the theoretical questions bear mentioning.

The Planck radiation law rests upon the assumption of a continuous distribution of radiation over an infinite frequency range[27], while the radiation spectrum of a gas is, on the contrary, discontinuous and finite. Hence it is not immediately obvious that it is justifiable to apply the Planck law to gases. The use of the Planck law for gases has been justified in the past mainly on empirical grounds[7-12,28]. However, it can be justified theoretically, by detailed analysis of energy exchange processes in a hot gas. It has been shown[29] that the Planck law holds for narrow bands in a discontinuous molecular spectrum, provided that the time constant (relaxation time) for interconversion of vibrational energy and translational energy is much smaller than the radiative lifetime of the spectral emission. This is always true for infrared bands[30,31], with the possible exception of radiation from very fast transients, such as shock waves and detonation waves. The latter are discussed later.

Contrasting to infrared radiation is the case of the very intense ultraviolet and visible bands of molecules, in which the radiative lifetimes are so short that there is often insufficient time for equilibrium to be reached between the radiative and kinetic degrees of freedom. For this reason, the

temperature values obtained from ultraviolet radiation measurements may not be equilibrium temperatures, but may correspond to abnormal excitation of the radiative degree of freedom giving rise to the emission. A well-known example is the ultraviolet emission of the OH radical, found in many combustion flames[32].

The essentially thermal origin of infrared emission bands of flames has been established theoretically by Shuler[33], who showed that there can be no appreciable chemiluminescent contribution to this radiation. The radiation emission process is a small "heat leak", which has negligible effect on the thermal state of the gas. This corresponds to the fact that significant amounts of energy are transferred in flames only by collision processes, rather than radiative processes. The case where radiative energy transfer is appreciable (e.g. in stars) has been discussed elsewhere[34].

III. INSTRUMENTATION AND EXPERIMENTAL RESULTS

A. Instrumentation

Figure 4 is a schematic diagram of an IMRA pyrometer for gas temperature measurement. As shown, the Source and Receiver are disposed opposite one another on either side of the flame. If the flame is small, it may be located at a common focal point of the Source and Receiver. If the flame or gas stream is very large, both the Source and Receiver are focused at infinity. The instrument functions as follows: infrared radiation from the glower G in the Source unit passes through chopper Ch_1, a rotating sector disc operating at a fixed frequency of 90 cycles per second. The resulting pulsed infrared beam is reflected from plane mirror M_1 to spherical mirror M_2. M_2 sends the pulsed beam through the flame to spherical mirror M_3. M_3 collects the steady radiation beam from the flame as well as the pulsed beam from M_2. Radiation collected by M_3 is reflected from plane mirror M_4 to plane mirror M_5. A second chopper Ch_2 is located at a focal point of M_3 between M_4 and M_5. Radiation relayed by M_5 is collected by spherical mirror M_6 and focused on the monochromator. The monochromator may be a prism or grating monochromator or an infrared filter; its function is to select radiation in a narrow wavelength band from the incoming radiation and transmit that narrow band radiation to the infrared detector. The detector converts the radiant energy it receives to an electric signal, which is stepped up by the amplifier and indicated on the recorder.

The reason for using two radiation choppers is to distinguish between the emission and absorption signals, which are measured by a common optical system, detector, and electronic system. To measure radiation from the hot gas, a shutter is interposed in front of the glower G, cutting off radiation from

the Source Unit. Chopper Ch_2 then periodically interrupts the radiation from the hot gas, thus producing an AC signal for the detector. To measure gas absorption, the shutter is removed from in front of the glower, and chopper Ch_1 provides a pulsating beam of radiation from the glower. In this latter mode of operation the chopper Ch_2 does not function. Then the radiation detector will pass on to the electronic system only the pulsating signal from the glower, reduced by absorption in the hot gas. The steady, unchopped radiation coming from the hot gas will not be passed by the AC electronics. In this way one may measure emission or absorption along the same optical path through the flame. An alternative technique is to operate both choppers simultaneously, but at different chopping frequencies. The emission and absorption signals, differing in frequency, can then be separated by frequency discrimination in the electronics, and the two signals indicated separately as before.

For calibration purposes, mirror M_4 can be rotated to illuminate the measuring system with radiation from the blackbody standard B.

A typical IMRA pyrometer is shown in Fig. 5. This instrument is set up to measure temperatures of combustion flames in a closed burner. Corresponding to schematic Fig. 4, the unit to the left of the burner in Fig. 5 is the Source Unit. The unit to the right of the burner is the Receiver Unit. The Recorder and Amplifier unit is located remotely. Figure 6 shows a close-up of the Receiver Unit without cover. The condensing mirror (M_6) and chopper (Ch_2) can be seen together with an auxiliary strip lamp and mirrors. The strip lamp is used as a secondary radiation standard in place of a blackbody radiator. The infrared monochromator is at the right rear.

B. Combustion Flame Temperatures

Figures 7, 8, and 9 illustrate measurements of flame radiation and temperature by the IMRA technique. Figure 7 shows the emission and emissivity of a 5-inch diameter methanol-oxygen flame between 2.5-μ and 3.6-μ, at a point $5\frac{1}{2}$ inches from the base of the flame. Figure 8 shows the corresponding IMRA-measured temperature, plotted against wavelength (Curve A), and a similar plot for a point $8\frac{1}{2}$ inches from the base of the flame (Curve B). Figure 9 shows a plot of temperature vs. wavelength in the 4.3-μ spectral band of CO_2, for the methanol-oxygen flame $8\frac{1}{2}$ inches downstream (Curve B), and a similar plot for measurements made $5\frac{1}{2}$ inches from the base of a hexane-oxygen flame (Curve A).

Figures 8 and 9 have a number of interesting features. The indicated temperature is different at different wavelengths, corresponding to the non-uniformity of the temperature distribution in the flame cross-section. Moreover, we obtain higher

temperatures from wavelengths at which the emissivity is low than from wavelengths where the emissivity is high. This can be seen by comparing the emissivity plot in Fig. 7, wavelength-by-wavelength, to Curve A in Fig. 8. (For convenience, alternate spectral lines are omitted in Fig. 8. This does not affect the comparison). The reason for this phenomenon is clear. When the emissivity is high, radiation emitted from the interior of the flame suffers considerable reabsorption; hence, in effect we measure primarily radiation from the outer, cooler layers of gas, and the indicated temperature is relatively low. At wavelengths where the emissivity is low, on the other hand, the pyrometer can "see deeper" into the hot core of the flame and the indicated temperatures are higher.

Comparison of the two curves of Fig. 9 brings out the effect of different temperature gradients. The data for Curve A were obtained near the base of the flame, where the core temperature is highest and the gradient steepest. At the long wavelength end of the band, where the emissivity falls, the temperature shows a sharp rise, corresponding to the temperature in the hot core. Contrasting to this, Curve B in Fig. 9 shows data measured further downstream, where substantial mixing has taken place and the temperature gradient is much less steep. Correspondingly, the indicated temperature levels off as a function of wavelength, and the sharp rise observed in Curve A is absent. A plot somewhat like Curve B was described by Silverman[9], for the $CO-O_2$ flame; the rising portion of the plot near 4.20-μ was omitted in Silverman's published figure. The effect of temperature gradients may be seen also in Fig. 8. The average temperature is higher and the slope of the temperature vs. wavelength plot is steeper for the measurements made near the base of the flame. Comparing Curve B of Fig. 8 with Curve B of Fig. 9, we find that the temperature is the same for both spectral regions, for wavelengths of equal emissivity. The mean temperature of the entire T vs. λ curve is about 100° higher for the 2.7-μ than for the 4.3-μ data. This is to be expected, since the average emissivity is higher in the 4.3-μ band.

The temperature values shown here are weighted averages of the temperatures across an inhomogeneous flame. The variation of temperature with wavelength reflects the temperature profile of the flame, although it does not provide a strict point-by-point temperature profile. Methods for determining the profile in detail have been discussed elsewhere for the case where the radial temperature distribution is uniform[35,36], and for the general case of an inhomogeneous temperature distribution[26,37].

C. Temperature Measurements in Plasmas

Plasma may be defined loosely as a gas which is partially ionized. Ordinarily, plasmas are hotter than combustion gases and are electrically conductive. Polyatomic molecules are not commonly found in plasmas, because they are dissociated by the high temperature. Plasmas in the range up to perhaps 15,000°K are composed of diatomic molecules and atoms. As one goes to higher and higher temperatures, dissociation and ionization become progressively greater, until eventually, at temperatures of some millions of degrees, the plasma consists entirely of stripped atomic nuclei and free electrons.

Monochromatic radiation pyrometry has been applied to plasmas at temperatures up to about 15,000°K. At these temperatures, infrared emission is obtained from a few diatomic molecules and from atoms. The instrumentation for measurement of plasma temperatures by monochromatic radiation pyrometry is basically similar to that used in measuring temperatures of flames and combustion gases. An example of plasma temperature measurement by monochromatic radiation pyrometry is given in Fig. 10, which shows temperatures determined from emission and absorption in the 4.015-μ line of helium. The experimental points are compared to a theoretical curve of gas enthalpy against temperature.

D. Measurement of Transient Gas Temperatures by Monochromatic Radiation Pyrometry

Transient gas temperatures can be determined as a function of time, by application of the principles already discussed. The measurements must be made and recorded at high speed. Instrumentation for this purpose has been described[38]. The high-speed IMRA pyrometer is similar in function to the instrument illustrated schematically in Fig. 4. The main difference is that a much higher chopping frequency (11,000 cycles per second) is used in the Source Unit than is the case for the steady-state instrument, and no chopper is used in the Receiver Unit. A very fast infrared detector is used and its output is indicated on an oscilloscope. Recordings are made by photographing the oscilloscope trace. Radiation from the blackbody standard is chopped at a different frequency (1600 cycles per second) from the Source Radiation, so that this signal can be readily identified on the oscillogram. Figure 11 shows a typical record of temperatures in a deflagration wave, measured with a high-speed IMRA pyrometer. These measurements were made at a wavelength of 4.4-μ, corresponding to the emission of hot carbon dioxide. The left third of the diagram shows the 11,000-cps modulated source radiation beam before the deflagration wave has arrived at the observation point. The low frequency (1600-cps) chopped signal is the calibrating signal from the blackbody standard. After 1½ milliseconds, the deflagration

wave reaches the observation station. The infrared emission from the combustion wave causes a transient signal to be indicated on the oscilloscope. The spectral emission at any time can be obtained by scaling off the amplitude from the oscillogram. The spectral emissivity is obtained by scaling off the peak-to-peak amplitude of the 11,000-cps modulated signal during the interval where emission occurs, and comparing this to the peak-to-peak amplitude of the 11,000-cps trace prior to arrival of the combustion wave. Thus both spectral emission and spectral emissivity as functions of time can be obtained from a single recording. The blackbody calibration trace enables conversion of the data to absolute temperature. The circles drawn on Fig. 11 connected by a dashed line are the temperatures calculated from the spectral emission and spectral emissivity values read off this oscillogram.

IV. PRECISION ANALYSIS

In order to evaluate the accuracy and precision of monochromatic gas radiation pyrometry, a series of measurements was made in which gas temperatures determined by monochromatic radiation pyrometry were compared to temperatures measured with accurately calibrated and corrected chromel-alumel thermocouples. The characteristics of the chromel-alumel thermocouples necessarily limited the comparison to temperature not exceeding 1800°F. However, since the principles used are independent of the temperature, it is reasonable to assume that a check of the accuracy of the method in this temperature range is also applicable at higher temperatures. This is particularly plausible, because the Planck radiation curve, against which monochromatic radiation pyrometry is calibrated, gets steeper as the temperature increases (see Fig. 3); hence the method is inherently more sensitive and less susceptible to measurement errors at higher temperatures.

In these tests, the fully-combusted exhaust of a gasoline-air burner was used as the sample gas. The gas stream was six inches in diameter, and was essentially isothermal, except for a negligibly thin boundary layer. Radiation data and thermocouple data were recorded simultaneously on a two-pen recorder. The radiation measurements were made at a fixed wavelength of 2.66-μ.

Tests were made at four nominal temperatures, near 1200°, 1400°, 1600°, and 1800°F. The results of the comparison are shown in Fig. 12. At each temperature, the horizontal line is the mean of repeated radiation temperature measurements. The measurements themselves are shown as solid circles. In each case, the mean thermocouple reading is shown as the short line segment near the right hand margin. At all four temperatures the standard deviation of the radiation pyrometer readings was ±2%. At the higher temperatures the accuracy of the measurement

was within 1% of the temperature indicated by the thermocouple. As lower temperatures are approached the accuracy becomes progressively poorer. This corresponds to the flattening out of the Planck curve at low temperatures. The accuracy of the radiation method improves as one goes to higher temperatures, because the Planck curve gets steeper. Of course the accuracy cannot increase indefinitely as one goes to higher temperatures; an accuracy somewhere between ½% and 1% is probably the practical limit for this type of measurement.

In such a comparison, one cannot distinguish between fluctuations in the measurement process and fluctuations of the hot gas under study. The temperature of the hot combustion gas was constantly fluctuating, with an amplitude of roughly +75°F. Accordingly, the indicated reproducibility in Fig. 12 includes both the random measurement errors and the fluctuations of the gas temperature.

A more definitive evaluation of accuracy would require a standard hot gas sample in equilibrium at a known temperature. Such a standard has recently been described, and preliminary results obtained with it bear out the analysis given in this paper[39].

V. ACKNOWLEDGEMENTS

Material for this paper was drawn from investigations conducted in this laboratory over the past fifteen years, in which many people participated. The instrumentation and equipment used to obtain the measurements described in this paper were designed by S. A. Dolin, E. T. Liang, and G. J. Penzias. P. M. Henry and M. L. Hecht contributed to the measurement of plasma and deflagration temperatures. The author is particularly indebted to L. R. Ryan, for Figs. 8 and 9, and to H. J. Babrov for helpful discussions and criticism.

REFERENCES

1. J. K. Roberts and A. R. Miller, Heat and Thermodynamics (Interscience Publishers, New York, 1960, 5th ed.), Ch. XX.

2. A. G. Worthing, Temperature (Reinhold, New York, 1941), p. 1164.

3. E. K. Plyler and C. J. Humphreys, J. Res. Natl. Bur. Standards 40, 449 (1948).

4. E. K. Plyler, J. Res. Natl. Bur. Standards 40, 113 (1948).

5. R. H. Tourin, Natl. Bur. Standards Circ. No. 523, 87 (1954).

6. R. H. Tourin, J. Opt. Soc. Am. 51, 175 (1961).

7. H. Schmidt, Ann. d. Physik 29, 971 (1909).

8. M. Grossman and R. H. Tourin, Air Technical Index Document #58331, Wright-Patterson Air Force Base, Ohio (1949).

9. S. Silverman, J. Opt. Soc. Am. 39, 275 (1949).

10. M. Grossman and R. H. Tourin, U. S. Air Force Tech. Report #6064 (Wright-Patterson Air Force Base, Ohio, 1950).

11. R. H. Tourin and M. Grossman, Combustion & Flame 2, 328 (1958).

12. M. Grossman and R. H. Tourin, U. S. Patents 2,844,032, 2,844,033 (1958).

13. H. J. Kostkowski and R. D. Lee, This Symposium.

14. H. P. Broida, Temperature, Vol. II, H. C. Wolfe, ed. (Reinhold Publishers, New York, 1955), p. 265.

15. G. H. Dieke, Temperature, Vol. II, H. C. Wolfe, ed. (Reinhold Publishers, New York, 1955), p. 19.

16. S. S. Penner, Amer. J. Phys. 17, 491 (1949).

17. S. S. Penner, This Symposium.

18. F. Seitz, The Modern Theory of Solids (McGraw-Hill, New York, 1940).

19. R. G. Breene, Jr., J. Chem. Phys. 29, 512 (1958).

20. Wentink, Planet, Hamerling, and Kivel, J. App. Phys. 29, 742 (1958).

21. N. Balazs, Optical Spectrometric Measurements of High Temperatures, P. J. Dickerman, ed. (U. of Chicago Press, 1961), p. 39.

22. G. R. Harrison, R. C. Lord, and J. R. Loofbourow, Practical Spectroscopy (Prentice-Hall, New York, 1948).

23. R. H. Tourin, Infrared Physics 1, 105 (1961).

24. H. J. Babrov, J. Opt. Soc. Am. 51, 171 (1961).

25. H. F. Stimson, J. Res. Natl. Bur. Standards 42, 209 (1949).

26. G. A. Hornbeck and L. O. Olsen, WADC Tech. Rep. 57-516 (Wright-Patterson Air Force Base, Ohio, 1957).

27. R. B. Lindsay, Physical Statistics (John Wiley, New York, 1941), pp. 222-226.

28. E. T. Child and K. Wohl, Seventh Symposium on Combustion (Butterworth's Scientific Publications, London, 1958), p. 215.

29. D. A. Dows, J. Chem. Phys. 27, 1430 (1957).

30. A. G. Gaydon, The Spectroscopy of Flames (John Wiley, New York, 1957), pp. 171-172.

31. W. S. Benedict, and E. K. Plyler, Natl. Bur. Standards Circ. #523, 64 (1954).

32. T. Carrington, J. Chem. Phys. 31, 1243 (1959).

33. K. E. Shuler, Seventh Symposium on Combustion (Butterworth's Scientific Publications, London, 1958), p. 87.

34. P. J. Dickerman, ed., Optical Spectrometric Measurements of High Temperatures (U. of Chicago Press, 1961).

35. W. J. Pearce, Conference on Extremely High Temperatures, Fischer and Mansur, eds. (John Wiley & Sons, New York, 1958), p. 123.

36. M. P. Freeman and S. Katz, J. Opt. Soc. Am. 50, 826 (1960).

37. R. H. Tourin, Combustion and Flame 2, 353 (1958).

38. R. H. Tourin, M. L. Hecht, and S. A. Dolin, J. Opt. Soc. Am. 50, 1129 (A) (1960).

39. G. A. Hornbeck, This Symposium.

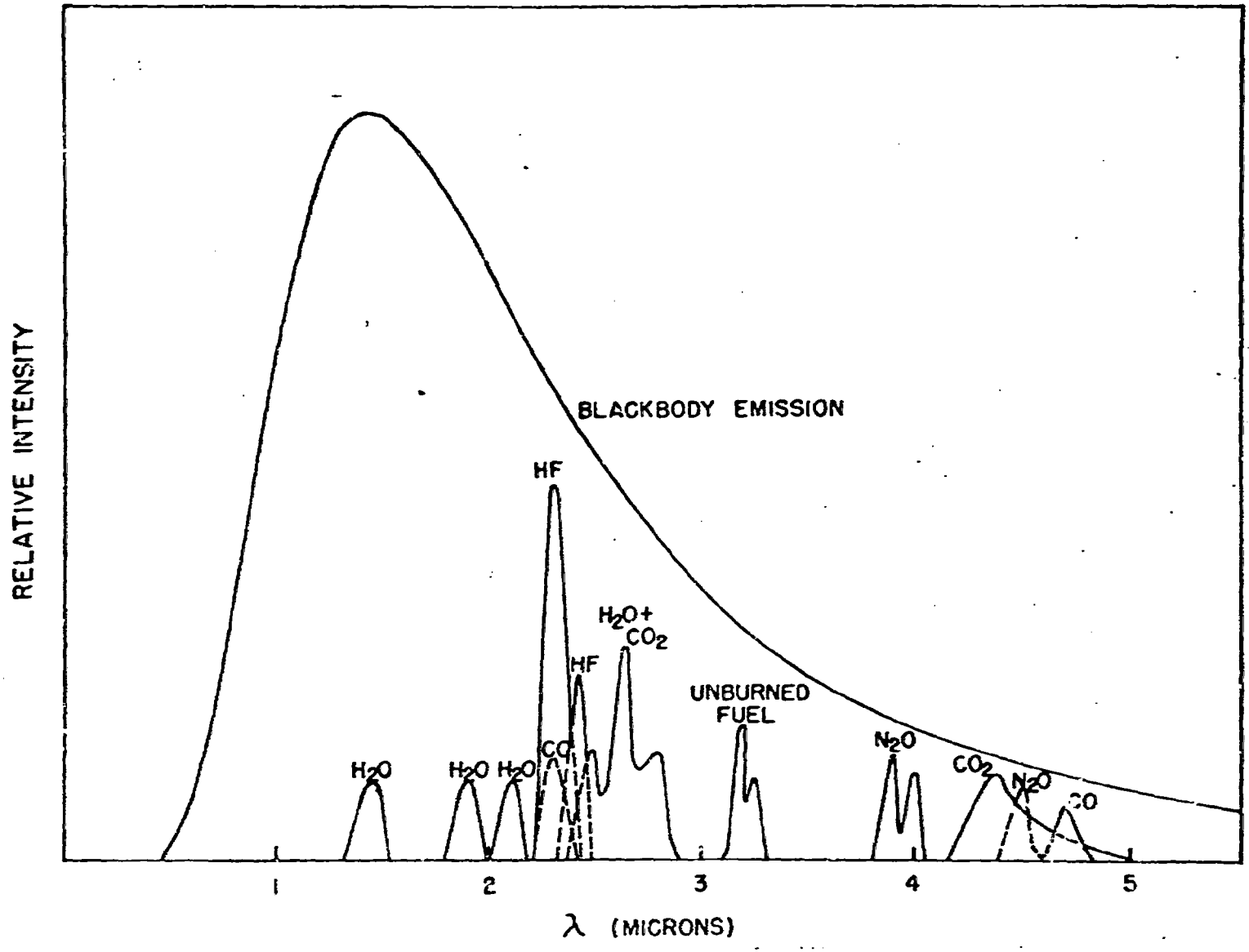

Fig. 1. Schematic infrared emission spectra of typical hot gas molecules, compared to blackbody emission.

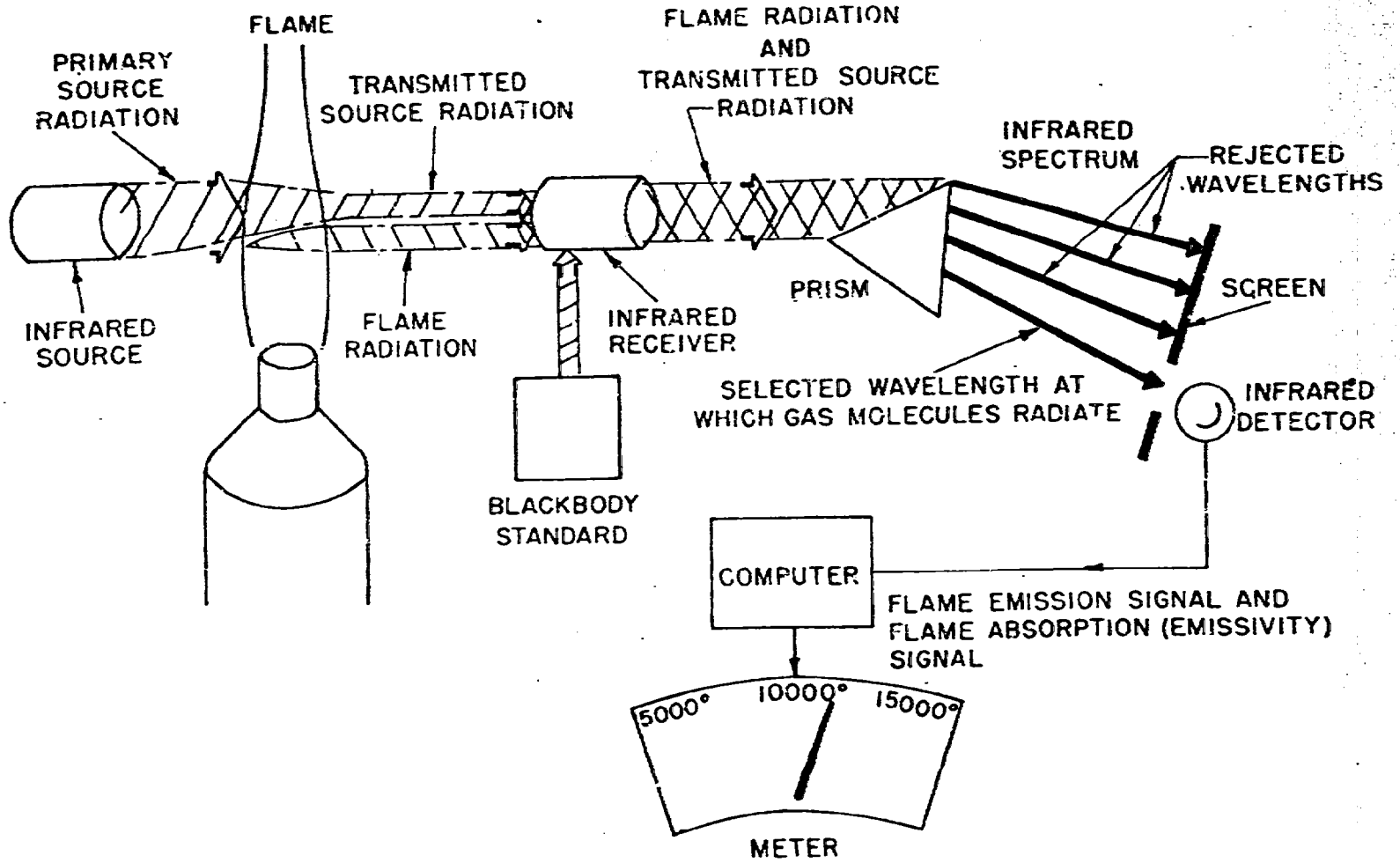

Fig. 2. Schematic diagram showing the principle of monochromatic radiation pyrometry for gas temperature measurement.

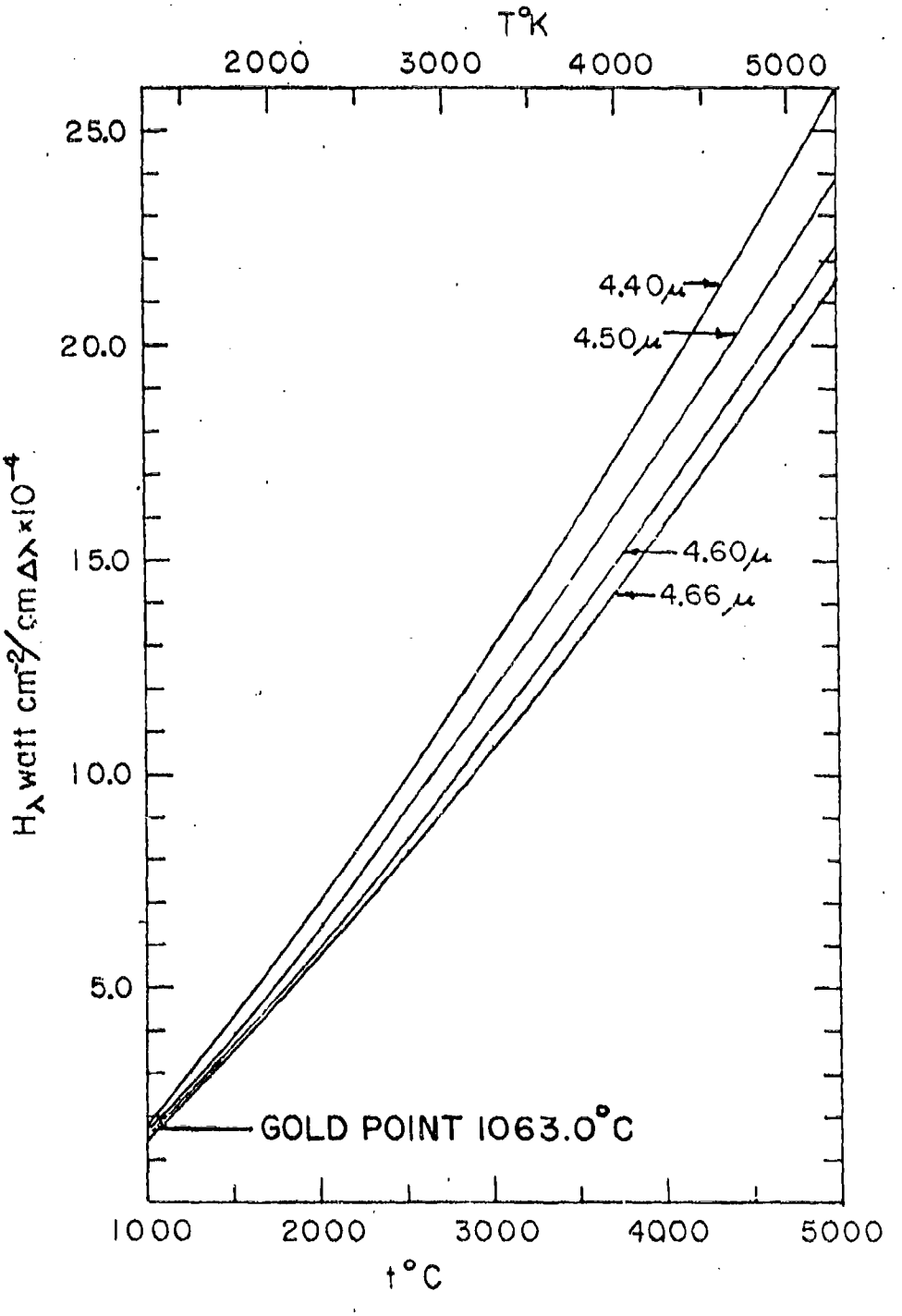

Fig. 3. Planck law curves for calibration of a monochromatic radiation pyrometer.

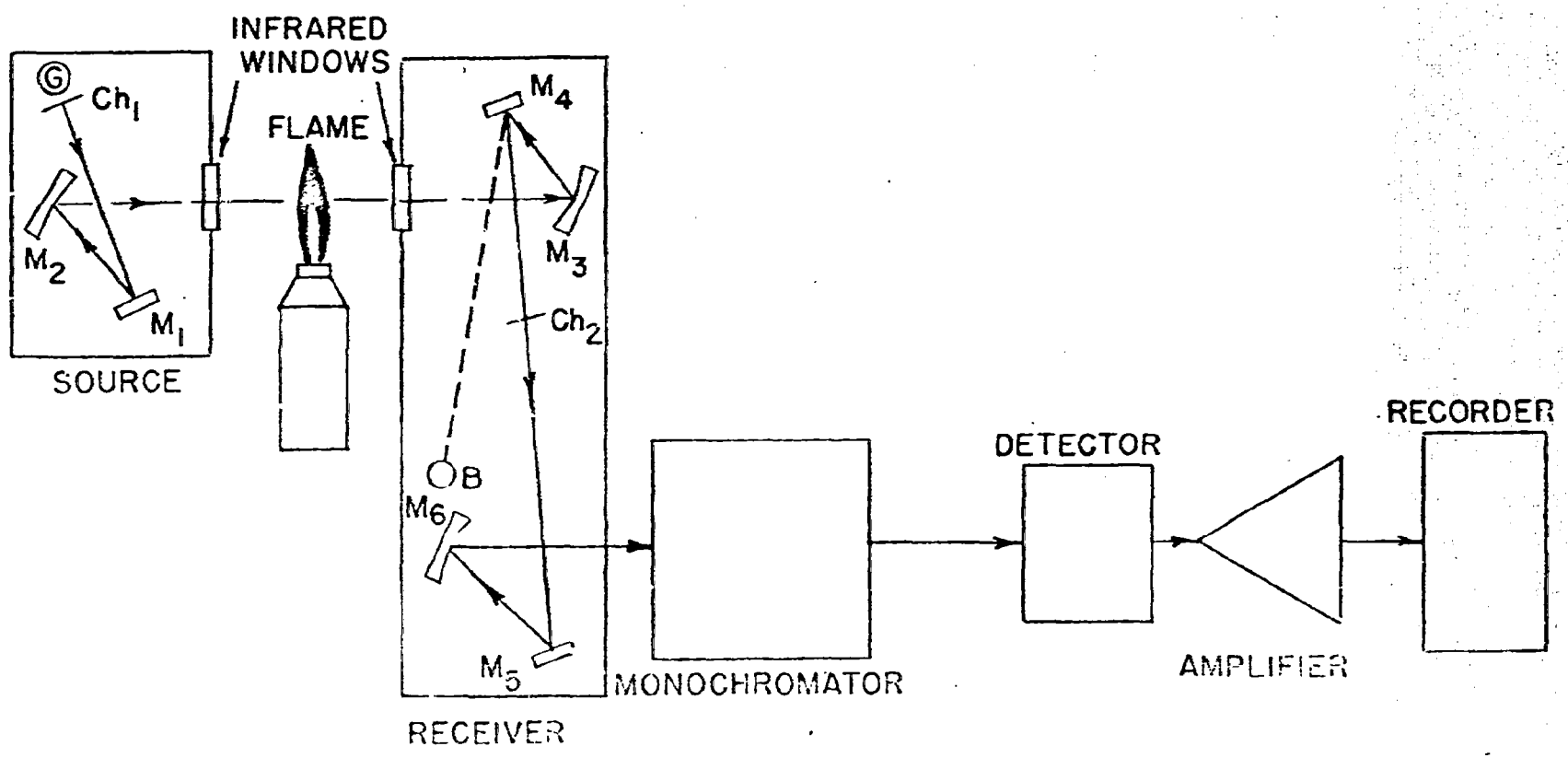

Fig. 4. Schematic diagram of a monochromatic radiation pyrometer.

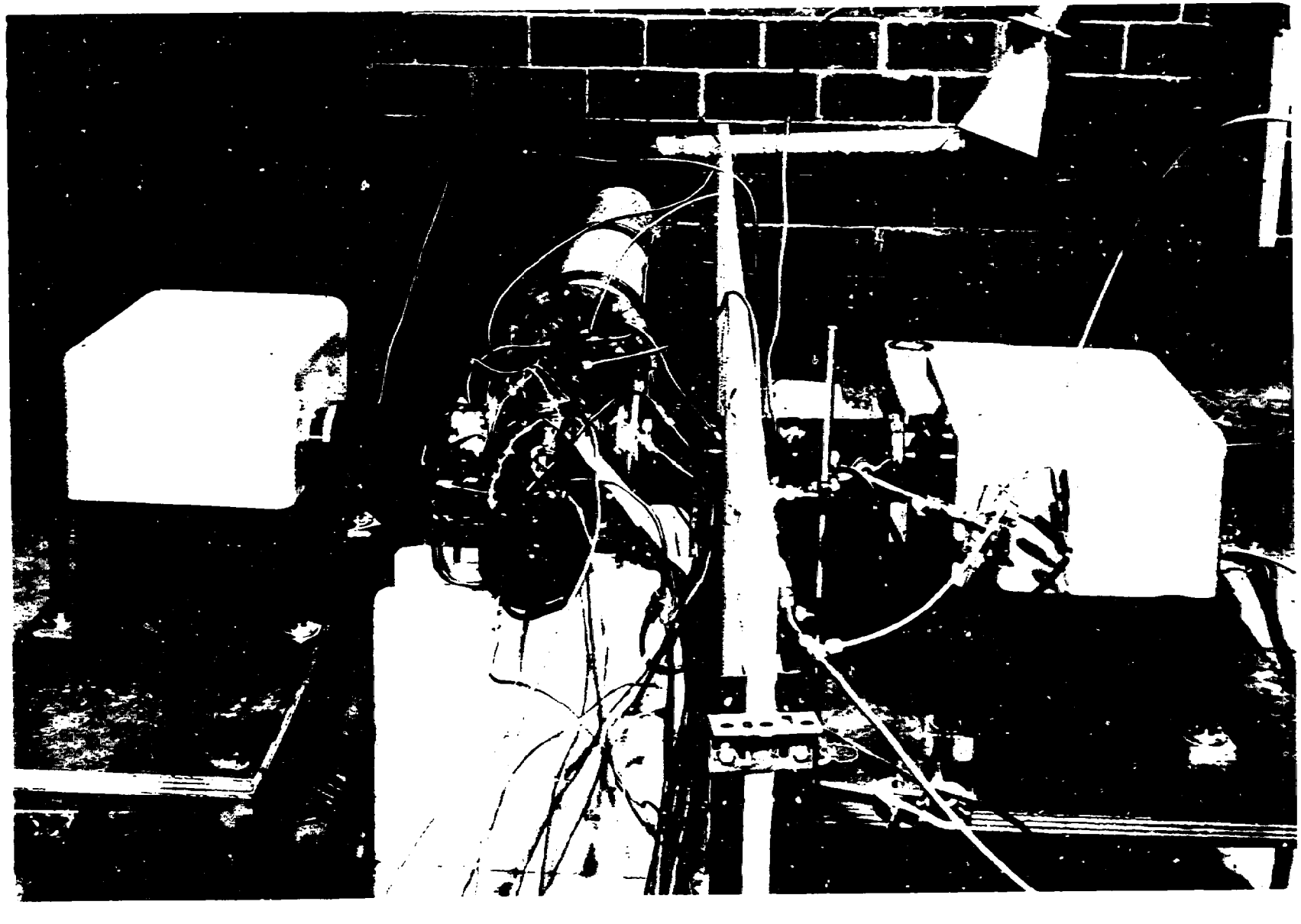

Fig. 5. A monochromatic radiation pyrometer for gas temperature measurement.

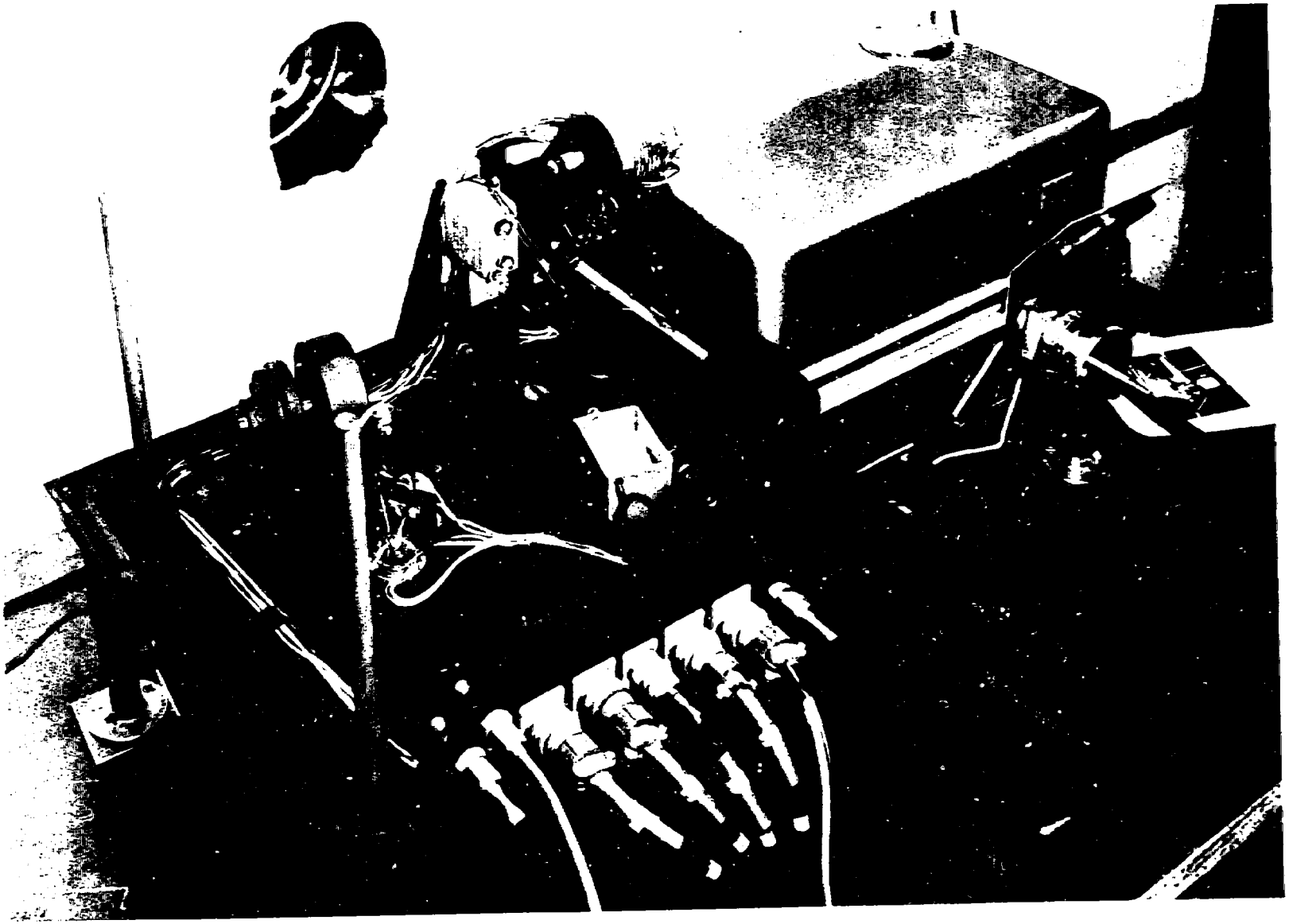

Fig. 6. Closeup view of Receiver Unit of monochromatic radiation pyrometer.

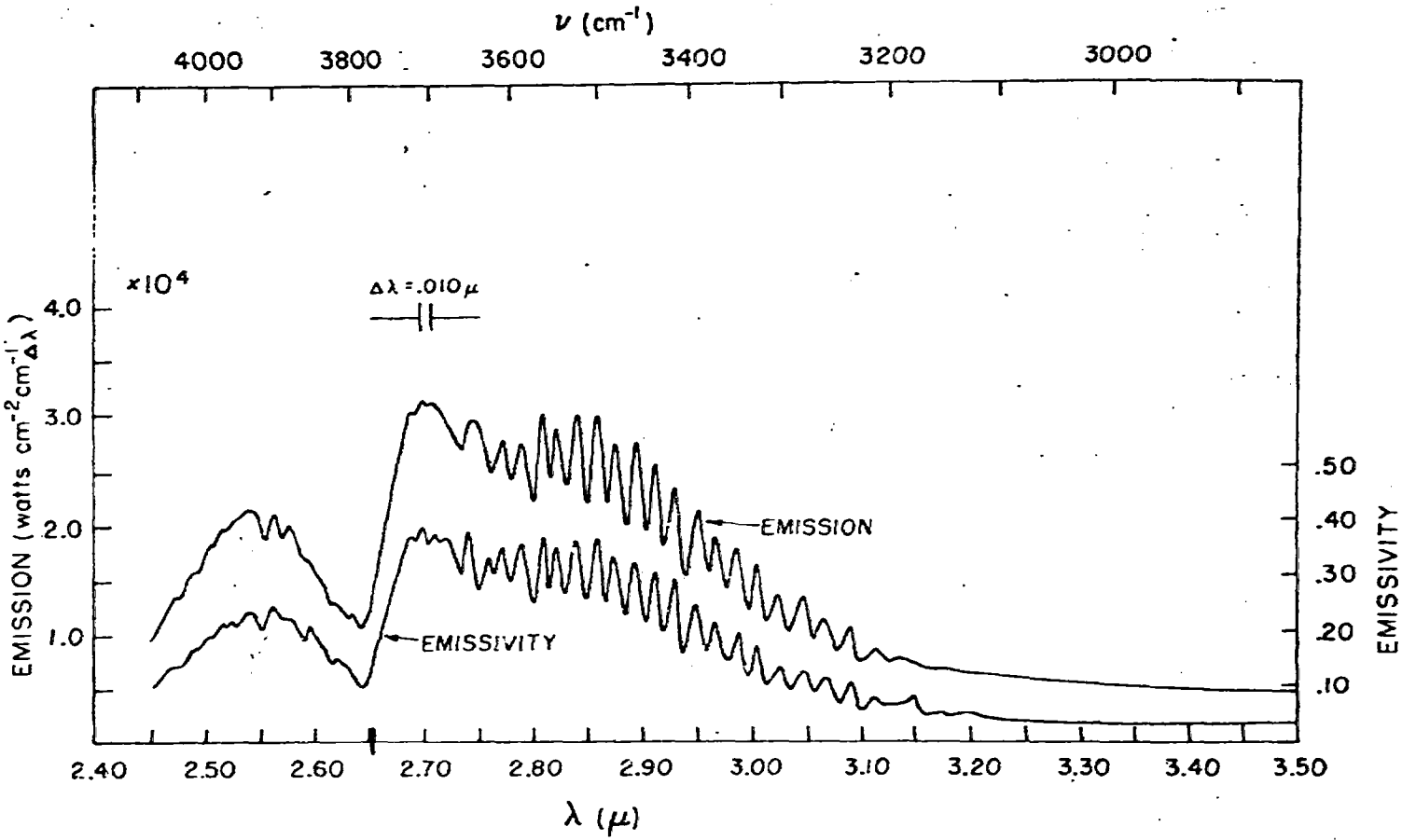

Fig. 7. Typical spectral emission and spectral emissivity plots for a flame. These curves were obtained from measurements of emission and absorption of a 5-inch diameter methanol-oxygen flame, $5\frac{1}{2}$ inches from the base of the flame.

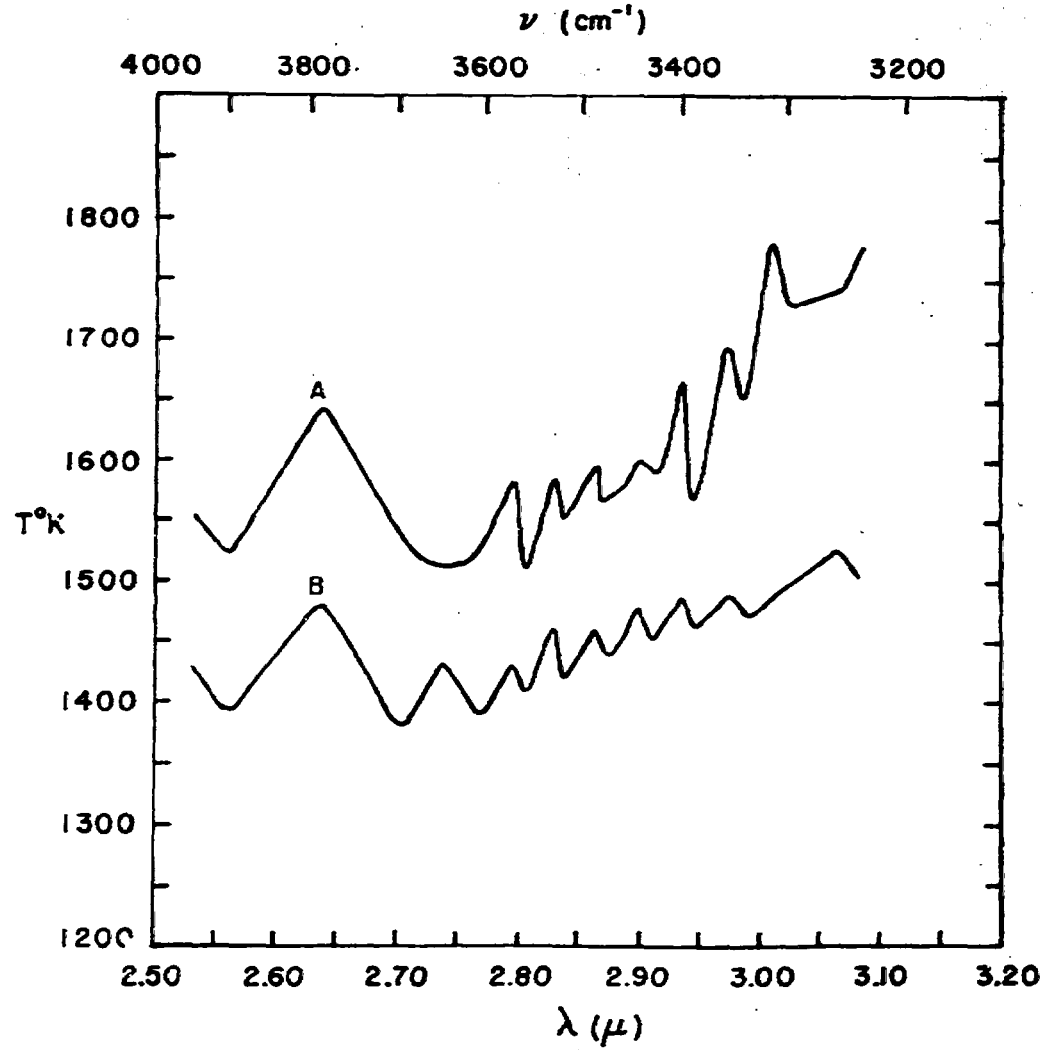

Fig. 8. Curve A is a plot of methanol-oxygen flame temperature vs. wavelength, obtained from the emission and emissivity data of Fig. 7. For convenience, alternate spectral peaks have been omitted. Curve B shows a corresponding plot for the same flame, measured $3\frac{1}{2}$ inches further downstream than for Curve A.

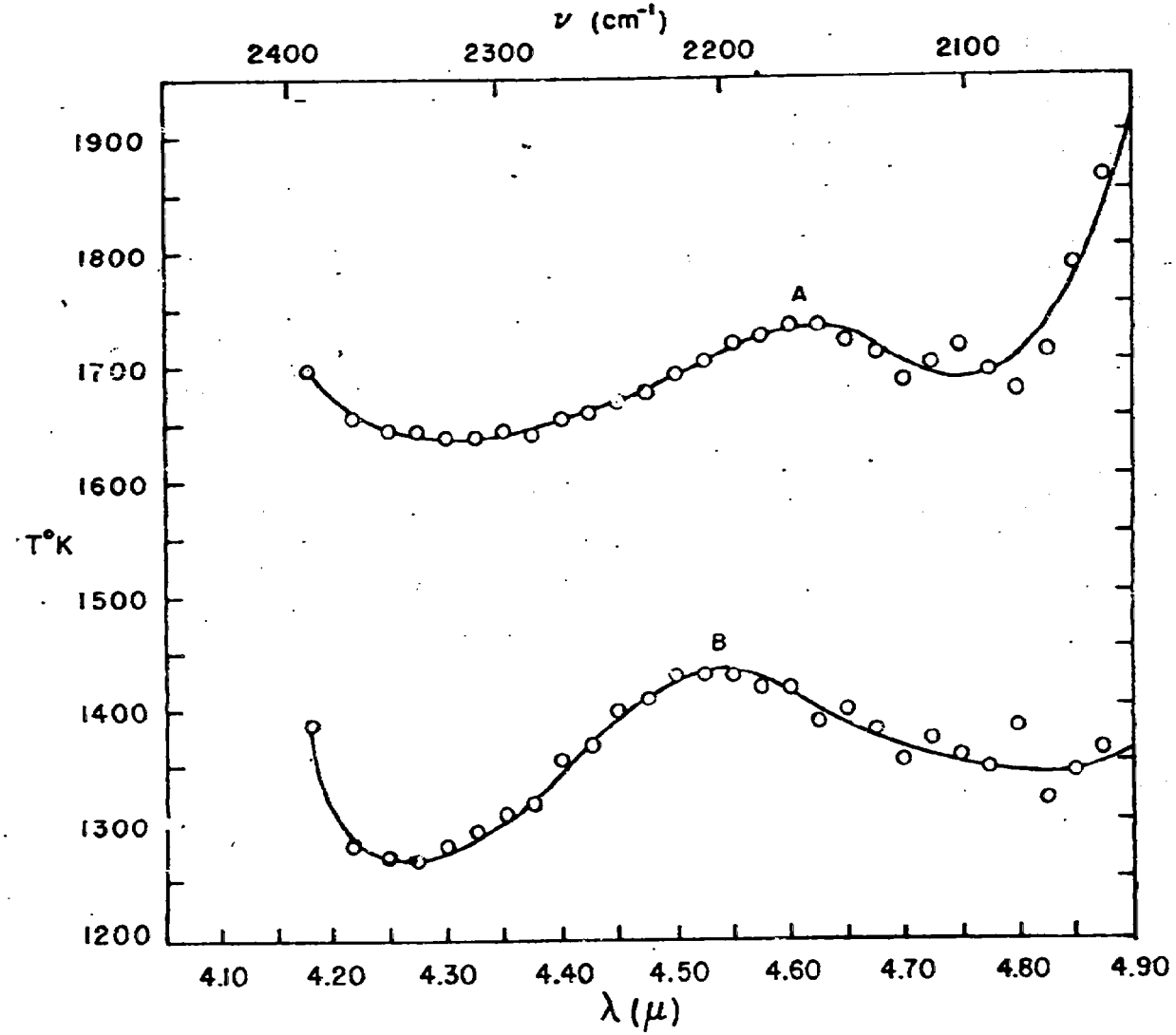

Fig. 9. Curve B is a temperature-wavelength plot for the methanol-oxygen flame, obtained at the same position as Curve B of Fig. 8. Curve A was obtained from measurements in a 5-inch diameter hexane-oxygen flame, $5\frac{1}{2}$ inches from the flame base.

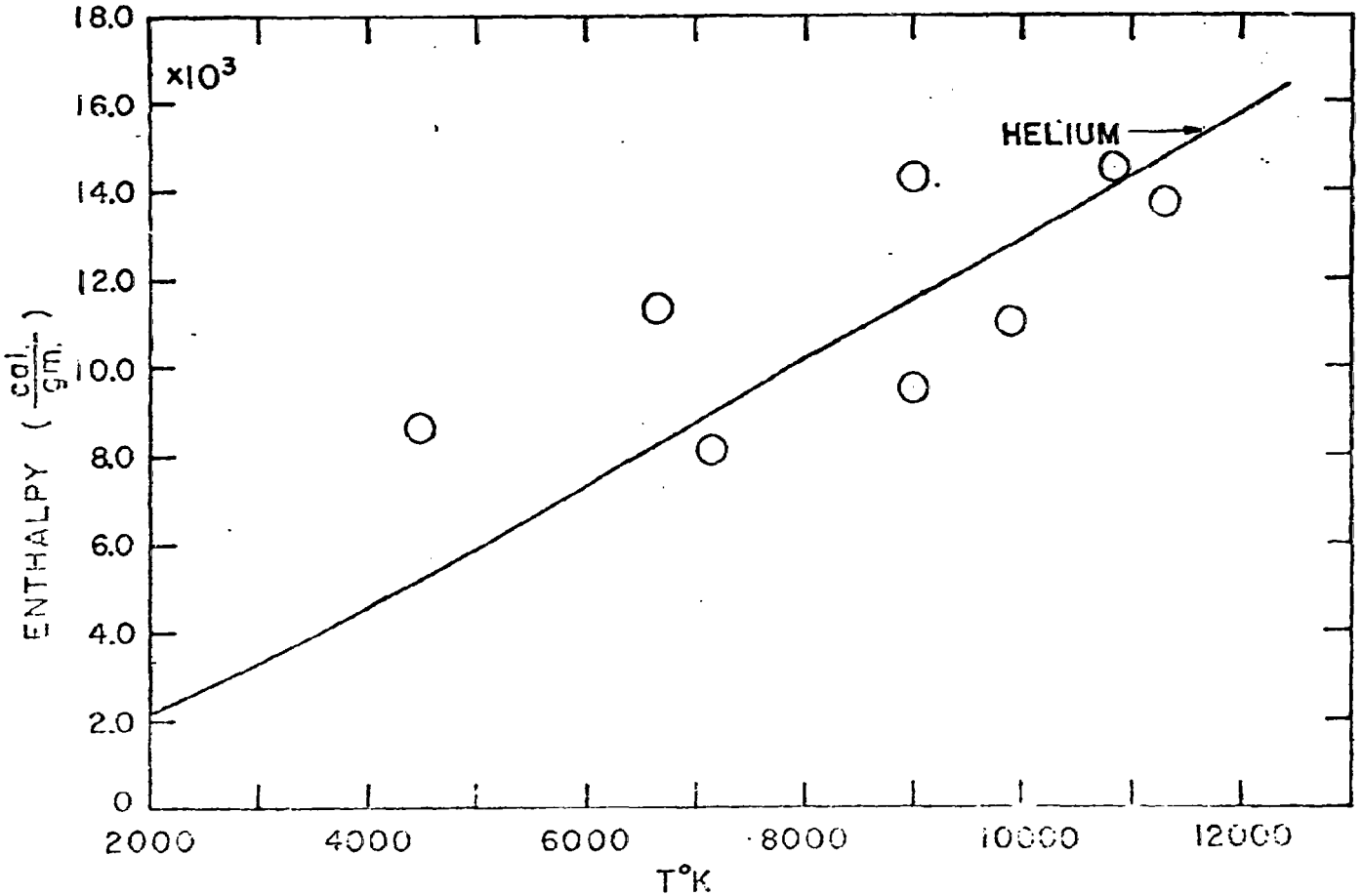

Fig. 10. Temperatures measured in a helium plasmajet by monochromatic radiation pyrometry.

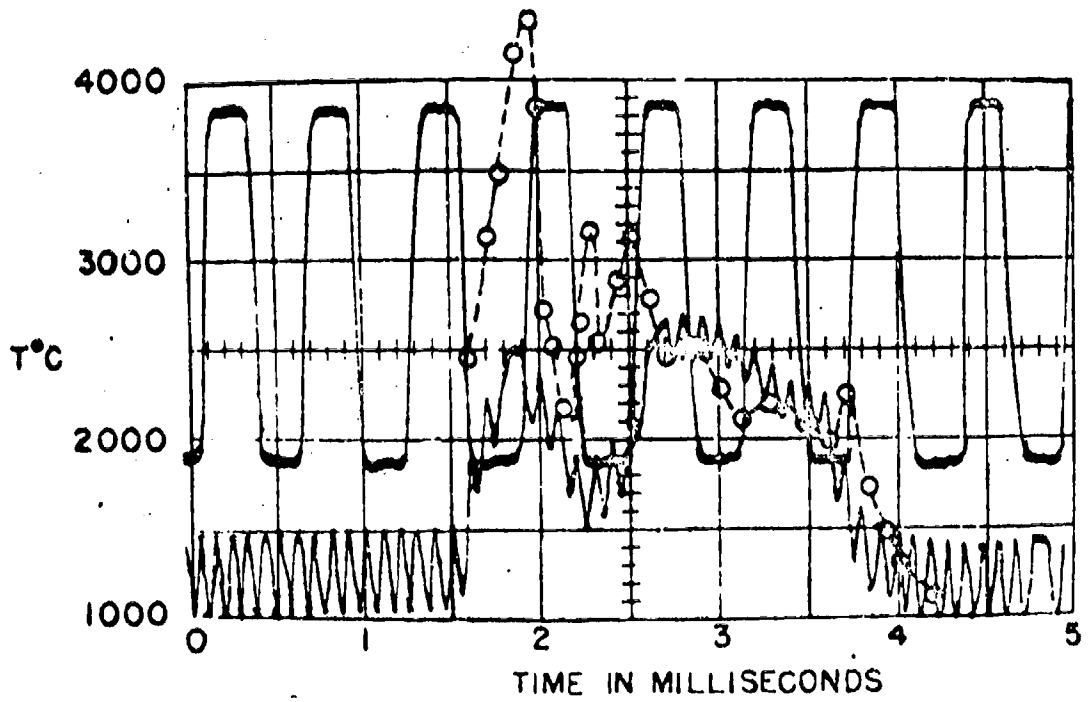

Fig. 11. Typical temperature record of a deflagration wave, obtained by the high-speed monochromatic radiation pyrometer. The circles drawn on the figure represent temperatures computed from the oscillogram, as described in the text. The temperature range 0–1000°C has been suppressed.

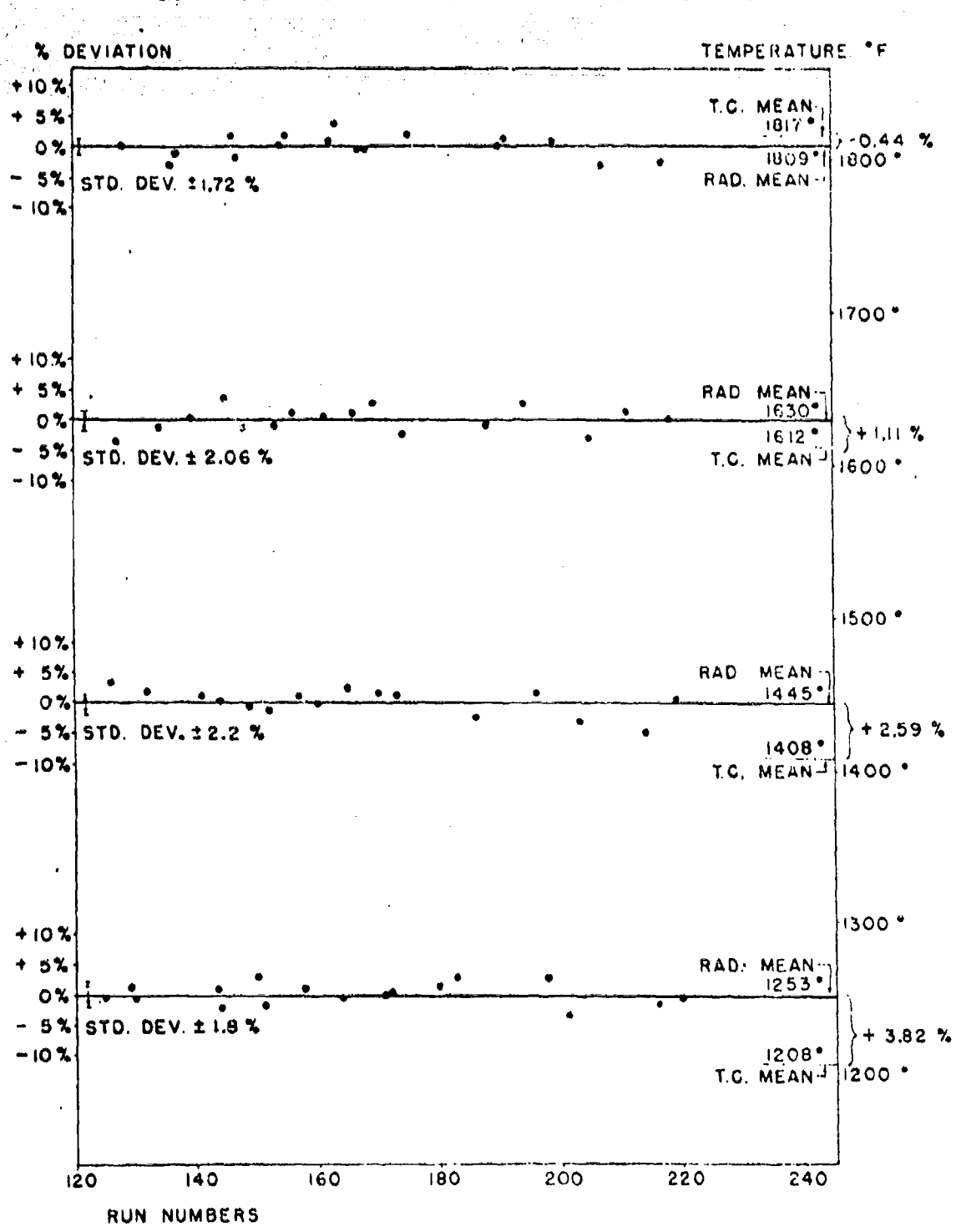

Fig. 12. Comparison of combustion gas temperatures measured by monochromatic radiation pyrometry and by chromel-alumel thermocouples. At each temperature the burning was maintained as steady as possible, and repeated measurements made. The reproducibility is shown by the distribution of each set of points about their mean value; the scatter includes the average gas temperature fluctuation of $\pm$ 75°F. Absolute accuracy is indicated by the agreement of the radiation mean temperature and the thermocouple mean temperature, given in the right hand margin.

* Infrared Physics, 1961, Vol. 1, pp. 105–110. Pergamon Press Ltd. Printed in Great Britain

INFRARED SPECTRAL EMISSIVITIES OF CO_2 IN THE 2·7 MICRON REGION*

R. H. TOURIN

The Warner & Swasey Company, Control Instrument Division,
32–16 Downing Street, Flushing 54, N.Y., U.S.A.

(*Accepted* 31 *October* 1960)

Abstract—Spectral emissivities of hot CO_2 in the 2·7 μ region were measured. Obscuration by H_2O emission, which occurs in flame spectra, was eliminated by use of CO_2 samples heated in a closed gas cell. These measurements of emissivity can be used to calculate radiant power of hot CO_2 over a given spectral region, by means of an approximate integration technique. The CO_2 absorption near 2·7 μ was found to be independent of pressure at 1273 °K, from 50 mm to 700 mm Hg. This contrasts with the case of CO_2 absorption at room temperature. It results from overlapping of vibration-rotation transitions of the types $v_1v_2^lv_3 - (v_1 + 1)\,v_2^l\,(v_3 + 1)$ and $v_1v_2^lv_3 - v_1(v_2 + 2)^l\,(v_3 + 1)$, originating from excited states as well as from the ground state. This overlapping produces "temperature-smearing" of the spectrum, analogous to pressure broadening.

INTRODUCTION

FLAMES and combustion gases exhibit strong infrared emission in the spectral region near 2·7 μ. This emission is contributed by infrared vibration-rotation bands of carbon dioxide and water vapor. The 2·7 μ carbon dioxide bands in a flame spectrum are obscured by the strong emission of the water vapor fundamental bands in the same spectral region. For this reason no detailed studies of these CO_2 bands in hot gases have been reported previously.

The present paper describes measurements of the 2·7 μ infrared absorption bands of carbon dioxide at high temperatures. The measurements were made primarily to determine spectral emissivities of CO_2 as a function of temperature and molecular concentration. The measurements were made with samples of pure, dry CO_2 heated in a special gas cell. Spectra were measured with a Perkin–Elmer Model 12C infrared spectrometer. The experimental methods and some of the results of measurements in the 4·3 μ region have been reported previously.[1, 2]

MEASUREMENTS

Figure 1 shows the spectral emissivity of CO_2 in the 2·7 μ bands for temperatures from 394 °K to 1300 °K, measured with an optical depth *ps* of 2·67 cm atm, at 700 mm Hg total pressure. The path length was 12·7 cm, and dry nitrogen was used to adjust the pressure. Most prominent in Fig. 1 are the CO_2 combination bands (00^00)–(02^01) and (00^00)–(10^01), centered at frequencies 3613 cm^{-1} and 3715 cm^{-1} respectively. Near 3560 cm^{-1}, there is an extra peak, suggesting additional bands. This peak is probably mainly due to the transition (01^10)–(03^11), for which ν_0 equals 3579 cm^{-1}.

* Supported in part by the U.S. Air Force, through the Geophysics Research Directorate, Bedford, Mass.

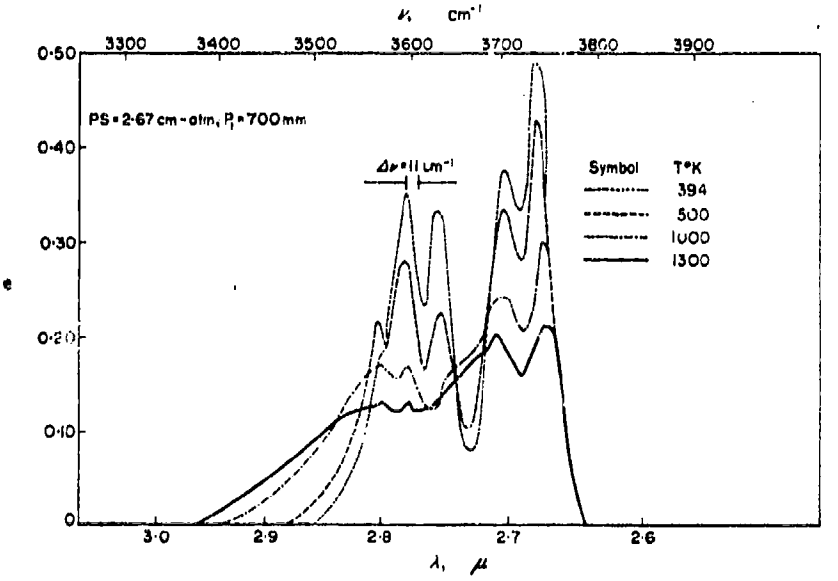

FIG. 1. Temperature variation of the spectral emissivity of CO_2 in the 2·7 μ region.

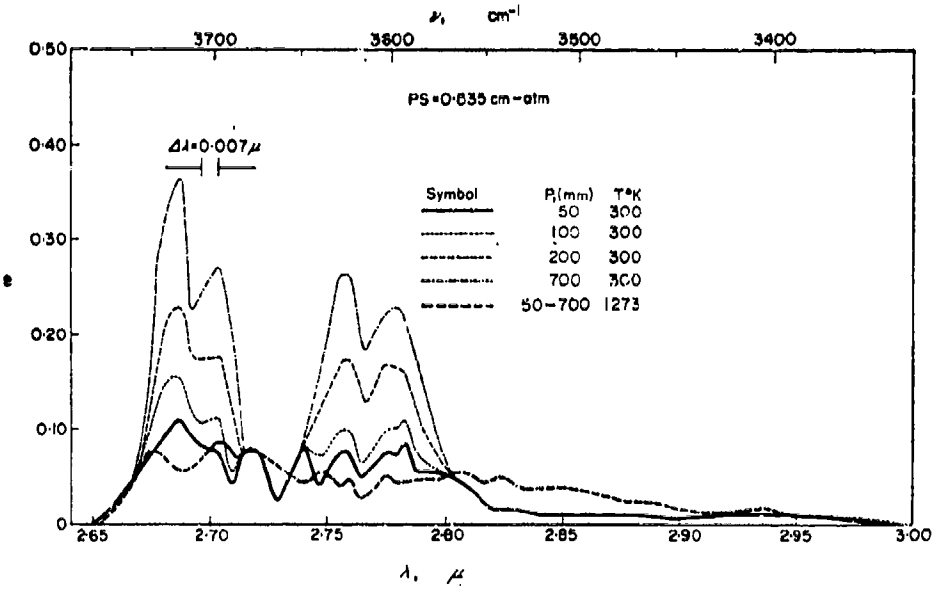

FIG. 2. Spectral emissivity of CO_2. Comparison of temperature and pressure effects in the 2·7 μ region.

The high-temperature spectrum is insensitive to pressure variation. Fig. 2 summarizes measurements at several pressures, at 300 °K and 1273 °K, for ps = 0·84 cm atm. The effect of pressure on the emissivity at room temperature is apparent, while at 1273 °K there

is no observable pressure effect, as can be seen from the fact that the curves for 50 mm and 700 mm total pressure coincide.

Although independent of pressure, the high-temperature spectrum is quite sensitive to absorber concentration, as indicated by Fig. 3. The lower curve of Fig. 3 reproduces the lower curve of Fig. 2. The upper curve in Fig. 3 corresponds to a much higher concentration, at the same temperature and pressure.

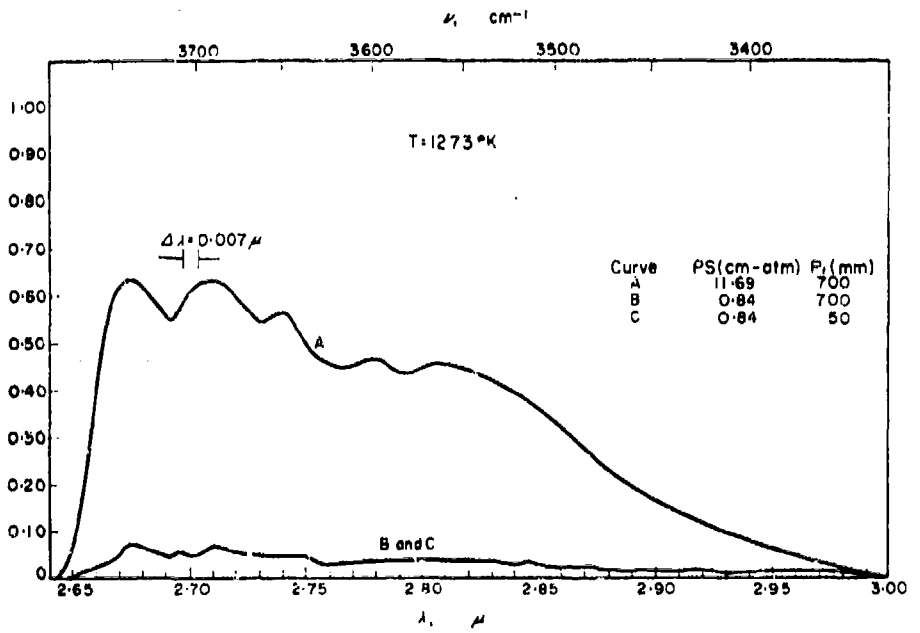

FIG. 3. Spectral emissivity of CO_2 at 1273 °K; the 2·7 μ region. Increasing the absorber concentration changes the emissivity by a comparable amount, while changing pressure by more than a factor of ten has no effect.

Absolute spectral radiance may be calculated from the spectral emissivity plots shown in Figs. 1, 2 and 3, by multiplying the emissivities point-by-point by the appropriate values of the Planck function. Fig. 4 shows the spectral radiance of carbon dioxide at 1273 °K calculated by this method. The power radiated in any spectral interval may be calculated from Fig. 4 by integrating over the interval. To simplify this calculation the approximation

$$P_{\Delta\lambda}(T) = \int_{\Delta\lambda} e(\lambda, T)J(\lambda, T)d\lambda \approx \bar{J}_\lambda(T) \int_{\Delta\lambda} e(\lambda, T)d\lambda,$$

may be used, where $P_{\Delta\lambda}(T)$ is the spectral radiant power of the hot gas in the interval $\Delta\lambda$, $e(\lambda, T)$ is the spectral emissivity at wavelength λ and temperature T, $J(\lambda, T)$ is the Planck function, and $\bar{J}_\lambda(T)$ is the average value of $J(\lambda, T)$ over $\Delta\lambda$. Table 1 compares integrated radiances calculated in this way to radiances obtained by multiplying the emissivities point-by-point by the Planck radiation function and integrating. The agreement between the approximate and exact calculations is very good.

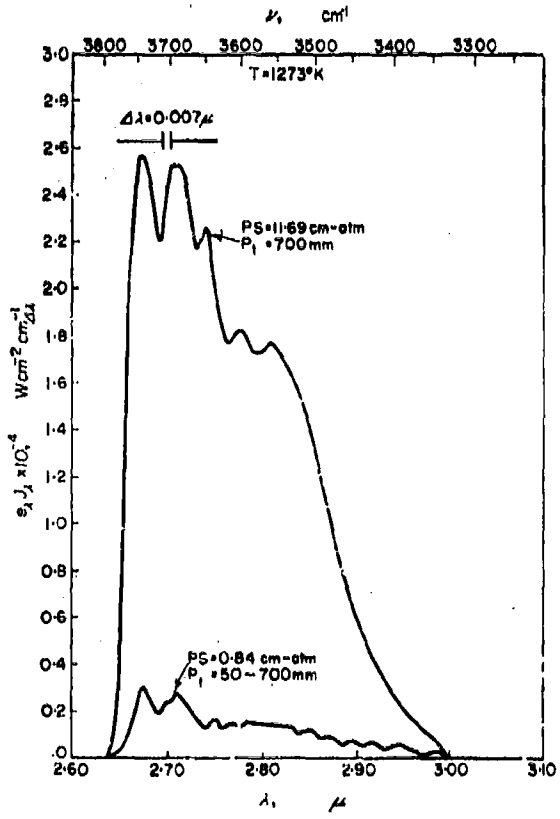

FIG. 4. Spectral radiance of CO_2 at 1273 °K, calculated from emissivity measurements; 2·7 μ region.

TABLE 1. CO_2 EMISSIVITY AND RADIANCE INTEGRALS IN THE 2·7 μ REGION

T °K	Band ($\Delta\lambda$)	P(atm)	PS(cm atm)	P_t (atm)	$\int e d\lambda$	$\int J e d\lambda$(W/cm²)	$\bar{J}\int e d\lambda$(W/cm²)	Difference %
1273	2·635–3·000	0·07	0·8	0·07	0·0109	$0·42 \times 10^{-1}$	$0·42 \times 10^{-1}$	0
1273	2·635–3·000	0·07	0·8	0·92	0·0109	$0·42 \times 10^{-1}$	$0·42 \times 10^{-1}$	0
1273	2·635–3·000	0·92	11·7	0·92	0·1182	0·48	0·46	− 4·2
305	2·656–2·820	0·07	0·8	0·07	0·00991	$0·81 \times 10^{-7}$	$0·86 \times 10^{-7}$	+ 6·2
305	2·656–2·856	0·07	0·8	0·92	0·02387	$0·20 \times 10^{-6}$	$0·23 \times 10^{-6}$	+ 15·0
305	2·656–2·865	0·92	11·7	0·92	0·1035	$0·90 \times 10^{-6}$	$1·01 \times 10^{-6}$	+ 12·2
1273	2·660–2·920	0·07	0·8	0·07	0·00960	$0·38 \times 10^{-1}$	$0·38 \times 10^{-1}$	0
1273	2·660–2·920	0·07	0·8	0·92	0·00960	$0·38 \times 10^{-1}$	$0·38 \times 10^{-1}$	0
1273	2·660–2·920	0·92	11·7	0·92	0·1116	0·45	0·44	− 2·2
305	2·670–2·800	0·07	0·8	0·07	0·00913	$0·76 \times 10^{-7}$	$0·79 \times 10^{-7}$	+ 3·9
305	2·670–2·800	0·07	0·8	0·92	0·0221	$0·19 \times 10^{-6}$	$0·19 \times 10^{-6}$	0
305	2·670–2·800	0·92	11·7	0·92	0·0896	$0·75 \times 10^{-6}$	$0·77 \times 10^{-6}$	+ 2·7

DISCUSSION

The radiation from CO_2 in the 2·7 μ region is contributed by two sets of vibration-rotation transitions: those for which $\Delta v_1 = 0$, $\Delta v_2 = 2$, $\Delta v_3 = 1$, $\Delta l = 0$, with band centers at frequencies of 3613 cm^{-1} and lower; and bands corresponding to transitions where $\Delta v_1 = 1$, $\Delta v_2 = 0$, $\Delta v_3 = 1$, $\Delta l = 0$, which occur at frequencies below 3715 cm^{-1}. Table 2 shows four transitions of each type, listed in order of relative population of the lower state. For each

TABLE 2. VIBRATIONAL POPULATION FACTORS AND TRANSITION PROBABILITIES FOR CO_2 BANDS IN THE 2·7 μ REGION

Lower state	Upper state	ν_0	Transition probability	Population of lower vibrational state at 300 °K	at 1273 °K
$(v_1 v_2^l v_3)$	$(v_1' v_2^{l'} v_3')$				
(a) $\Delta v_1 = 0$, $\Delta v_2 = 2$, $\Delta v_3 = 1$, $\Delta l = 0$					
(00^00)	(02^01)	3613 cm^{-1}	2	0·920	0·211
(01^10)	(03^11)	3579	6	0·074	0·199
(02^00)	(04^01)	3565	12	0·002	0·049
(10^00)	(12^01)	3593	2	0·001	0·044
(b) $\Delta v_1 = 1$, $\Delta v_2 = 0$, $\Delta v_3 = 1$, $\Delta l = 0$					
(00^00)	(10^01)	3715	1	0·920	0·211
(01^10)	(11^11)	3722	1	0·074	0·199
(02^00)	(12^01)	3696	1	0·002	0·049
(10^00)	(20^01)	3716	2	0·001	0·044

transition in Table 2, the vibrational population factor for the lower state is shown at 300 °K and at 1273 °K. The calculation of these factors is described in a report by Tourin and Henry [3] The transition probabilities shown in Table 2 were calculated from a formula given by W. S. Benedict. [4]

The intensities of the overlapping CO_2 bands occurring in the 2·7 μ spectral region are proportional to the product of transition probability and initial state population. It can be seen from Table 2 that at high temperatures there may be many overlapping bands of approximately equal intensity.

The absorption coefficients in this region are not extremely high, as shown by Fig. 3. Nevertheless, the large pressure effect observed in the room temperature spectrum vanishes at high temperatures, as shown by Fig. 2. Evidently the spectrum is not fully pressure broadened at 700 mm. Another effect occurs instead, which has the same effect as pressure broadening in smearing out the rotational structure. Each of the overlapping bands has a P and an R branch; hence there are many rotational lines of slightly different frequency for each value of rotational quantum number J. As a result of the manifold vibrational and rotational overlapping, the high-temperature spectrum is virtually continuous.

REFERENCES

1. TOURIN, R. H., *J. Chem. Phys.* **20**, 1651 (1952). See also *Nat. Bur. Stands. Circ.* #523, 87 (1954).
2. TOURIN, R. H., *J. Opt. Soc. Amer.* **51**, 175 (1961).
3. TOURIN, R. H., and P. M. HENRY, AFCRC TN-59-262, Geophysics Research Directorate, Bedford, Mass., December 1958.
4. BENEDICT, W. S., *Rep. Nat. Bur. Stand.* 1123, 49 (1951).

Reprinted from JOURNAL OF THE OPTICAL SOCIETY OF AMERICA, Vol. 51, No. 11, 1225–1228, November, 1961
Printed in U. S. A.

Some Spectral Emissivities of Water Vapor in the 2.7-μ Region*

RICHARD H. TOURIN
The Warner & Swasey Company, Control Instrument Division, 32-16 Downing Street, Flushing 54, New York
(Received December 30, 1960)

Spectral emissivities of water vapor were measured in the 2.7-μ region, at temperatures up to 1273°K. The measurements were used to calculate spectral and integrated infrared radiance of hot water vapor for several cases of interest. The spectrum of hot H_2O is relatively poor in strong "hot" bands, in contrast to the case of CO_2. The general character of the rotational structure in the spectrum of the hot gas is similar to the case of room temperature, although some additional lines are observed at high temperatures. Consequently, care must be taken in selecting the spectral intervals over which radiance integrals are to be calculated.

I. INTRODUCTION

INFRARED spectral emissivities of hot water vapor are of interest in studies of radiant emission from flames and in problems of atmospheric transmission. In most cases, gas emissivities are best determined from absorption measurements. The basis for this practice is Kirchhoff's law,[1] which states that for any thermal radiator in equilibrium at temperature T,

$$\epsilon_\lambda(T) = a_\lambda(T),$$

where $\epsilon_\lambda(T)$ is the spectral emissivity at wavelength λ, defined as the ratio of the spectral radiant emittance of the thermal radiator to the spectral radiant emittance of a blackbody at the same temperature; and $a_\lambda(T)$ is the spectral absorptivity at wavelength λ, defined as the fraction of incident radiation (or arbitrary magnitude) absorbed at wavelength λ. The absorptivity $a_\lambda(T)$ can be measured by infrared absorption spectrophotometry.

The determination of spectral emissivities of gases from absorption measurements obviates the difficult task of comparing emission measurements directly to blackbody radiation. The absorption technique is unsatisfactory for weak absorption (less than a few percent) because small values of absorptivity cannot be measured accurately; in this case the more laborious procedure of direct emission measurement must be resorted to. This paper reports on emissivities obtained from absorption measurements.

The infrared spectrum of the water vapor molecule in the 2.7-μ region was studied in detail by Benedict and Plyler.[2] The spectrum of atmospheric water vapor was measured by Taylor *et al.*,[3] at temperatures up to 500°C. These investigators observed and identified a large number of lines in the vibration-rotation spectrum of H_2O, and checked the line frequencies against theoretical predictions. The magnitude of H_2O absorption at room temperature was studied quantitatively by Howard *et al.*[4] who developed formulas for calculating H_2O absorption over long atmospheric paths.

The H_2O spectrum near 2.7-μ corresponds to vibrational transitions of the type

$$(v_1v_2v_3) - (v_1v_2v_3+1) \text{ and } (v_1v_2v_3) - (v_1+1v_2v_3).$$

In flames and in the atmosphere, the 2.7-μ water vapor

* Supported in part by the U. S. Air Force, through the Geophysics Research Directorate, Bedford, Massachusetts.
[1] J. K. Roberts and A. R. Miller, *Heat and Thermodynamics* (Interscience Publishers, Inc., New York, 1960), 5th Ed., Chap. 20, p. 490.
[2] W. S. Benedict and E. K. Plyler, J. Research Natl. Bur. Standards **46**, 236 (1951).
[3] J. H. Taylor, W. S. Benedict, and J. Strong, J. Chem. Phys. 20, 528 (1952).
[4] J. N. Howard, D. F. Burch, and D. Williams, J. Opt. Soc. Am. **46**, 186, 237, 242, 334, 452 (1956).

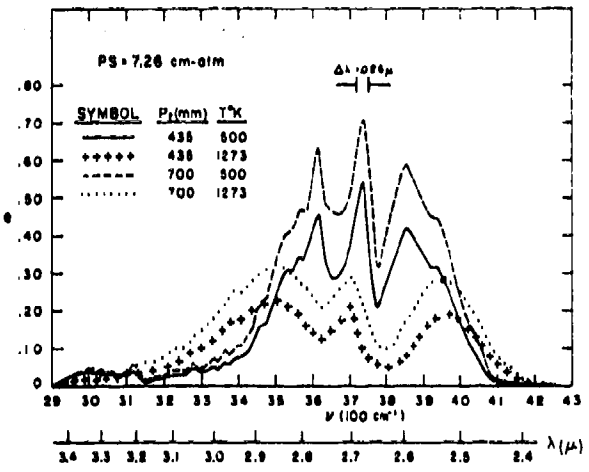

FIG. 1. Spectral emissivity of water vapor in the 2.7-μ region; optical depth 7.26 cm-atm.

spectrum is partially obscured by overlapping carbon dioxide bands of the type

$$(v_1v^l{}_2v_3)-((v_1+1)v^l{}_2(v_3+1))$$

and

$$(v_1v^l{}_2v_3)-(v_1(v_2+2)^l(v_3+1)).$$

The effect of this overlapping was avoided in the present work by measuring spectra of pure samples of CO_2 and H_2O heated in a furnace. The CO_2 measurements have been reported previously.[6,7] The present paper reports similar measurements of emissivities of heated water vapor, at temperatures up to 1273°K. The water vapor spectrum was pressure-broadened with nitrogen.

II. EXPERIMENTAL

The experimental setup used for measurement of hot CO_2 absorption spectra[5] was modified for use with water vapor. Steam produced by heating distilled water in a flask was admitted to a quartz gas cell, up to the desired pressure of H_2O. Sufficient nitrogen was then added to make up the desired total pressure. The gas cell was then sealed off from the gas-handling system. The water vapor samples, contained in the gas cell, were maintained at selected temperatures by means of an electric furnace. The gas-handling system was maintained at about 100°C, to prevent condensation of water. Absorption spectra were measured with a modified Perkin-Elmer 12C infrared spectrometer; auxiliary optics were used to provide an intermediate focal point at the center of the gas cell. The water vapor samples were studied at temperatures from 500° to 1273°K. The path through the samples was 12.7 cm in all measurements.

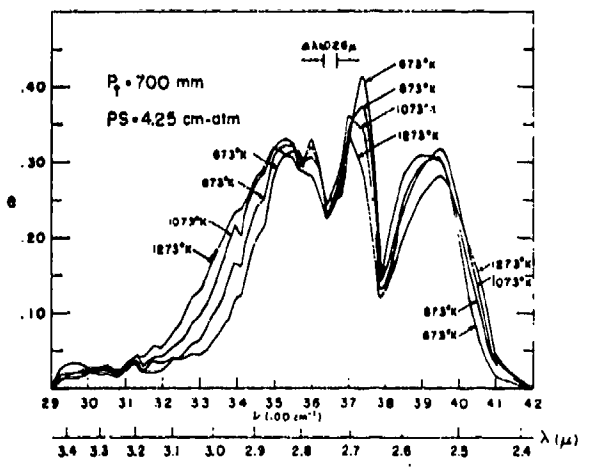

FIG. 2. Spectral emissivity of water vapor in the 2.7-μ region, at 700 mm Hg and various temperatures; optical depth about 4 cm-atm.

[5] R. H. Tourin, Natl. Bur. Standards Circ. No. 523, 87 (1954).
[6] R. H. Tourin, J. Opt. Soc. Am. 51, 175 (1961).
[7] R. H. Tourin, Infrared Phys. 1, 105 (1961).

III. RESULTS

Figure 1 shows water-vapor emissivities at 500° and 1273°K, at two different pressures, for an optical depth of 7.26 cm-atm of H_2O. The effect of pressure on the observed spectral emissivity is relatively greater for the higher temperature. This contrasts with the case of CO_2, where the pressure effect in the 2.7-μ region is observable at room temperature, but vanishes at high temperatures.[7] Figure 2 shows typical plots of H_2O spectral emissivities at an optical depth of 4¼ cm-atm, at four temperatures from 673° to 1273°K, at a total pressure of 700 mm Hg. In the central region of the band the emissivity decreases slightly with increasing temperature. In the wings, the order is reversed, the emissivity increases with temperature. It should be kept in mind that this is not purely a temperature effect. At constant pressure of H_2O, the density decreases with temperature, hence the number of absorbers is lower at the higher temperatures. However, the effect of density variation is considerably less than the effect of temperature; this is particularly evident in the wings, where the emissivity increases with temperature despite the reduction in density.

TABLE I. Slopes of some Beer's law plots for H_2O, measured at 700 mm Hg, pressure-broadened with N_2. The average spectral slit was 30 cm^{-1}. In all cases, the range of optical depth is 1–5 cm-atm. The uncertainty of the slope k varies with the magnitude of the transmittance τ, thus $\Delta k/k=[\ln(1/\tau)]^{-1}[\Delta(1/\tau)]/(1/\tau)$ +(higher order terms). The uncertainties given here are for an optical depth of 5 cm-atm, for which τ has its smallest value (strong absorption). Hence the values shown are lower limits.

Frequency	Temperature	Slope	Frequency	Temperature	Slope
cm^{-1}	°K	cm^{-1} atm^{-1}	cm^{-1}	°K	cm^{-1} atm^{-1}
3400	673	0.061±0.033	3618	673	0.14 ±0.033
3400	873	0.061±0.033	3618	873	0.10 ±0.031
3400	1073	0.059±0.030	3618	1073	0.093±0.033
3400	1273	0.058±0.029	3618	1273	0.084±0.033
3520	673	0.094±0.028	3700	673	0.10 ±0.029
3520	873	0.090±0.028	3700	873	0.113±0.031
3520	1073	0.083±0.028	3700	1073	0.098±0.028
3520	1273	0.086±0.028	3700	1273	0.10 ±0.030

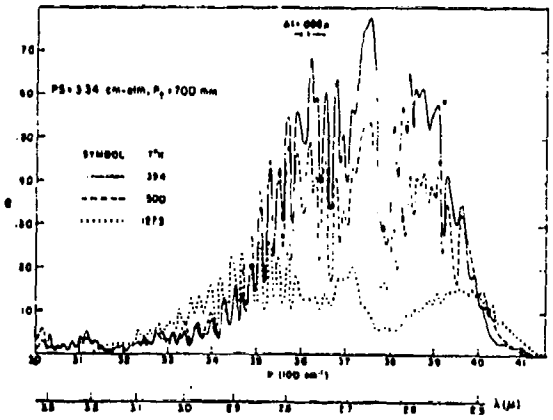

FIG. 3. Spectral emissivity of water at three temperatures, under moderate spectral resolution. Individual spectral lines are not resolved, but the general character of the structure is very similar at all three temperatures.

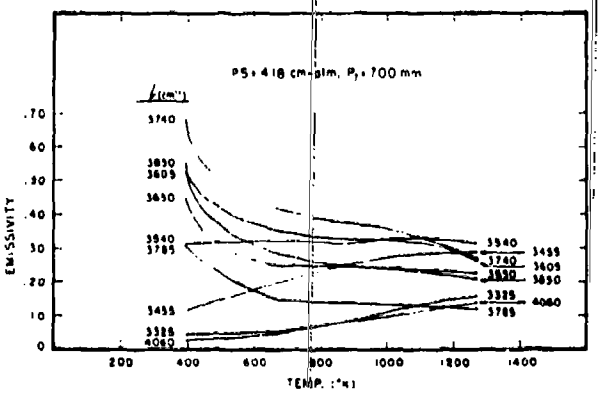

FIG. 4. Temperature dependence of H_2O spectral emissivity, at various frequencies in the 2.7-μ region.

The measurements were made for a range of optical depth from 1 to 5 cm-atm. The results can be fitted to linear ("Beer's Law") plots over this range. In Table I the slopes of some linear plots are given, for four spectral frequencies, at four temperatures, based on data of the type shown in Fig. 2. These slopes are not true absorption coefficients, because the low-resolution spectra from which they were computed contain much unresolved rotational structure. The slopes can be used for interpolation over the range of optical depth shown in Table I, but not for extrapolation much beyond this range.

Unlike the case of CO_2, the H_2O absorption spectra show considerable structure at all the temperatures observed. Figure 3 shows spectral emissivity of H_2O at three temperatures, measured with a moderately narrow spectral slit. Individual lines are not resolved, but the gross rotational structure is apparent, and there is no striking difference between the structures in the low and high temperature cases.

Some examples of the variation of H_2O spectral emissivity with temperature are given in Fig. 4, at several frequencies in the 2.7-μ region. This figure exhibits none of the regularity of comparable plots for carbon dioxide,[6,8] reflecting the greater complexity of the H_2O asymmetric rotor spectrum as compared to the relatively simple, regular spectrum of linear, symmetrical CO_2.

As in the case of CO_2, spectral radiant emittances of H_2O over a given spectral bandwidth can be calculated from emissivity data of the type given in Figs. 1 and 2. However, because of the persistence of rotational structure at high temperatures, these low-resolution emissivities are numerically valid only as averages over a bandwidth great enough to include many rotationa

TABLE II. Infrared radiant emittance of H_2O, calculated from emissivity measurements.

T°K	Band (μ)	P(atm)	PS(cm-atm)	P_t(atm)	$\int e d\lambda$	$W\int e d\lambda$ watt/cm²	$\int We d\lambda$ watt/cm²	Percent difference
1273	2.35–3.45	0.13	1.7	0.13	0.0297	0.11	0.11	0
1273	2.35–3.45	0.13	1.7	0.92	0.0572	0.26	0.21	−19.2
500	2.40–3.40	0.13	1.7	0.13	0.0370	0.28×10^{-3}	0.35×10^{-3}	+25.0
500	2.40–3.40	0.13	1.7	0.92	0.0554	0.38×10^{-3}	0.53×10^{-3}	+39.5
1273	2.35–3.45	0.57	7.3	0.57	0.1027	0.37	0.38	+ 2.7
1273	2.35–3.45	0.57	7.3	0.92	0.1671	0.61	0.62	+ 1.6
500	2.35–3.45	0.57	7.3	0.57	0.1517	0.11×10^{-2}	0.14×10^{-2}	+27.3
500	2.35–3.45	0.57	7.3	0.92	0.2153	0.15×10^{-2}	0.20×10^{-2}	+33.3
1273	2.5–2.9	0.13	1.7	0.13	0.0158	0.64×10^{-1}	0.64×10^{-1}	0
1273	2.5–2.9	0.13	1.7	0.92	0.0356	0.16	0.14	−12.5
500	2.5–2.9	0.13	1.7	0.13	0.0289	0.19×10^{-3}	0.18×10^{-3}	− 5.3
500	2.5–2.9	0.13	1.7	0.92	0.0444	0.28×10^{-3}	0.28×10^{-3}	0
1273	2.5–2.9	0.57	7.3	0.57	0.0602	0.24	0.24	0
1273	2.5–2.9	0.57	7.3	0.92	0.1061	0.39	0.43	+10.3
500	2.5–2.9	0.57	7.3	0.57	0.1283	0.80×10^{-3}	0.80×10^{-3}	0
500	2.5–2.9	0.57	7.3	0.92	0.1814	0.11×10^{-2}	0.11×10^{-2}	0

[8] G. N. Plass, J. Opt. Soc. Am. 49, 821 (1959).

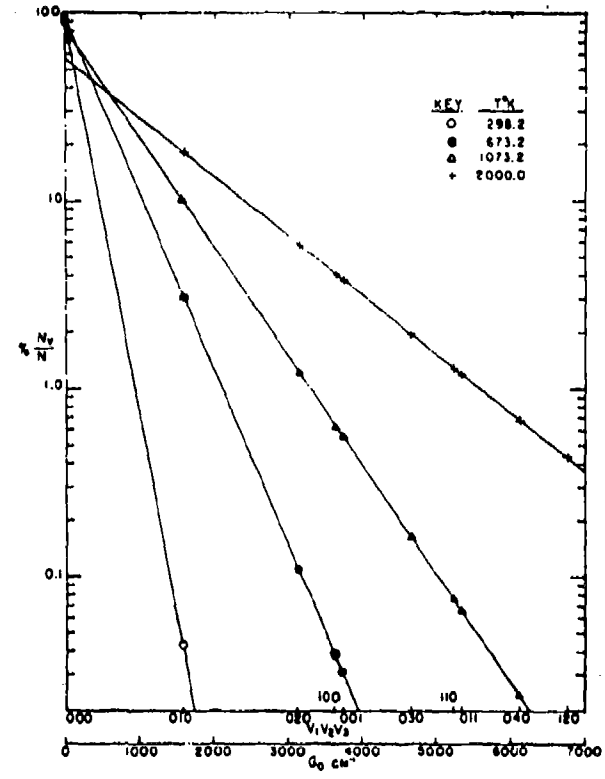

FIG. 5. Energy distribution of H_2O vibrational population. The population is concentrated in the ground state, even at high temperatures.

lines. Referring to Fig. 3, a reasonable bandwidth in this case is about 0.05 μ.

In calculating infrared radiant emittances from emissivities, the necessity for point-by-point multiplication with the Planck function may be obviated by using the approximation

$$W_{\Delta\lambda}(T)=\int_{\Delta\lambda} W(\lambda,T)e(\lambda,T)d\lambda \approx \bar{W}_{\lambda}(T)\int_{\Delta\lambda} e(\lambda,T)d\lambda,$$

where $W_{\Delta\lambda}(T)$ is the spectral radiant emittance over the interval $\Delta\lambda$, $W(\lambda,T)$ is the Planck function, $e(\lambda,T)$ the spectral emissivity, and $\bar{W}_{\lambda}(T)$ the average value of the Planck function over $\Delta\lambda$. The approximation is useful for emissivities greater than about 5%. Table II compares some calculated results obtained by the exact emittance integral and by the approximation. Within the limitations on bandwidth mentioned above, the accuracy of the spectral emissivities reported here is estimated to be of the order of $\pm$10–20%.

IV. DISCUSSION

As compared to carbon dioxide, the spectrum of hot water vapor is much less rich in "hot" bands. The reason for this can be deduced from Fig. 5, which shows how the H_2O molecules in a gas are distributed among the vibrational energy states, at four temperatures. At 2000°K, which is higher than the temperatures attained in this study, the population of the ground vibrational state is still 55%, which is three times as great as the state of next highest population, and there are only seven states, aside from the ground state, having populations as great as 1%. At 1273°K the relative ground-state population is 80%. As a result, the absorption spectrum of hot water vapor is due predominantly to transitions from the ground vibrational state, with relatively modest contributions from excited levels. Therefore the H_2O band structure maintains its discrete character over a wide range of temperature. One should not expect the H_2O absorption in these spectra to follow Beer's law, because emissivities measured with low resolution are averages, over the spectrometer slitwidth, of contributions from narrow spectrum lines, within which absorption is strong, and wide spaces between lines, where absorption is very weak. Typical H_2O linewidth is $\approx$0.1 cm^{-1} atm^{-1}, while line spacing is $\approx 0.1-1.0$ cm^{-1}. The linear plots from which Table I was computed are presumably approximations to segments of a more complicated function.

The H_2O spectrum contrasts strongly to the case of CO_2, where the high-temperature spectrum is virtually continuous, due to overlapping of many hot bands of comparable intensity.[6] The rotational structure of the H_2O bands must be taken into account even at the high temperatures of flames and combustion gases. Hence, caution must be used in applying the results of measurements made with low-resolution spectrometers and filters to calculation of infrared radiance of hot gases containing H_2O.

Reprinted from JOURNAL OF THE OPTICAL SOCIETY OF AMERICA, Vol. 51, No. 2, 171-174, February, 1961
Printed in U. S. A.

Instrumental Effects in Infrared Gas Spectra and Spectroscopic Temperature Measurements*

HAROLD J. BABROV
The Warner & Swasey Company, Control Instrument Division, Flushing, New York
(Received August 15, 1960)

The effect of a most general spectrometer response function (slit function) on the measured transmission and emission of gases is investigated. It is shown that, although both the measured absorption and emission of hot gases are distorted by the slit function, the temperature determined by the infrared monochromatic radiation method is independent of the slit function. It is also shown that the conditions for the invariance of the integrated transmission are much milder than those previously assumed.

I. INTRODUCTION

PREVIOUS work in this laboratory[1] on the spectra of heated gases has shown that for some molecular bands the measured emissivity (and emission) is independent of the spectral slit width of the spectrometer, whereas for other bands the measured emissivity is a very strong function of the slit width. Similarly, it was found that the addition of a gas such as nitrogen, which does not absorb infrared radiation, sometimes caused a great change in the apparent transmission of a molecular band, and had no effect on the transmission of another band. In general, the effect of varying slit width and foreign-gas pressure was small in a spectral region where there are a great many overlapping spectral lines, such as the 4.3-μ absorption of hot CO_2. Where the spacing between lines was large, both the effect of the slit width and of foreign (non-absorbing) gases was quite noticeable.

The explanation for these effects is quite simple. When a spectrometer is set to a certain frequency ν, it responds not only to radiation of that frequency but also to adjacent frequencies ν'. Of course, the response at these adjacent frequencies is not as great as the response at ν. The curve of spectrometer response vs ν' is called the slit function $g(\nu,\nu')$ of the spectrometer. The slit function of a poorly adjusted spectrometer with wide slits might look like the one in Fig. 1. The slit function of a properly adjusted spectrometer usually looks somewhat like that shown in Fig. 2.

II. EFFECT OF SLIT FUNCTION ON THE TRANSMISSION MEASURED AT A GIVEN FREQUENCY

The measured transmission when the spectrometer is set at ν is

$$T_m(\nu)=\int_{\Delta\nu'} I(\nu')g(\nu,\nu')d\nu' \Big/ \int_{\Delta\nu'} I_0(\nu')g(\nu,\nu')d\nu', \quad (1)$$

where $I_0(\nu')$ is the intensity at the frequency ν' in the absence of absorption, and $I(\nu')$ is the transmitted intensity at the frequency ν', i.e.,

$$I(\nu')=I_0(\nu')T(\nu').$$

The interval of integration $\Delta\nu'$ is the region over which $g(\nu,\nu')$ is nonzero; I_0 is usually so slowly varying over this narrow interval that it may be considered constant. Thus we obtain

$$T_m(\nu)=\frac{I_0(\nu)\int_{\Delta\nu'} T(\nu')g(\nu,\nu')d\nu'}{I_0(\nu)\int_{\Delta\nu'} g(\nu,\nu')d\nu'} = \frac{\int_{\Delta\nu'} T(\nu')g(\nu,\nu')d\nu'}{\int_{\Delta\nu'} g(\nu,\nu')d\nu'}. \quad (2)$$

If $T(\nu')$ is nearly constant, as is the case when there are many overlapping lines in the spectral interval covered by the slits, then

$$T_m(\nu)=T(\nu)\int_{\Delta\nu'} g(\nu,\nu')d\nu' \Big/ \int_{\Delta\nu'} g(\nu,\nu')d\nu'=T(\nu). \quad (3)$$

In this case the measured transmission is the same as the true transmission at ν and is independent of the spectral slit width $\Delta\nu'$. Another case in which the measured transmission is independent of the slit width is the case where many lines of approximately equal intensity and spacing are included within $\Delta\nu'$. This case is shown diagramatically in Fig. 3.

In Fig. 3 $g_1(\nu,\nu')$ is the response function for a spectrograph with narrow slits and $g_2(\nu,\nu')$ the response function of that spectrograph with wide slits. It is evident from the diagram that for neither slit width will the spectrograph give the true transmission at ν (100% transmission), but the measured transmission will be an average of the true transmission over the

* This work was supported in part by the U. S. Air Force through the Geophysics Research Directorate, ARDC, Bedford, Massachusetts.
[1] R. H. Tourin and P. M. Henry, Final Report AFCRC-TR-60-203, Geophysics Research Directorate, Bedford, Massachusetts (1959).

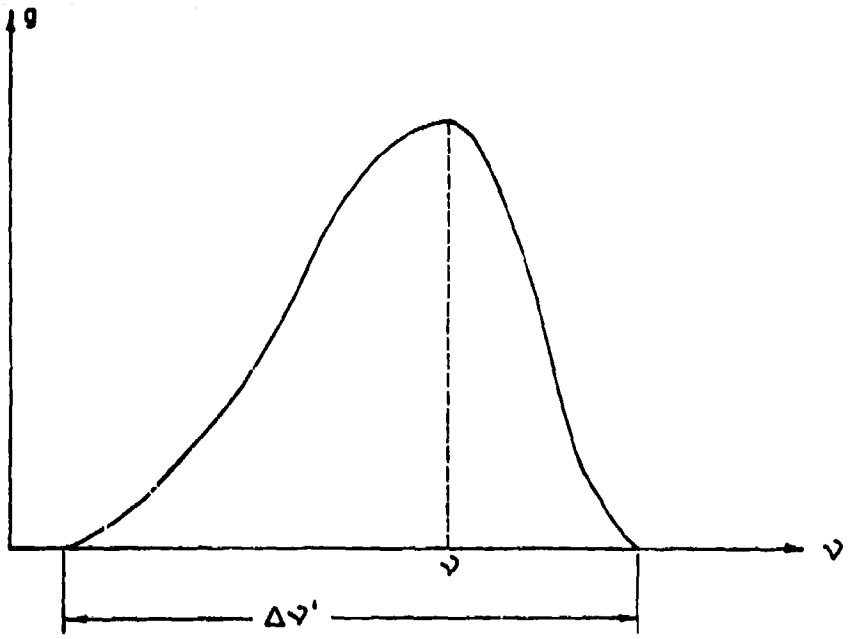

FIG. 1. Asymmetric response function which can result from a poorly adjusted spectrometer. The spectrometer is set at the frequency ν. The ordinate scale is arbitrary.

interval $\Delta\nu'$. Since the average transmission over the interval $\Delta\nu_1'$ is the same as that over $\Delta\nu_2'$, the measured transmission will be the same for both settings of the slit. Although the measured transmission in this case is independent of the slit width, it is not independent of the effect of foreign-gas broadening of the spectral lines. The addition of a foreign gas will cause the measured transmission to decrease. This is not surprising, because the average transmission in the spectral region $\Delta\nu'$ will decrease due to the collision broadening of the lines.

If a small number of lines ($\approx$1–3) of unequal spacing and/or intensity (or width) are included in $\Delta\nu'$, then the measured transmission is severely distorted by the response function of the spectrograph, and the measured absorption at a given spectrometer setting ν will depend very strongly on the spectral slit width and on the presence of nonabsorbing foreign gases. Changes of 200 or 300% in the measured transmission at a given spectrometer setting when the slit width is doubled are not at all uncommon. Needless to say, the measured transmission at a given spectrometer setting [given by Eq. (1)] can be many-fold different from the true transmission at this frequency. Several attempts[2–4] have been made to calculate corrections to the measured transmission by assuming a particular shape for $g(\nu,\nu')$ and $T(\nu')$. It is usually left to the experimenter to determine whether the slit function of his spectrometer has the shape used for the calculated corrections. These corrections are quite useful when the widths of the spectral lines are comparable to the spectral slit widths. However, the spectral slit width of a prism spectrometer is usually much greater than the width of a molecular vibration-rotation line, so the corrections are usually quite impractical for measurements in the infrared with prism spectrometers.

III. INVARIANCE OF THE INTEGRATED TRANSMISSION

Although the measured transmission at any given frequency can be greatly distorted by the slit function, the total (or integrated) transmission of a line or a band is independent of the slit function and is equal to the true integrated transmission, under some very mild conditions on the nature of the slit function and the procedure of integration. To prove this statement, we integrate Eq. (2) over the spectral interval for which

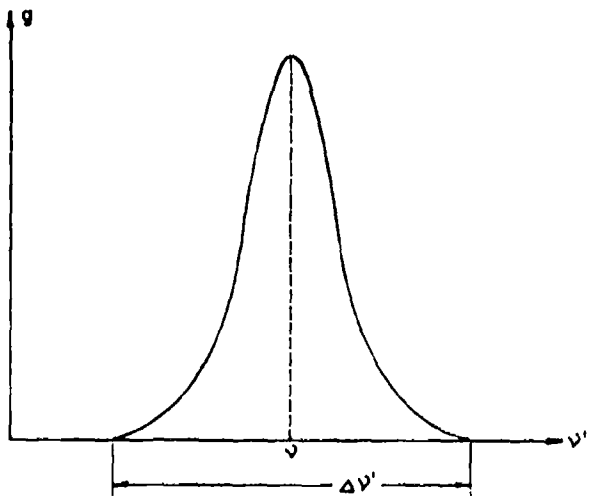

FIG. 2. Symmetric response function of a properly adjusted spectrometer. The spectrometer is set at frequency ν. The ordinate scale is arbitrary.

[2] H. J. Kostkowski and A. M. Bass, J. Opt. Soc. Am. 46, 1060 (1956).
[3] M. T. Pigott and D. H. Rank, J. Chem. Phys. 26, 384 (1957).
[4] G. A. Kulpers, J. Mol. Spectroscopy 2, 75 (1958).

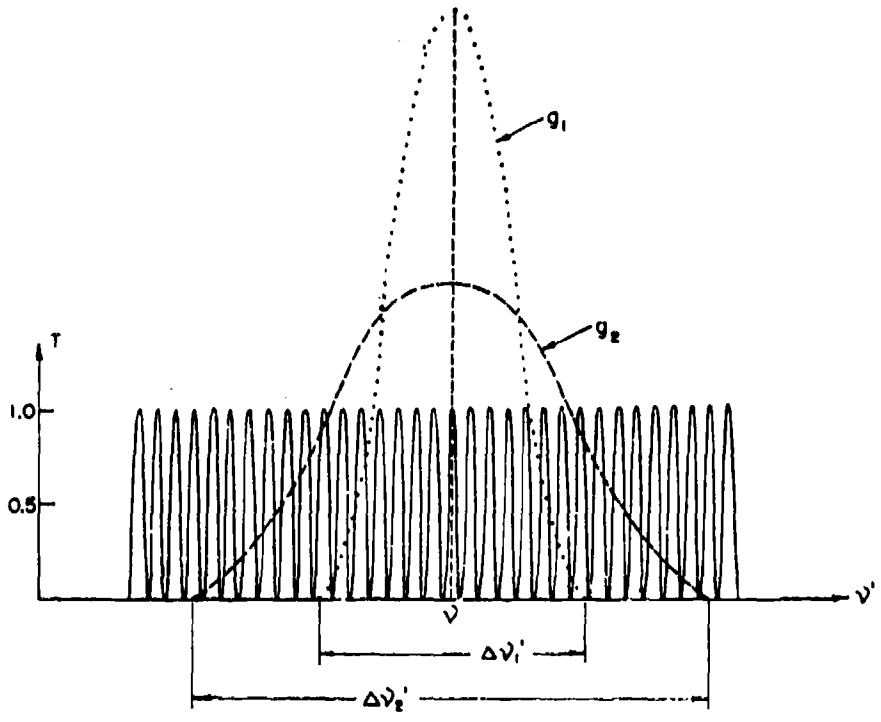

FIG. 3. The response function g_1 of a spectrometer with narrow slits and with wide slits g_2 superimposed on a spectrum of many uniformly spaced lines of equal intensity. In both cases the spectrometer is set at the frequency ν. The ordinate scale for the spectrum is the transmission T of the gas.

the absorption is nonzero; this is equivalent to scanning a spectrum with an infrared spectrograph. We get

$$T_m^{\text{total}} = \int T_m(\nu)d\nu = \int d\nu \left\{ \frac{\int T(\nu')g(\nu,\nu')d\nu'}{\int g(\nu,\nu')d\nu'} \right\}. \quad (4)$$

Interchanging the order of integration in Eq. (4) leads to

$$T_m^{\text{total}} = \int \frac{T(\nu')d\nu'}{\int g(\nu,\nu')d\nu'} \int g(\nu,\nu')d\nu. \quad (4a)$$

Thus we find that

$$T_m^{\text{total}} = \int T(\nu')d\nu' = T_{\text{true}}^{\text{total}},$$

provided that

$$\int g(\nu,\nu')d\nu = \int g(\nu,\nu')d\nu'. \quad (5)$$

Obviously, if $g(\nu,\nu')$ is symmetric in ν and ν' i.e., $g(\nu,\nu')=g(\nu',\nu)$, then Eq. (5) holds. But even if g is not symmetric, Eq. (5) can hold if $g(\nu,\nu')=g(\nu-\nu')$, i.e., if g is independent of the spectrometer setting (if g depends only on the difference between ν and ν'). Thus, even the asymmetric slit function for a poorly adjusted spectrometer shown in Fig. 2 would give

$$T_m^{\text{total}} = T_{\text{true}}^{\text{total}}.$$

The only other important restriction on the procedure is that the limits of the spectral scan be at places where the measured absorption is zero. This requirement is necessary for the interchange of the order of integration to be permissible.

The statement that the total transmission (or absorption) is independent of the slit function has often been made, and occasionally the conditions required for the truth of this statement have been examined.[5] However, it is not usually realized how mild the restrictions are for this statement to be true. For example, De Prima and Penner[5] restrict $g(\nu,\nu')$ to a subclass of the class of symmetric functions for which $g(\nu,\nu')=g(|\nu-\nu'|)$ holds. Examples of this subclass are the Gaussian function and the triangular function. However, the type of slit function shown in Fig. 1 does not belong to this subclass. Nevertheless, the integrated transmission is invariant to the slit function even for a spectrometer with this asymmetric slit function.

IV. EFFECTS IN TEMPERATURE MEASUREMENTS

The measurement of the temperature of hot gases by the infrared monochromatic radiation (IMRA) method[6,7] is a very important part of the measurement program of this laboratory. The IMRA method is based on the fact that the ratio of the monochromatic emission to absorption of a gas in thermal equilibrium is equal to the Planck function (a function of temperature only). Thus, if the absorption and emission are

[5] C. R. DePrima and S. S. Penner, J. Chem. Phys. 23, 757 (1955).
[6] R. H. Tourin and M. Grossman, Combustion and Flame 2, 330 (1958).
[7] R. H. Tourin, Seminar on High Temperature Thermometry, Oak Ridge, Tennessee (1959).

measured at a frequency ν the temperature of the gas is determined. Both the emission and the absorption of the gas at the frequency ν are distorted by the slit function, but the ratio of the measured emission to the measured absorption is equal to the true ratio of these quantities. Therefore, the IMRA temperature is independent of the slit function. That this is so can be seen by considering the mathematical expressions for the (monochromatic) emission and absorption of the gas. Thus

$$I_m^g(\nu)=\int_{\Delta\nu'} I^b(\nu')\{1-[I(\nu')/I_0(\nu')]\}g(\nu,\nu')d\nu'$$

$$I_m^g(\nu)=I^b(\nu)\left[\int_{\Delta\nu'} g(\nu,\nu')d\nu' - \int_{\Delta\nu'} T(\nu')g(\nu,\nu')d\nu'\right], \quad (6)$$

where $I_m^g(\nu)$ is the measured intensity of emission from the gas and $I^b(\nu')$ is the blackbody intensity at the frequency ν'. $I^b(\nu')$ is almost constant over the interval $\Delta\nu'$, so it can be brought in front of the integral sign. From Eq. (2) we have

$$\int T(\nu')g(\nu,\nu')d\nu'=T_m(\nu)\int g(\nu,\nu')d\nu'.$$

Therefore

$$I_m^g(\nu)=I^b(\nu)\left[\int g(\nu,\nu')d\nu'\right][1-T_m(\nu)]. \quad (6a)$$

But by definition

$$1-T_m(\nu)\equiv A_m(\nu) \quad (7)$$

and

$$I^b(\nu)\int g(\nu,\nu')d\nu'\equiv I_m^b(\nu), \quad (8)$$

where $A_m(\nu)$ and $I_m^b(\nu)$ are the measured absorption and blackbody intensity, respectively. Substitution of Eqs. (7) and (8) into Eq. (6a) leads to

$$I_m^g(\nu)/A_m(\nu)=I_m^b(\nu). \quad (6b)$$

In other words, the ratio of the measured emission to the measured absorption is equal to the measured blackbody intensity.

A word of caution is in order at this point. Implicit in the above proof was the assumption that $g(\nu,\nu')$ was the same for the emission measurement, the absorption measurement, and the calibration (blackbody) measurement. In order to ensure this, the optics which illuminate the entrance slit of the spectrometer must be equivalent for all three measurements, i.e., the slit must be evenly illuminated by all three sources (gas I_0 and calibration source) and all three sources must subtend the same solid angle at the detector of the spectrometer.

ACKNOWLEDGMENTS

It is a pleasure to acknowledge the many helpful discussions and criticism by G. A. Ameer and W. M. Benesch of the University of Pittsburgh and P. M. Henry and R. H. Tourin of The Warner and Swasey Company.

Reprinted from JOURNAL OF THE OPTICAL SOCIETY OF AMERICA, Vol. 51, No. 2, 175–183, February, 1961
Printed in U. S. A.

Measurements of Infrared Spectral Emissivities of Hot Carbon Dioxide in the 4.3-μ Region*

RICHARD H. TOURIN
The Warner & Swasey Company, Control Instrument Division, Flushing, New York
(Received August 15, 1960)

Infrared spectral emissivities of hot carbon dioxide have been determined by measurement of the infrared absorption spectra of gas samples heated under controlled conditions. Measurements in the 4.3-μ region are described and are discussed in relation to molecular energy distributions, theoretically calculated emissivities, and flame radiation.

I. INTRODUCTION

THE determination of the radiant power emitted by hot gases in narrow bands of the infrared spectrum is a problem of great interest. Hot gases radiate at characteristic spectral frequencies and do not normally exhibit a continuous blackbody spectrum. The amount and spectral character of radiation from hot gases are dependent on molecular constants and on temperature, pressure, and composition. The radiation of a hot gas cannot be readily calculated from theory alone, because the required constants are imperfectly known, and because the idealized models used in the theory are often inadequate to describe a complex spectrum. Measurements of hot-gas emission are therefore desirable. In the work reported here controlled gas samples of known composition, pressure, and temperature were heated in a quartz gas cell to temperatures up to 1273°K. The infrared spectra of the samples were measured under various conditions.

The present paper gives some results of studies of radiation from heated carbon dioxide in the 4.3-μ region. Several interim accounts of this work have been given previously.[1–5] Most of the measurements reported here are absorption measurements. Accurate gas-emission measurements are very difficult to make, because of the difficulty of comparing to an accurate standard of blackbody radiation, and because of the large corrections necessary for radiation from the gas-cell windows. Some preliminary results of emission measurements are given in Sec. IV of this paper.

One purpose of this work was to obtain data for predicting flame radiation. Most published flame spectra[6,7] cannot be quantitatively compared to theory or to heated gas data, because of large uncertainties in temperature and composition. Correlation of heated gas measurements and flame measurements will be discussed in a future publication.

II. PROCEDURES

A. Experimental

The apparatus used has been described previously.[1,2] The data were obtained by measuring the infrared absorption spectra of samples of hot CO_2. The samples were heated in a quartz gas cell, maintained at temperatures up to 1273°K by an electric furnace. Pressure and composition of the sample were kept constant in the course of a given spectral scan. Spectra were measured with a Perkin-Elmer 12C infrared spectrometer, using a lithium fluoride prism.

B. Treatment of Data

It is convenient to express radiant emission of a hot gas in terms of the spectral emissivity of the hot gas as a function of wavelength and temperature. The spectral emissivity may be combined with the Planck blackbody function to compute the absolute power radiated in any given spectral interval.

The radiant power emitted by a thermal radiator in a finite spectral range $\Delta\lambda$ is given by

$$P_{\Delta\lambda}(T)=\int_{\Delta\lambda} e(\lambda,T)J(\lambda,T)d\lambda, \qquad (1)$$

where $e(\lambda,T)$ is the emissivity at wavelength λ and $J(\lambda,T)$ is the Planck radiation function.

The emissivity $e(\lambda,T)$ is generally a rapidly varying function of λ with irregular amplitude and nonuniform spacing. It also depends on composition, path length, and pressure. It is therefore usually impractical to evaluate the radiant power integral [Eq. (1)] analytically. To obtain a value of the integral in any given case, one must measure the emissivity, multiply point-by-point by the appropriate values of the Planck function,

* This work was supported in part by the U. S. Air Force through the Geophysics Research Directorate, Bedford, Massachusetts.
[1] R. H. Tourin, Industrial Scientific Company Repts. Nos. 224–1 and 224–2, under contract, Wright-Patterson Air Force Base, Dayton, Ohio (1952).
[2] R. H. Tourin, J. Chem. Phys. 20, 1651 (1952). See also Natl. Bur. Standards Circ. No. 523, 87 (1954).
[3] R. H. Tourin, Warner & Swasey Research Corporation, Report No. 258 under contract, Air Force Office of Scientific Research, Baltimore, Maryland (1954).
[4] R. H. Tourin and P. M. Henry, AFCRC TN-59-262, Geophysics Research Directorate, Bedford, Massachusetts (1958).
[5] R. H. Tourin and P. M. Henry, AFCRC-TR-60-203, Geophysics Research Directorate, Hanscom Field, Bedford, Massachusetts (1959).
[6] E. E. Bell *et al*, Study of infrared emission from flames, final report, Parts 1–3, Ohio State University, Columbus, Ohio (1955).
[7] E. K. Plyler and C. J. Humphreys, J. Research Natl. Bur. Standards 40, 449 (1948).

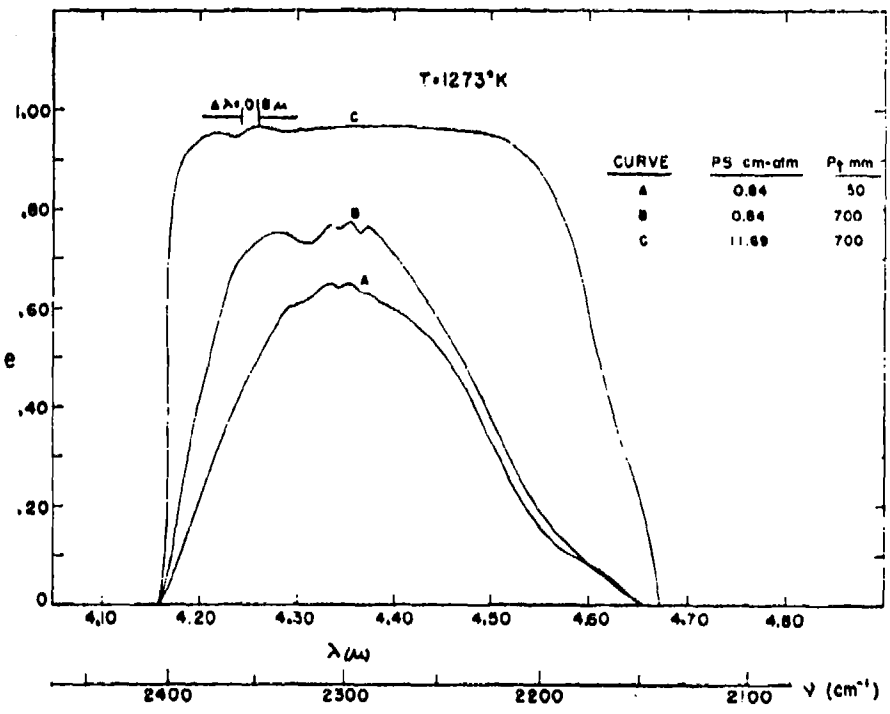

FIG. 1. Spectral emissivity of carbon dioxide at 1273°K; the 4.3-μ region.

plot the results, and evaluate the integral by mechanical means, e.g., by a planimeter.

In order to reduce the work involved in evaluating radiant power integrals, simplifying assumptions can be used. If the spectral band is sufficiently narrow, one may neglect the variation of the Planck function $J(\lambda,T)$ with λ. Then $J(\lambda,T)$ may be taken outside the integral sign, and we have

$$P_{\Delta\lambda}(T)=J_{\lambda}(T)\int_{\Delta\lambda}e(\lambda,T)d\lambda, \tag{2}$$

where

$$J_{\lambda}(T)=(1/\Delta\lambda)\int_{\Delta\lambda}J(\lambda,T)d\lambda. \tag{3}$$

It is then only necessary to evaluate graphically the integral $\int_{\Delta\lambda}e(\lambda,T)d\lambda$. This eliminates the necessity for point-by-point multiplication by the Planck function.

C. Instrument Factors

In practice, one does not measure the radiant power $P_{\Delta\lambda}(T)$ directly, but in terms of the reading of an instrument, $I_{\Delta\lambda}(T)$, given by

$$I_{\Delta\lambda}(T)=K\int_{\Delta\lambda}\int_{\Delta\lambda'}\rho(\lambda,\lambda')e(\lambda',T)J(\lambda,T)d\lambda'd\lambda, \tag{4}$$

where $\rho(\lambda,\lambda')$ is the slit function of the spectrometer,[8–10] $\Delta\lambda'$ is the width of the slit function, and K is a calibration constant, which contains those parameters of the measuring system, such as amplifier gain, which are not dependent upon wavelength. The apparent emissivity $e_{\lambda}(T)$ measured for any given slit width is equal to the area under the spectrum curve divided by the base, i.e.,

$$e_{\lambda}(T)=1/\Delta\lambda'\int_{\Delta\lambda'}e(\lambda',T)\rho(\lambda,\lambda')d\lambda'. \tag{5}$$

The apparent emissivity will be sensitive to slit-width variation if the slit encompasses only a few spectrum lines, widely spaced. However, if the spectrum consists of many lines which overlap to such an extent that the envelope of the spectrum is virtually continuous, the integral of Eq. (5) will be practically invariant with slit width. At the high temperatures with which we are concerned, the infrared spectrum of a polyatomic molecule consists of many bands contributed by vibrational transitions from highly excited states. Many of these "hot" bands differ only slightly from each other in frequency. Consequently, there is a great deal of overlapping among them, and this tends to fill in the gaps in the spectrum, making it approximate a uniform function. The multiplicity of spectral lines at high temperatures produces a situation equivalent to pressure broadening, in which the spectrum is smeared out to a virtual continuum, in a limited spectral range. The case of the CO_2 bands in the 4.3-μ region is unusually favorable in this respect. Measurements by Neill[11] have shown that the CO_2 absorption measured with a continuous radiator as background source does

[8] J. Strong, Phys. Rev. 37, 1661 (1931).
[9] J. Strong, J. Opt. Soc. Am. 39, 320 (1949).
[10] H. J. Kostkowski and A. M. Bass, Natl. Bur. Standards Rept. No. 4418 (1956), p. 32.
[11] H. W. Neill, J. Opt. Soc. Am. 49, 505 (1959).

not differ measurably from the absorption measured with a hot-gas source having the same spectrum as the absorbing sample. The effect of the slit function has been neglected in this paper. Dr. H. J. Babrov[12] of this laboratory has recently shown explicitly that this is justifiable, even if $\rho(\lambda,\lambda')$ is strongly asymmetric.

III. SUMMARY OF CO_2 EMISSIVITIES

This section summarizes some emissivity measurements in the 4.3-μ band, and their application to calculating absolute radiant intensities of hot gases and flames. In all measurements, the geometrical path s was 12.7 cm. The range of temperature T was 300°K to 1273°K, the range of CO_2 partial pressure p was 50–700 mm Hg, the optical depth ps (partial pressure ×path) ranged from 0.84 to 11.7 cm atm, and the total pressure range was 50–700 mm Hg. The total pressure was adjusted by adding nitrogen to the CO_2 samples.

Figure 1 shows the emissivity of CO_2 in the 4.3-μ region at 1273°K, for ps equal to 0.84 and 11.69 cm atm, and total pressure 50 and 700 mm Hg. In this case, there is an apparent pressure effect. This effect virtually disappears between 100 mm and 200 mm pressure, at wavelengths longer than 4.26-μ, as shown in Fig. 2.

The variation of emissivity with temperature is nonuniform with respect to wavelength. Figure 3 illustrates this for selected frequencies in the 4.3-μ band. The interpretation of this temperature dependence is discussed in Sec. VI.

The molecular density, as well as the temperature, varies along the curves shown in Fig. 3. Hence, these curves do not exhibit merely a temperature effect. This is a result of the general practice, followed here, of

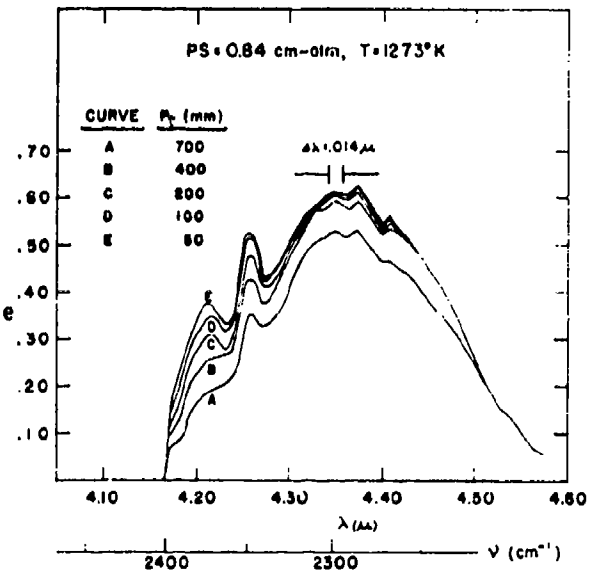

FIG. 2. Effect of pressure on the spectral emissivity of carbon dioxide at 1273°K; the 4.3-μ region.

[12] H. J. Babrov, J. Opt. Soc. Am. 51, 171 (1961).

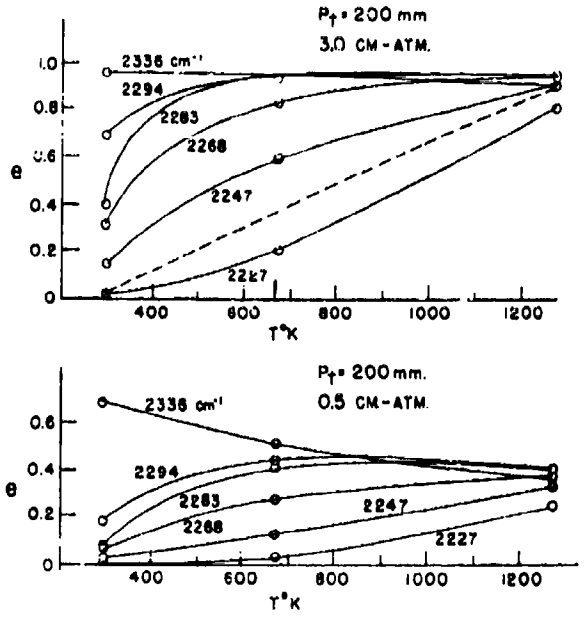

FIG. 3. Spectral emissivity of carbon dioxide as a function of temperature, at several frequencies in the 4.3-μ band. Concentrations 0.5 and 3.0 cm atm, at a total pressure of 200 mm Hg.

expressing concentrations in terms of partial pressure, rather than in terms of radiating particle density. At constant temperature, the distinction is unimportant, because the two quantities are proportional, but at different temperatures the same partial pressure corresponds to different absorber densities. The dotted curve in Fig. 3 shows the variation of spectral emissivity at one frequency when the density is kept constant at its value for 1273°K. The values of $e_\lambda(T)$ for this plot were computed from the 1273°K data, assuming that Beer's law and the ideal gas law were applicable.

The absolute spectral radiance of hot CO_2, for a combination of variables within the ranges shown in the preceding curves, may be computed by multiplying the emissivity by the value of the Planck function for the corresponding temperature and wavelength.

The relative effects of temperature and concentration upon CO_2 emission are illustrated by Figs. 4 and 5. Emissivity data are given in Fig. 4 for the long-wavelength portion of the 4.3-μ band of CO_2 at two temperatures and two concentrations. From 4.35-4.45 μ the effects of changing concentration and changing temperature are moderate. At longer wavelengths the effect of temperature is much greater. When the emissivity data of Fig. 4 are applied to calculating spectral radiance, by means of Eq. (1) or (2), we get a somewhat different picture, as can be seen in Fig. 5. The effect of changing concentration on spectral radiance is hardly appreciable, compared to the temperature effect.

Figure 6 shows the effect of temperature in shifting the CO_2 spectrum. The 1273 and 673°K curves at 200 and 700 mm agree within experimental error; the precision of these measurements is not high.

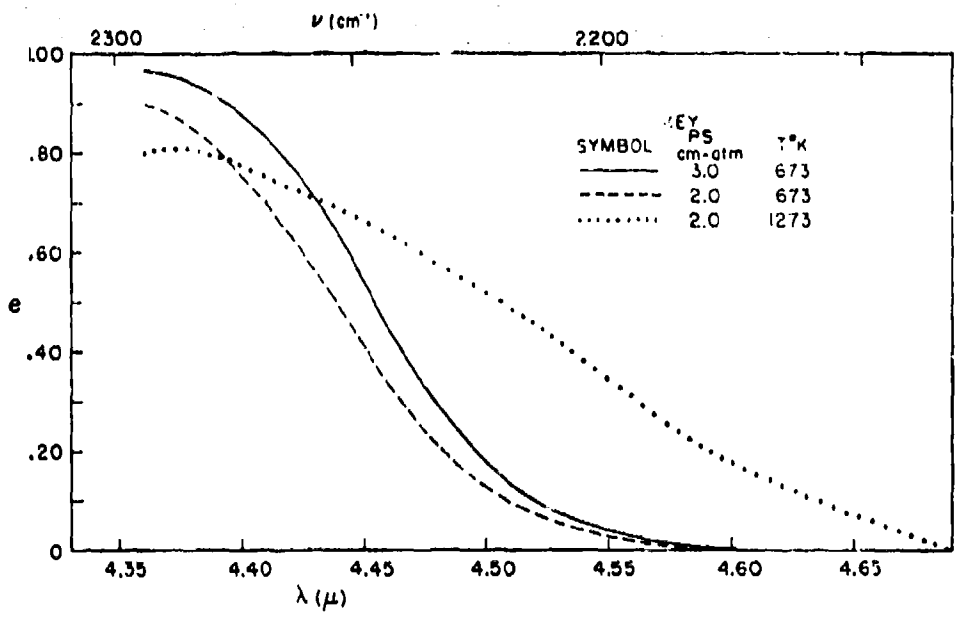

FIG. 4. Spectral emissivity of carbon dioxide in the 4.3-μ region, illustrating the relative effects of temperature and concentration.

Emissivity data of the type given in this paper can be used to calculate the absolute radiance of portions of the 4.3-μ band of CO_2 of variant width. A summary of emissivity integrals and radiant power integrals is given in Table I for 305 and 1273°K. The integrals in Table I were evaluated by measuring the areas under spectral emissivity plots by means of a planimeter. The last column of Table I gives the percentage deviation of the approximate radiant power integral [Eq. (2)] from the exact value [Eq. (1)]. For most applications, the approximation is sufficiently accurate. The approximation is not usuable for very low emissivities, because there the relative experimental error is too large. The approximation seems to be somewhat better

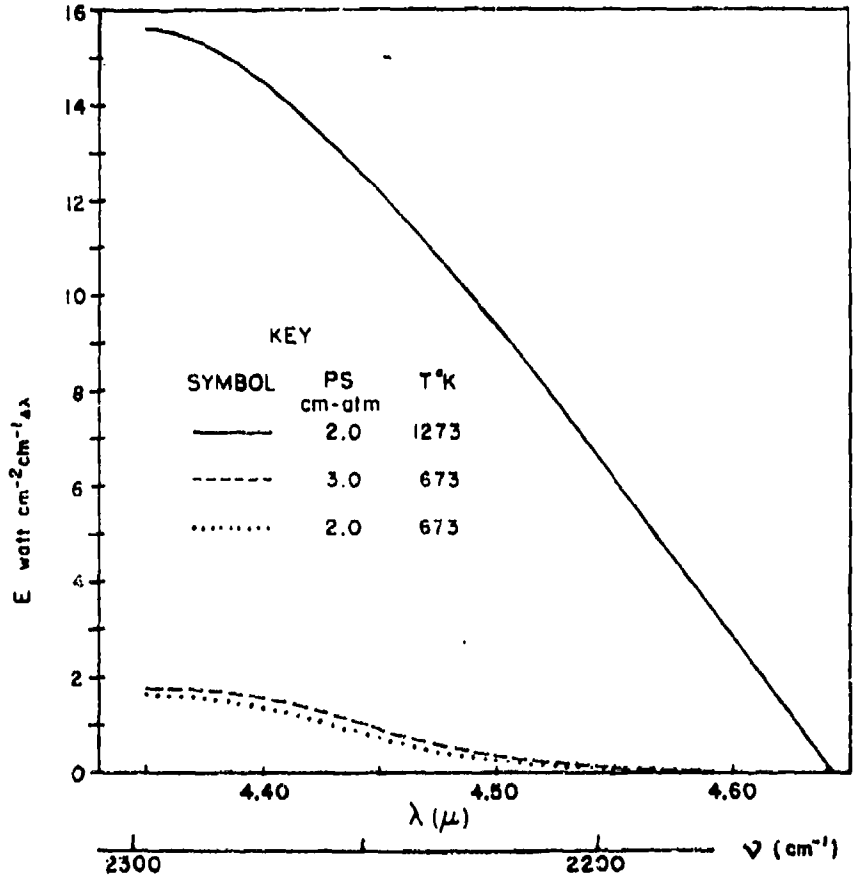

FIG. 5. Spectral radiance of carbon dioxide in the 4.3-μ region, illustrating the relative effects of temperature and concentration.

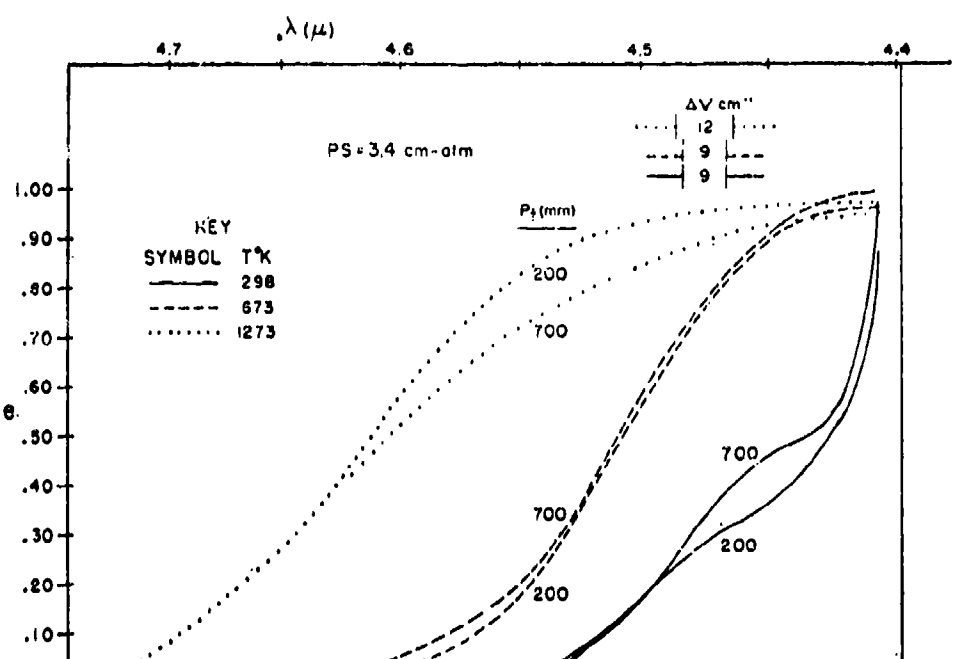

FIG. 6. Pressure and temperature effects on the spectral emissivity of carbon dioxide.

for narrower spectral regions. This is illustrated by comparison of parts (A) and (B) of Table I. The relative uncertainties of these results are estimated to be within ±5–10%. Additional data are given the work cited in footnote 5. Many deficiencies still exist in the data, and will require additional work to clear up.

IV. EMISSION SPECTRA OF HEATED CO_2

In regions of the spectrum where the emissivities are very small, it is difficult to measure them accurately. In such cases, it is preferable to determine the absolute emission of the hot gas by comparison to blackbody radiation at the same temperature.

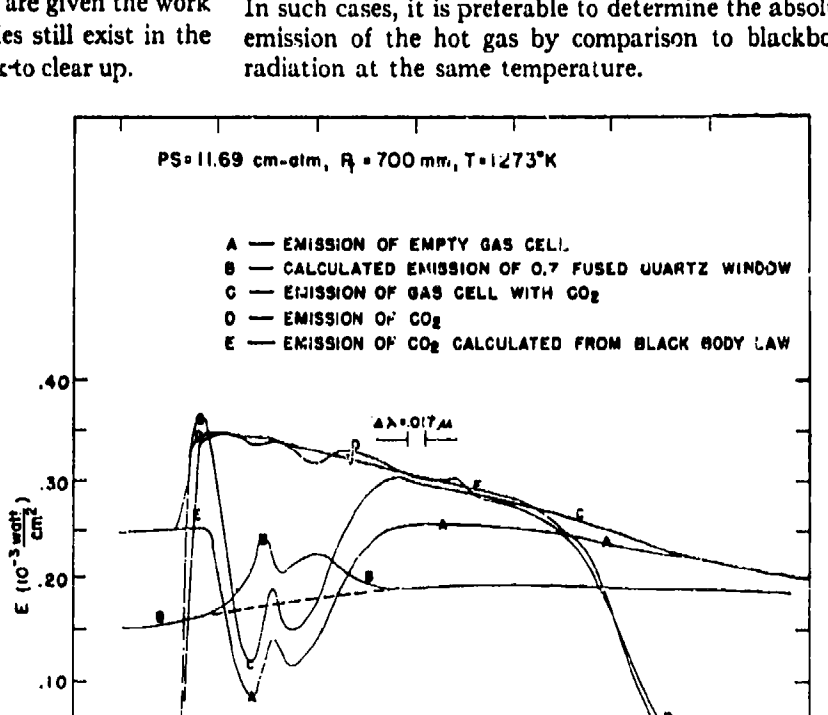

FIG. 7. Correction of gas emission spectra for window radiation.

TABLE I. Emissivity and radiant power integrals of carbon dioxide in the 4.3-μ region.

T°K	$\lambda(\mu)$	p(atm)	ps(cm atm)	p_i(atm)	$\int e d\lambda$	$\int eJ d\lambda$ watt/cm²	$J_\lambda \int e d\lambda$ watt/cm²	% Diff.
(A) Integrated over the full spectral range of appreciable absorption								
305	4.165–4.490	0.07	0.8	0.07	0.0973	0.43×10^{-4}	0.46×10^{-4}	+7.0
305	4.165–4.490	0.07	0.8	0.92	0.1682	0.76×10^{-4}	0.80×10^{-4}	+5.3
305	4.100–4.515	0.92	11.7	0.92	0.2677	0.12×10^{-3}	0.12×10^{-3}	0
1273	4.155–4.650	0.07	0.8	0.07	0.1812	0.34	0.34	0
1273	4.155–4.650	0.07	0.8	0.92	0.2263	0.44	0.42	−4.5
1273	4.155–4.675	0.92	11.7	0.92	0.4247	0.79	0.78	−1.3
(B) Integrated over part of the absorption region								
305	4.2–4.4	0.07	0.8	0.07	0.0809	0.40×10^{-4}	0.42×10^{-4}	+5.0
305	4.2–4.4	0.07	0.8	0.92	0.1522	0.68×10^{-4}	0.71×10^{-4}	+4.4
305	4.2–4.4	0.92	11.7	0.92	0.1926	0.88×10^{-4}	0.89×10^{-4}	+1.1
1273	4.2–4.5	0.07	0.8	0.07	0.1574	0.30	0.30	0
1273	4.2–4.5	0.07	0.8	0.92	0.1955	0.38	0.37	−2.6
1273	4.2–4.5	0.92	11.7	0.92	0.2876	0.55	0.55	0

Emission measurements are also of value as a further check on the influence of instrument parameters, such as spectral slit width. Some measurements of the emission of hot-gas samples were made in the present work. These measurements proved very difficult, primarily because of the relatively high emissivity of the quartz windows in the gas cell. It is possible to make corrections for window effects, but in the present case the emissivity of the windows is of the same order of magnitude as the emissivity of the gas, which makes the correction very difficult to accomplish. Tourin and Henry[5] may be consulted for details of the correction procedure.

Figure 7 shows an example of heated CO_2 emission in the 4.3-μ band, corrected for window absorption and emission. Curves A, B, and C in Fig. 7 were used to calculate curve D, which represents the emission that would have been measured were the windows non-absorbing. For comparison purposes, curve E was calculated from Eq. (2), using measured emissivities. The agreement between the corrected experimental emission and the emission calculated from absorption data is apparently good throughout the band. However the emission correction is a tedious calculation and is

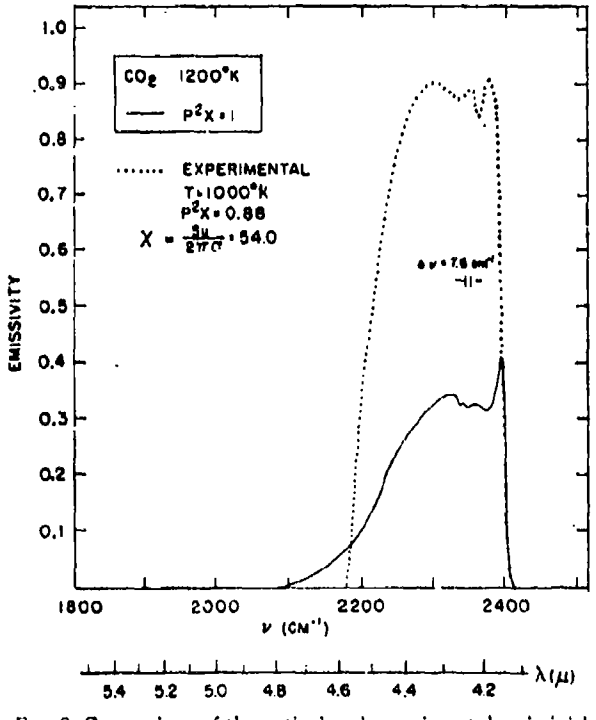

FIG. 8. Comparison of theoretical and experimental emissivities of CO_2 for $x = (Su/2\pi\alpha) > 1.63$. The solid curve is a theoretical curve from Plass.[18]

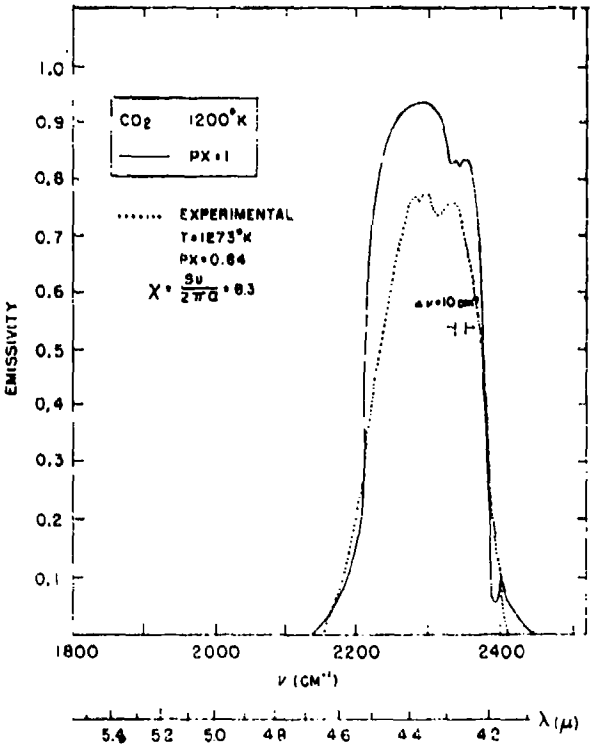

FIG. 9. Comparison of theoretical and experimental emissivities of CO_2, for $x = Su/2\pi\alpha) < 0.2$. Theoretical curve from Plass.[18]

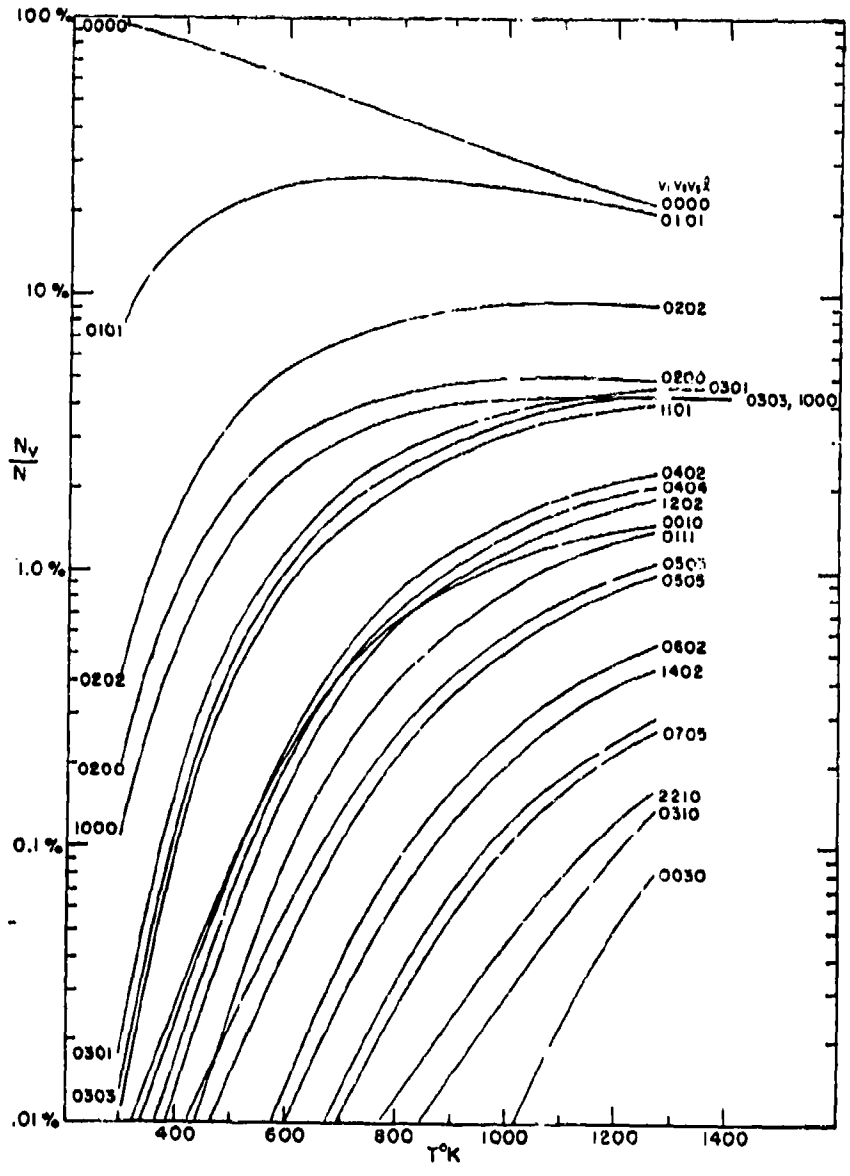

FIG. 10. Vibrational level populations of CO_2.

susceptible to many cumulative errors, so this close agreement should not be taken too seriously.

V. COMPARISON TO THEORY

Theoretical calculations of CO_2 spectral emissivities in the 4.3-μ region have been made by Plass.[13] Figures 8 and 9 show comparisons of Plass' calculations to the present measurements. The values of temperature, pressure, and optical depth for the measured spectra were not identical with the values used for the calculations, but were close enough for a reasonable comparison to be made. Plass plotted two sets of CO_2 emissivities for two extreme cases, $x<0.2$ and $x>1.63$, where $x=Su/2\pi\alpha$. Here S is the total intensity of a rotational line, u the mass of absorbing gas per unit area, and α the half-width of a spectrum line. For $x>1.63$ (Fig. 8) the agreement is poor, the measured data being about 2½ times the calculated values. A similar result has been reported by Ferriso.[14]

In the comparison of Fig. 8, the experimental data corresponded to $x=54$. This was calculated as follows. The value of S was interpolated from data of Benedict and Plyler,[15] the value of u was measured, and α was estimated from the work of Kostkowski.[16] The calculated value $x=54$ is for the strongest line in the band and is believed accurate to within $\pm 25\%$. Making generous allowance for error and for downward weighting of the average line intensity by weak lines, x is

[13] G. N. Plass, J. Opt. Soc. Am. 49, 821 (1959).

[14] C. Ferriso, private communication (1959).

[15] W. S. Benedict and E. K. Plyler, Natl. Bur. Standards Circ. No. 523 (1954), p. 57.

[16] H. J. Kostkowski, Progress Report on Contract Nonr. 248(01), The Johns Hopkins University, Baltimore, Maryland (1955).

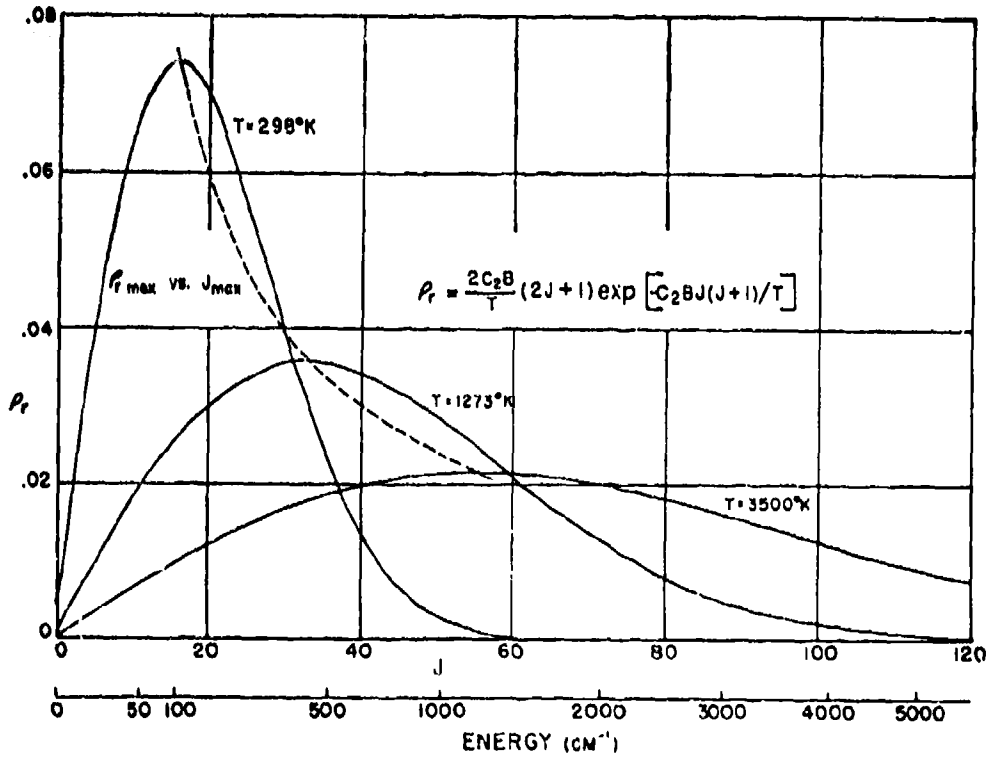

FIG. 11. Rotational distribution function of CO_2.

clearly greater than 1.63, so that it is justifiable to make the comparison.

No measurements were taken in which $x<0.2$. Therefore, a direct comparison to Plass' calculation for this case could not be made. However, when the calculated curve for 1200°K was compared to an experimental curve for which $x\gg0.2$, the theoretical and experimental curves were very close together. In Fig. 9 the value of x corresponding to the experimental curve was $x=8.3$, calculated in the same manner as the preceding case. Again allowing for error and for the variation of intensity from line to line, the experimental value of x clearly does not fall in the range $x<0.2$; hence, the correspondence between the theoretical and experimental curves is anomalous.

VI. DISCUSSION

The distribution of molecular population over the vibrational energy states appears to be a major factor in the temperature dependence of CO_2 emission near 4.3 μ. Figure 10 shows plots of relative population of the CO_2 levels appreciably populated at 1273°K. In calculating the levels and populations for Fig. 10, the effects of higher-order accidental degeneracy, of the Fermi resonance type, have been taken into account. These effects cannot be neglected, particularly when considering radiation in the wings of the band. The dependence of vibrational population on temperature shown in Fig. 10 can be roughly correlated with the observed temperature dependence of Fig. 3.

The relatively minor role of variation in rotational-level population is illustrated by Fig. 11. At high temperatures, the rotational population factor does not vary much, over a wide range of J. At 1273°K the population values fall in the range 1–3½% for J from $J=15$ to $J=75$. In addition, the fall in population at high J is counterbalanced by the increase in transition probability, which is proportional to J and ν.

TABLE II. Some CO_2 transitions giving bands in the 4.3-μ region.

Lower state	Upper state	Lower-state population			
$v_1v_2^lv_3$	$v_1v_2^lv_3$	300°K	1273°K	P	ν_0
00^00	00^01	0.920	0.211	1	2349 cm^{-1}
01^10	01^11	0.074	0.199	1	2337
02^20	02^21	0.003	0.094	1	2324
03^30	03^31	<0.001	0.044	1	2320
04^40	04^41	<0.001	0.021	1	2304
00^01	00^02	≪0.001	0.015	2	2323
00^02	00^03	≪0.001	0.001	3	2301

Table II shows a few of the many transitions giving rise to absorption bands in the 4.3-μ region. At room temperature, the transition from the ground state is predominant, although there is an appreciable contribution from the transition 01^10-01^11. At higher temperatures, no single transition is predominant. Since each band has a rotational structure, and these overlap, the high-temperature spectrum is a virtual continuum.[11] The overlapping of multiple bands has the same effect on the spectrum as pressure broadening for a room temperature, even though the line widths

are actually of the order of 0.1 cm^{-1}, while the line spacing in a single band is about 0.8 cm^{-1}.

The relative transition probabilities, in the harmonic oscillator approximation, are[17]

$$P=\frac{(v_1''+\Delta v_1'')!(v_2''+\Delta v_2'')^d!(v_3''+\Delta v_3'')!}{v_1''!v_2''^d!v_3''!}, \quad (6)$$

[17] W. S. Benedict, Natl. Bur. Standards Rept. No. 1123 (1951), p. 49.

where $d=2$ for CO_2. For bands in the 4.3-μ region $\Delta v_3=1$, while $\Delta v_1=\Delta v_2=0$, so Eq. (6) reduces to $P=v_3+1$. Values of P are listed in Table II.

VII. ACKNOWLEDGMENTS

The author is grateful to Paul M. Henry for assistance in making the measurements and reducing the spectral data, and to George A. Hornbeck and Harold J. Babrov for many stimulating discussions.

Reprinted from JOURNAL OF THE OPTICAL SOCIETY OF AMERICA, Vol. 51, No. 7, 799-800, July, 1961
Printed in U. S. A.

Spectral Emissivities of Hot CO_2-H_2O Mixtures in the 2.7-μ Region*

RICHARD H. TOURIN
The Warner & Swasey Company, Control Instrument Division, Flushing 54, New York

(Received January 30, 1961)

THIS laboratory has been engaged in measuring infrared spectral emissivities of hot gases.[1-3] In this work, emissivities have been determined from infrared absorption spectra of gas samples heated under controlled conditions. For a gas in thermal equilibrium, spectral emissivity and spectral absorptivity are equal at every wavelength (Kirchhoff's law). Emissivities can therefore be read directly from the measured absorption spectrum. This method of measuring emissivities is usually more accurate and convenient than the alternative procedure of comparing gas emission to blackbody emission. It is desired to extrapolate from these laboratory measurements, to predict spectral emissivities of hot gases in various cases of practical interest. The simplest extrapolation formula is Beer's law. Beer's law applies to spectral regions of finite width, if the observed spectrum is continuous over the experimental spectral slot width. The 4.3-μ and 2.7-μ bands of hot CO_2 are favorable cases for Beer's law, because they show continuous absorption even under high resolution, due to overlapping of "hot" bands.[2,3] The 2.7-μ H_2O bands do not appear favorable for Beer's law; only a few "hot" bands occur, and the line spacing is substantially greater than the linewidths.

Of particular interest is the region 2.65–3 μ, where the H_2O fundamentals ν_1 and ν_3 overlap the CO_2 combination bands $(2\nu_2+\nu_3)$, and $(\nu_1+\nu_3)$. Absorption spectra of CO_2-H_2O mixtures were measured in the 2.65–3-μ region, to determine whether emissivities of H_2O and CO_2 measured separately could be combined by means of Beer's law to give the emissivity of a mixture of these gases. Spectra were measured with a prism spectrometer, using a spectral slit of about 11 cm^{-1}. The gas mixtures were maintained at 1273°K in a heated quartz gas cell. Mixture ratios used corresponded to CO_2 and H_2O concentrations in a propane-air

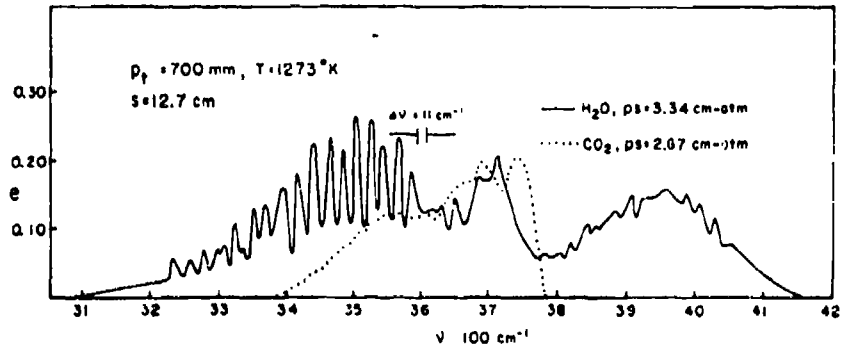

FIG. 1. Emissivities of CO_2 and H_2O independently measured in a hot gas cell, for optical depths corresponding to a stoichiometric propane-air flame.

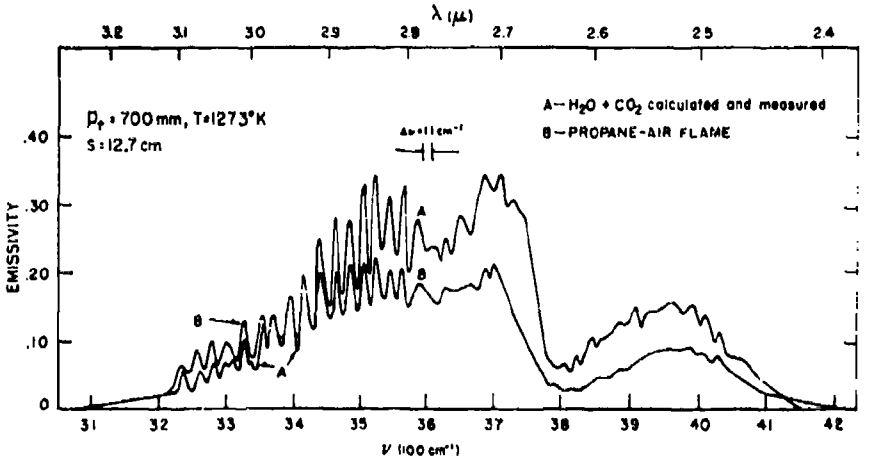

FIG. 2. Spectral emissivity of a CO_2-H_2O mixture of stoichiometric proportions compared to emissivity of a stoichiometric propane-air flame.

flame; optical depths ranged from 1.67 to 4.18 cm atm of H_2O, and 1.67 to 10.0 cm-atm of CO_2, at 127.3°K. Varying the pressure from 350 mm to 700 mm Hg, by adding nitrogen, did not change the measured absorption. The emissivity ϵ of each mixture was calculated from Beer's law, which yields the explicit formula

$$\epsilon(\text{mixture}) = \epsilon(CO_2) + \epsilon(H_2O) - \epsilon(CO_2)\epsilon(H_2O). \quad (1)$$

Measured emissivities of CO_2 and H_2O, corresponding to stoichiometric concentrations of CO_2 and H_2O in a propane-air flame, are shown in Fig. 1. The H_2O emissivities are numerically valid as averages over spectral regions wide enough to include many unresolved rotational lines; this restriction does not apply to CO_2, since its spectrum in this case is effectively continuous. Curve A of Fig. 2 is a plot of the measured spectral emissivities of a synthetic stoichiometric mixture of heated CO_2 and H_2O, and of the spectral emissivities of the same mixture calculated by Eq. (1) from the separate CO_2 and H_2O emissivities of Fig. 1. There are no measurable differences between the calculated and experimental values of the mixture emissivities within the experimental error, which is $\pm 1\%$. Curve B in Fig. 2 shows the measured emissivity of a stoichiometric propane-air flame, of approximately the same optical depth as the synthetic mixture. The comparison to the flame emissivity is qualitative, because the flame temperature (about 2000°K) is higher than that of the gas mixture, and the flame is inhomogeneous.

On comparing the curves in Fig. 2 to the H_2O curve of Fig. 1, it is evident that the basic H_2O structure is preserved throughout; only the relative shape of the spectral emissivity curve is changed by the addition of CO_2 and by changing the temperature. The numerical values of the mixture emissivities are valid as averages over reasonably broad spectral regions, as in the case of pure H_2O; no additional restrictions are introduced by the calculation procedure described here.

This example is typical of emissivities of hot H_2O-CO_2 mixtures. In the mixture spectra, the CO_2 spectrum behaves like a true continuum. This should hold also for mixtures of CO_2 with other gases than H_2O.

* Supported in part by Geophysics Research Directorate, Bedford, Massachusetts.

[1] R. H. Tourin, J. Chem. Phys. **20**, 1651 (1952); Natl. Bur. Standards Circ. No. **523**, 87 (1954).
[2] R. H. Tourin, J. Opt. Soc. Am. **51**, 175 (1961).
[3] R. H. Tourin, *Infrared Physics* (to be published).
[4] H. W. Neill, J. Opt. Soc. Am. **49**, 505(A) (1959).
[5] W. S. Benedict (private communication, 1960).